International Atomic Energy Agency

INDC-260E
FEB 1969

INDC

INTERNATIONAL NUCLEAR DATA COMMITTEE

USSR STATE COMMITEE ON THE UTILIZATION OF ATOMIC ENERGY NUCLEAR DATA INFORMATION CENTRE

NUCLEAR PHYSICS RESEARCH IN THE USSR (Collected Abstracts) No.6

English translation of an original in Russian published by Atomizdat, 1968

IAEA NUCLEAR DATA UNIT, KÄRNTNER RING 11, A-1010 VIENNA

International Atomic Energy Agency

INDC-260E
FEB 1969

INDC

INTERNATIONAL NUCLEAR DATA COMMITTEE

USSR STATE COMMITEE ON THE UTILIZATION OF ATOMIC ENERGY NUCLEAR DATA INFORMATION CENTRE

NUCLEAR PHYSICS RESEARCH IN THE USSR (Collected Abstracts) No.6

English Translation of:

Ядерно-физические исследования в СССР

IAEA NUCLEAR DATA UNIT, KÄRNTNER RING 11, A-1010 VIENNA

Russian original published by Atomizdat, 1968.

Institute of Physics and Power Engineering*/

FAST-NEUTRON RADIATIVE CAPTURE CROSS-SECTIONS OF ^{55}Mn, ^{69}Ga, ^{71}Ga AND ^{98}Mo

A.G. Dovbenko, V.E. Kolesov,
V.P. Koroleva, V.A. Tolstikov

(Submitted to 'Atomnaja Energija') AE 26 (1) 67 1/69

The radiative capture cross-sections of ^{55}Mn, ^{69}Ga, ^{71}Ga and ^{98}Mo for 0.2-3.0 MeV neutrons were measured by the activation technique. The T(p,n)^{3}He reaction was used as the fast-neutron source. The fast-neutron flux was monitored by means of a fission chamber containing ^{235}U. (The fission cross-sections were taken in accordance with the recommendations in W.C. Davey's article in Nuclear Science and Engineering, Vol. 26, 149, 1966.) The cross-sections obtained are compared with the calculated values obtained on the basis of the statistical theory of nuclear reactions, using the optical model of the nucleus for the purpose of calculating neutron penetration factors.

The results obtained are set out in Tables I-IV below.

Table I

Fast-neutron radiative capture cross-sections of ^{69}Ga

En keV	200	266	340 ±35	420 ±35	455	535	635 ±35	680	740 ±35	770	845 ±35	920 ±55
σ mb	50,2 ±3,2	42,6 ±2,3	37,8 ±I,9	33,3 ±I,7	30,I ±I,9	26,6 ±I,7	25,2 ±I,5	24,6 ±I,7	20,4 ±I,7	2I,4 ±I,4	20,9 ±I,2	I9,4 ±I,0
En keV	I025 ±55	I335 ±55	I400	I550	I745 ±50	I885	I945 ±50	22I0	2350 ±50	2745 ±50	3I50 ±50	
σ mb	I8,I ±0,9	I5,5 ±0,8	I5,0 ±I,2	I3,9 ±0,8	I2,0 ±0,6	I2,0 ±0,9	II,I ±0,7	II,2 ±0,9	9,I ±0,5	8,0 ±0,5	6,8 ±0,4	

The table shows errors, including experimental errors and errors in the fission cross-section of ^{235}U.

*/ Edited by A.V. Ignatyuk.

Table II

Fast-neutron radiative capture cross-sections of ^{55}Mn

En keV	420 ±35	530 ±35	635 ±35	710	800	890	950 ±35	975	1050 ±35	1155 ±35	
σ mb	4,5 ±0,6	3,7 ±0,5	3,6 ±0,5	3,2 ±0,5	3,3 ±0,5	3,2 ±0,5	2,7 ±0,4	2,65 ±0,4	2,5 ± 0,4	2,45 ±0,35	
En keV	1255 ±35	1430 ±35	1555 ±35	1630 ±60	1945 ±50	2150 ±50	2350 ±50	2745 ±50	3050 ±50	3260 ±50	3430 ±50
σ mb	2,4 ±0,4	2,0 ±0,3	2,0 ±0,3	1,9 ±0,3	1,7 ±0,3	1,6 ±0,25	1,65 ±0,25	1,7 ±0,25	1,5 ±0,2	1,45 ±0,2	1,35 ±0,2

The table shows errors, including experimental errors and errors in all reference cross-sections.

Table III

Fast-neutron radiative capture cross-sections of ^{71}Ga

En keV	222	265	340 ±40	420 ±35	455	535	635 ±35	680	740	770	845 ±35	920 ±55	1030 ±55
σ mb	49,4 ±3,5	43,3 ±2,9	42,3 ±2,4	39,1 ±2,2	28,7 ±1,7	23,0 ±1,9	21,1 ±1,2	18,5 ±1,7	18,1 ±1,1	17,8 ±1,4	17,1 ±1,0	15,6 ±0,9	14,2 ±0,8
En keV	1295	1335 ±50	1610 ±75	1690	1745 ±50	1860	1945 ±50	2120 ±70	2210	2350 ±50	2745 ±50	3150 ±50	
σ mb	10,7 ±0,8	10,1 ±0,7	8,8 ±0,7	8,1 ±0,7	7,5 ±0,5	7,5 ±0,5	7,4 ±0,5	6,6 ±0,5	6,6 ±0,5	6,4 ±0,5	6,7 ±0,5	6,3 ±0,5	

The table shows errors, including experimental errors and errors in the fission cross-section of ^{235}U.

Table IV

Fast-neutron radiative capture cross-sections of ^{98}Mo

En keV	230	400 ±60	435	550	600 ±55	770	815 ±60	845	960
σ mb	45,8 ±4,I	35,6 ±I,9	4I,I ±3,4	36,9 ±2,2	37,2 ±2,4	36,3 ±2,8	33,5 ±2,5	25,0 ±2,I	24,0 ±2,3

En keV	I025 ±60	I240 ±50	I300	I6I0 ±80	I770	2220 ±70	2725 ±75
σ mb	23,3 ±I,9	I8,5 ±I,2	I6,2 ±I,6	I4,I ±I,4	I3,0 ±I,2	I2,6 ±I,3	9,8 ±I,0

The table shows errors, including experimental errors and errors in the fission cross-section of ^{235}U.

RADIATIVE CAPTURE OF 0.01-3 MeV NEUTRONS

V.E. Kolesov, V.P. Koroleva, A.V. Malyshev,
V.A. Tolstikov, Yu.Ya. Stavissky

(Presented at the Anglo-Soviet Seminar on Nuclear Constants for Reactor Computations, Dubna, 18-22 June 1968. ASS-68/5)

The authors present the results of measurements of the radiative capture cross-sections of ^{74}Ge, ^{69}Ga, ^{71}Ga, ^{80}Se, ^{121}Sb and ^{192}Os, using the activation method. The thermal- and fast-neutron-induced fission cross-sections of ^{235}U were used as reference cross-sections. The cross-sections are given for the $^{80}Se(n,\gamma)^{81m}Se$ (Fig. 1) and $^{80}Se(n,\gamma)^{81g}Se$ (Fig. 2) reactions, and also the isomeric ratios $\sigma_m/\sigma_m + \sigma_g$ (Fig. 3) for the reaction involving radiative capture of fast neutrons by ^{80}Se. The results of the measurements are compared with calculations performed according to the statistical theory of nuclear reactions (Fig. 4 for ^{80}Se and Fig. 5 for ^{192}Os). The black dots on the graphs denote the results of this work, the solid, unbroken lines the calculated values for the total neutron radiative capture cross-section and the thin and broken lines the contributions made by neutron waves with ℓ = 0, 1, 2 and 3 to $\sigma(n,\gamma)$.

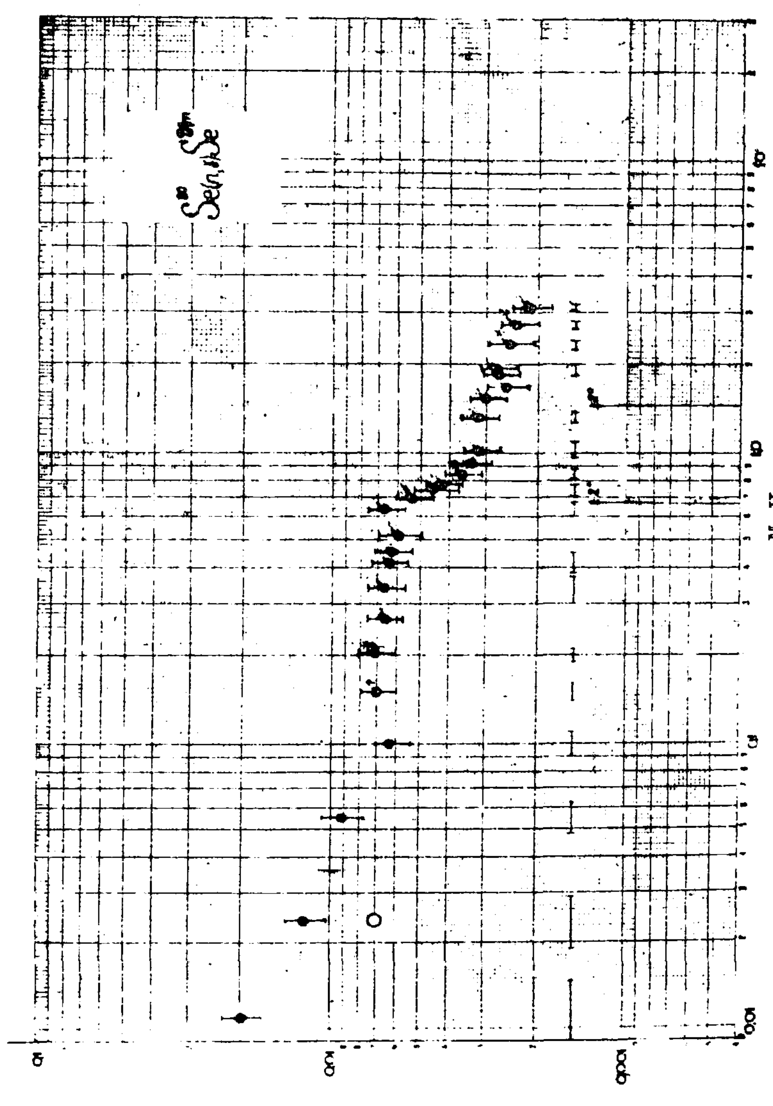
MeV
barns

POOR QUALITY ORIGINAL

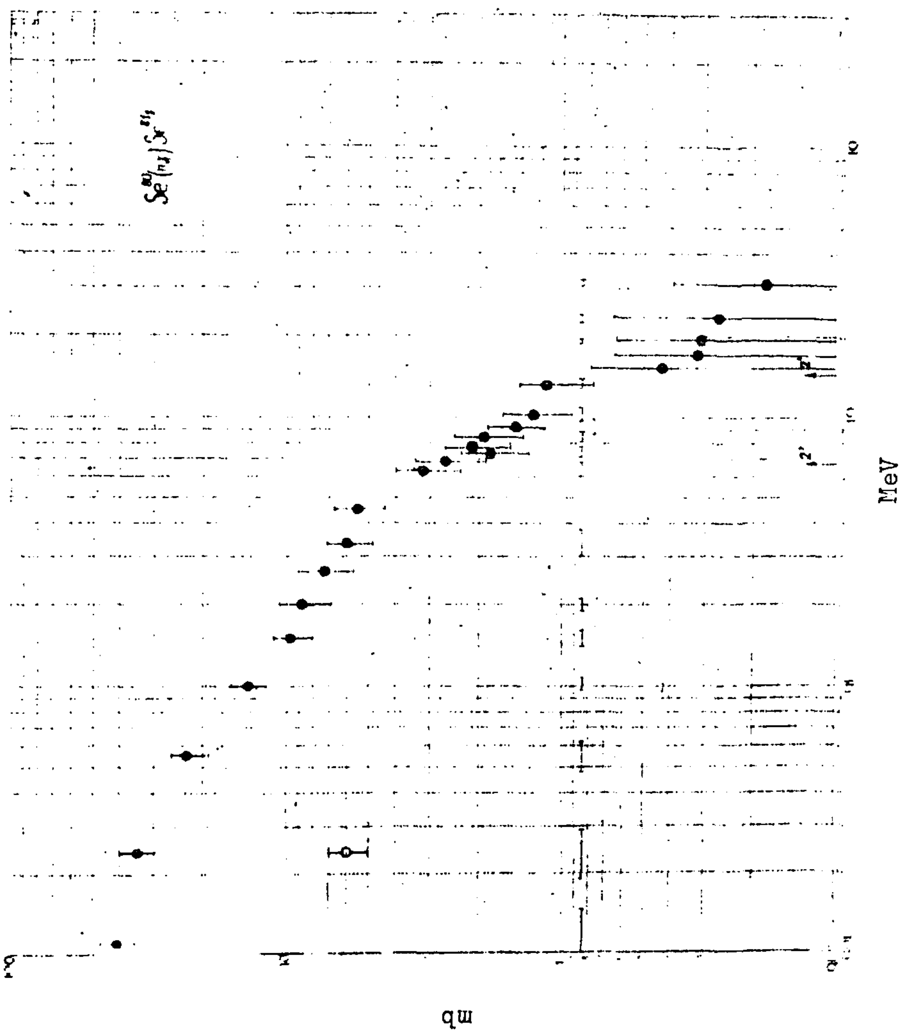

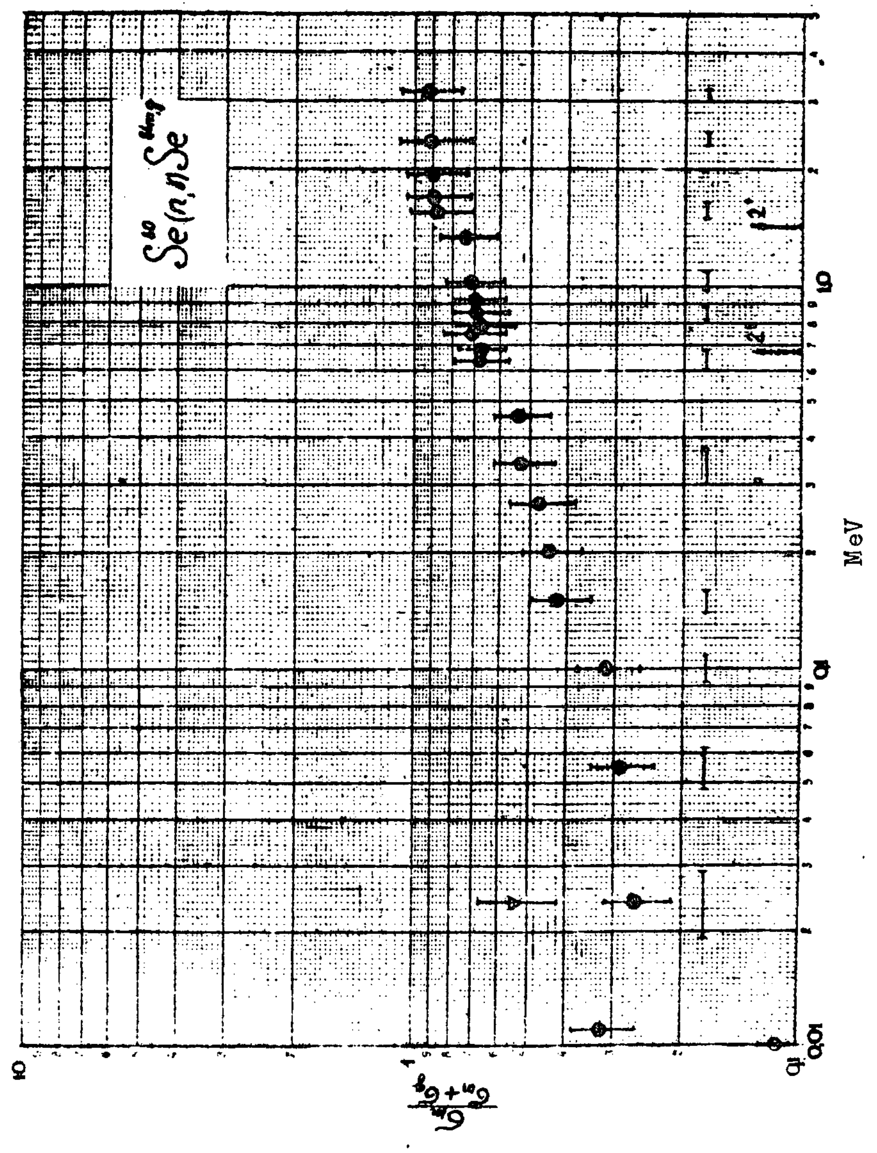
MeV
0.01
0.1
1.0
10

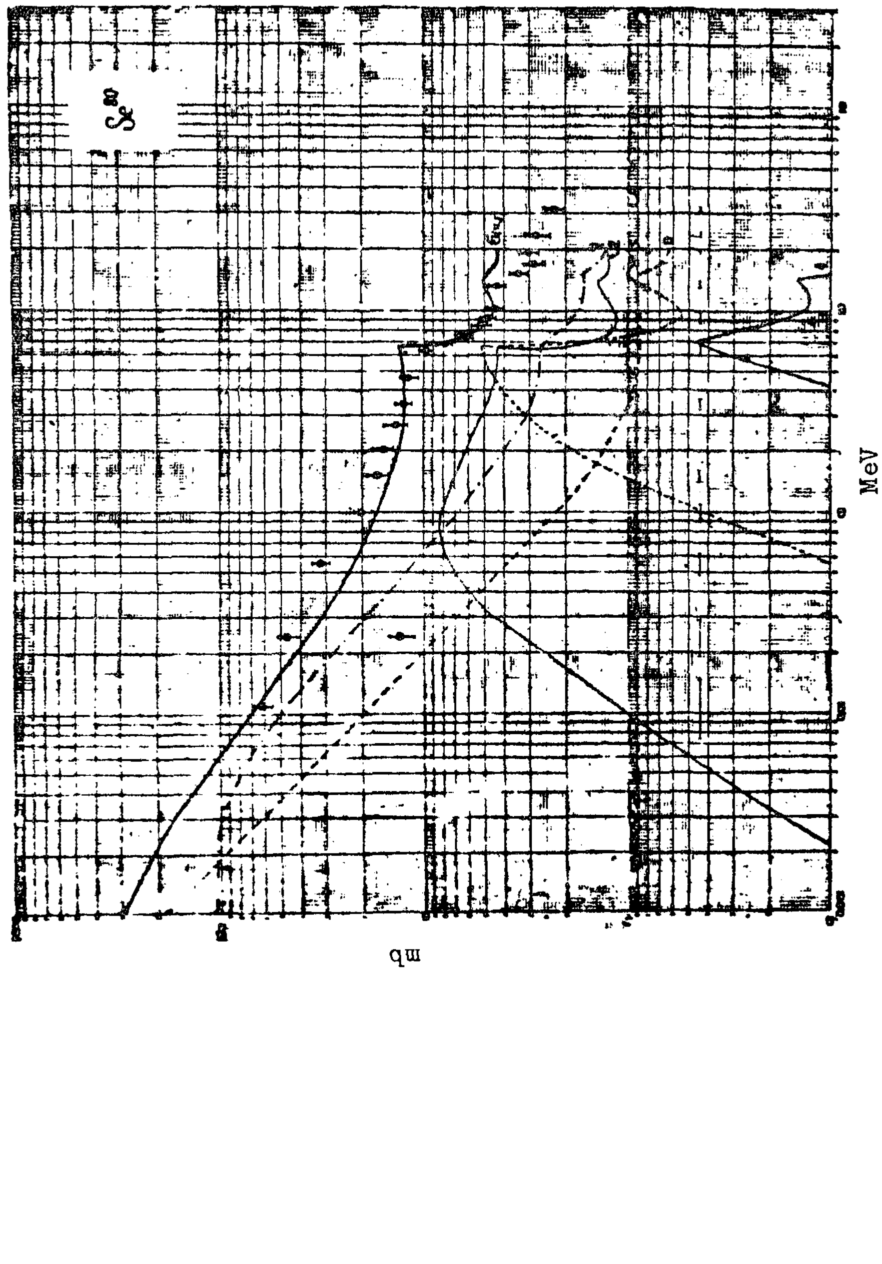
MeV
mb

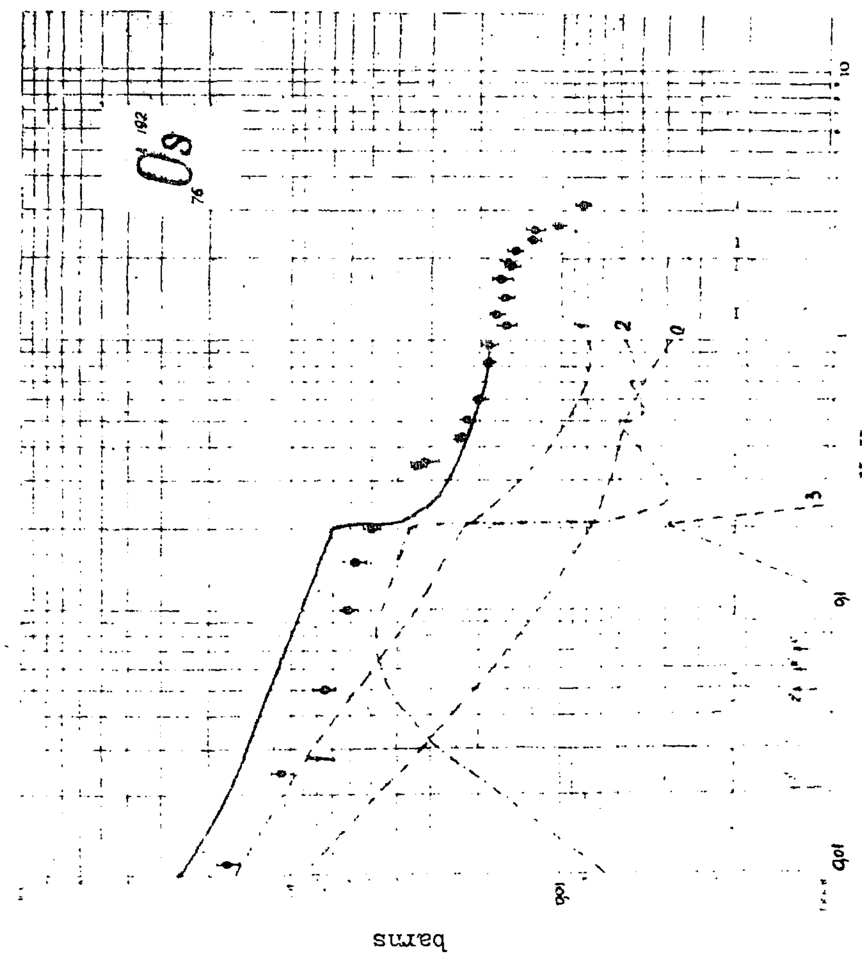
Os
192
76
MeV
barns

RADIATIVE CAPTURE CROSS-SECTIONS FOR FAST NEUTRONS IN THE 10-350 keV FIELD

A.G. Dovbenko, V.E. Kolesov, V.P. Koroleva, V.A. Tolstikov

(Submitted to 'Atomnaja energija')

The authors present measured and calculated results for the radiative capture cross-sections of ^{63}Cu, ^{69}Ga, ^{71}Ga, ^{74}Ge, ^{80}Se, ^{87}Rb, ^{121}Sb, ^{124}Sn, ^{128}Te, ^{130}Te, ^{192}Os, and ^{193}Ir for 10-350 keV neutrons.

The measurements were carried out by the relative activation method on a Van de Graaf accelerator in annular geometry at an angle of 105^{o} to the direction of the proton beam. The neutron flux was monitored by a fission chamber with a layer of ^{235}U. The induced activity of the samples was measured by end-window beta counters. The relative values of $\sigma(n,\gamma)$ were normalized in overlapping neutron energy regions, using data obtained by the authors previously. The calculated cross-sections were obtained by means of the statistical theory of nuclear reactions, using the optical model for the purpose of calculating neutron penetration factors. The results of the measurements are shown in Tables 1-15, which give the total errors taking into account the indeterminacies in the reference cross-sections - the fission cross-sections of ^{235}U for thermal and fast neutrons - and also in the thermal-neutron capture cross-sections of the isotopes in question.

Table 1

Fast-neutron radiative capture cross-sections of ^{63}Cu

E_n, кэв	9 ± 5	20 ± 6	5I ± 9,4	I03 ± I3	303 ± 30
$\sigma(n,\gamma)$, мб	I38 ± I5	85,2 ± 6,9	44,2 ± 4,8	29 ± 2,6	21,3 ± I,6

Table 2

Fast-neutron radiative capture cross-sections of ^{69}Ga

E_n, кэв	II ± 3,6	27 ± 5,3	53 ± 6,7	100 ± 8,5	I50 ± I0,5
$\sigma(n,\gamma)$, мб	247,8 ± 56	I72,I ± 39	99,8 ± 23	60,7 ± I3,9	56,7 ± I3,2
E_n, кэв	202 ± II	266 ± I3	338 ± I7		
$\sigma(n,\gamma)$, мб	5I,6 ± II,8	42,6 ± 9,6	37,8 ± 8,5		

Table 3

Fast-neutron radiative capture cross-sections of ^{71}Ga

E_n, кэВ	II±3,6	27±5,3	53±6,7	I00±8,5	I50±I0,5	202±II	266±I5	338±I7
σ(n,γ), мб	300,6±64	I64±34	87,7±20	63,I±I5	54,5±I3,5	49,4±I0,7	43,3±9,I	42,3±9

Table 4

Fast-neutron radiative capture cross-sections of a natural mixture of $_{31}Ga$ isotopes

E_n, кэВ	II±3,6	27±5,3	53±6,7	I00±8,5	I50±I0,5	202±II	338±I7
σ(n,γ), мб	268,8±42	I69±27	95±I6	62±10	56±9,6	53±8,3	39,6±6,I

Table 5

Results of cross-section measurements on the $^{80}Se(n,\gamma)^{81g}Se$ reaction

E_n, кэВ	II ± 3,6	24 ± 4,8	55 ± 7	I00 ± 8,5	I50±II	338 ± I7
σ(n,γ), мб	4I,6±6,2	346±5	22,7±3,2	I3,8±2,0	9,6±I,6	5,9±I,I

Table 6

Results of cross-section measurements on the $^{80}Se(n,\gamma)^{81m}Se$ reaction

E_n, кэВ	II±3,6	24±4,8	55±7	I00±8,5	I50±I0,5	202±II	266±I5	338±I7
σ(n,γ), мб	I9,9±3,I	I2±2	9,2±I,5	6,3±0,9	7±I,I	7±I	6,5±0,9	6,5±0,9

Table 7

Fast-neutron radiative capture cross-sections of ^{80}Se

E_n, кэВ	11±3,6	24±4,8	55±7	100±8,5	150±11	338±17
σ(n,γ), мб	61,5±6	48,8±4,7	32±3,1	20±1,9	16,6±1,5	12,5±1,1

Table 8

Isomeric ratios for the $^{80}Se(n,\gamma)^{81m,g}Se$ reaction

E_n, кэВ	11±3,5	24±4,8	55±7	100±8,5	150±11	336±17
σ(n,γ), мб	0,324±0,06	0,262±0,05	0,289 ±0,0054	0,315 ±0,057	0,422 ±0,076	0,524 ±0,091

Table 9

Fast-neutron radiative capture cross-sections of ^{87}Rb

E_n, кэВ	11±3,6	24±4,8	50±5,8	102±8	150±10	300±17
σ(n,γ), мб	51,5±13,5	34±8,9	18±5	9,3±2,6	10±2,8	8,6±2,3

Table 10

Fast-neutron radiative capture cross-sections of ^{121}Sb

E_n, кэВ	11±3,6	24±4,8	50±5,8	102±8	152±10	200±12	394±18
σ(n,γ), мб	1418±217	1096±165	685±103	310±47	227±35	221±35	161±24

Table 11

Results of cross-section measurements on the $^{124}Sn(n,\gamma)^{125g}Sn$ reaction

E_n, кэВ	9±5	20±6,4	51±9	103±13	155±17	217±28	250±30
σ(n,γ), мб	28.5±6,5	18,1±4,1	10,2±2,6	6,8±1,6	5,4±1,2	5,8±1,3	5,1±1,2

E_n, кэВ	338±30
σ(n,γ), мб	4,7±[illegible]

Table 12

Results of cross-section measurements on the $^{128}Te(n,\gamma)^{129g}Te$ reaction

E_n, кэв	II±3,6	24±5,3	50±5,8	56±5	I02±9	I50±I0	250±I3
$\sigma(n,\gamma)$, мб	77,5±22	53,5±I5	27±7,3	24±7,2	I7±5	I5±4,5	I2,7±3,5

E_n, кэв	338±I7
$\sigma(n,\gamma)$, мб	I2,2±3,3

Table 13

Results of cross-section measurements on the $^{130}Te(n,\gamma)^{131g}Te$ reaction

E_n, кэв	II±3,6	24±5,3	50±6,7	76±7	I02±9	200±I2
$\sigma(n,\gamma)$, мб	I6,3±5,5	I4±4,3	I2±4	8,6±2,9	5,5±2	5,9±2

E_n, кэв	289±25	338±I7
$\sigma(n,\gamma)$, мб	5,3±I,8	5,I±I,7

Table 14

Fast-neutron radiative capture cross-sections of ^{192}Os

E_n, кэв	II±3,6	24±4,8	50±5,8	I02±8	I52±I0	202±II
$\sigma(n,\gamma)$, мб	I73±46	I08±29	75±20	62±I6	58±I6	52±I4

E_n, кэв	338±37	350±I8
$\sigma(n,\gamma)$, мб	34±8,7	32±9

Table 15

Fast-neutron radiative capture cross-section of ^{193}Ir

E_n, кэв	I0±4,5	25±5,3	5I±9	I03±I3	I55±I7	377±I7
$\sigma(n,\gamma)$, мб	2662±650	I50I±370	I2I4±300	662±I62	559±I37	29I±7I

METHODS OF INTERPOLATION, EVALUATION AND COMPACT REPRESENTATION OF DATA ON ELASTIC AND INELASTIC NEUTRON SCATTERING

V.I. Popov, V.M. Sluchevskaya, V.I. Trykova

(Presented at the Anglo-Soviet Seminar on Nuclear
Constants for Reactor Computations
Dubna, 18-22 June 1968
ASS-68/11)

The authors propose a method of interpolating experimental results on inelastic neutron scattering with a view to calculating recommended spectra for inelastically scattered neutrons. As a result of the interpolation, all the data on inelastic neutron scattering for one nucleus are reduced to values for 120 constants, from which the neutron spectra for any initial neutron energy from 0 to 15 MeV can be calculated using a simple algorithm.

In order to interpolate the angular distributions of elastically scattered neutrons, the authors use the optical model of the nucleus. As a first step, the experimental results are analysed in order to find the neutron energy dependence of the coefficients for Legendre polynomial expansion of the angular distributions. Subsequently, machine searching programmes are used to determine the energy dependences of the optic potential parameters which provide satisfactory agreement between the calculated angular distributions and the smoothed experimental results.

The energy dependences found for these parameters are then used to calculate the differential elastic cross-sections in initial neutron energy regions not previously investigated.

DIFFERENTIAL INELASTIC SCATTERING CROSS-SECTIONS OF ^{238}U, ^{232}Th, Nb, Cu AND Fe FOR NEUTRONS WITH AN INITIAL ENERGY OF 14.3 MeV

O.A. Salnikov, G.N. Lovchikova, G.V. Kotelnikova,
V.I. Moroka, A.M. Trufanov, N.I. Fetisov, A.A. Ivanov

(Presented at the Anglo-Soviet Seminar on Nuclear
Constants for Reactor Computations
Dubna, 18-22 June 1968
ASS-68/6)

The authors present the results of measurements of the angular distributions of inelastically scattered neutrons with an initial energy of 14.3 MeV on ^{238}U, ^{232}Th, Nb, Cu and Fe nuclei. The measurements were carried out on a time-of-flight spectrometer in cylindrical geometry; the resolving time of the spectrometer was 5-7 seconds, the path length 2 m, the neutron recording threshold 100 keV and the pulse repetition frequency 2 Mc/s. The detector used was a liquid scintillator working in an assembly with 2 FEU-36 photomultipliers. The inelastically scattered neutron spectra measured for various angles made it possible to obtain not only the angular distribution but also the nuclear temperatures and nuclear level density parameters. The results are given in Table 1.

Table 1

Nucleus	T_{eff} (MeV) 30°	60°	90°	120°	150°	T_{eff} av.	T_1 (MeV) 30°	60°	90°	120°	150°	T_1 av.	a_p MeV^{-1} This work	Ref. [5]	$\frac{\sigma_{in.}(\theta^\circ)}{\sigma_{in.}(90^\circ)}$ (0.0–4 MeV) 30°	60°	90°	120°	150°	$\frac{\sigma_{in.}(\theta^\circ)}{\sigma_{in.}(90^\circ)}$ (4–14 MeV) 30°	60°	90°	120°	150°
Fe	0,86 ± 0,09	0,85 ± 0,09	0,80 ± 0,08	0,77 ± 0,08	0,72 ± 0,07	0,72 ± 0,07	1,66 ± 0,17	1,48 ± 0,15	1,55 ± 0,15	1,54 ± 0,15	1,53 ± 0,15	1,55 ± 0,15	5,25 ± 1,0	6,9	0,89 ± 0,04	0,99 ± 0,05	1	0,84 ± 0,09	0,88 ± 0,04	1,20 ± 0,12	0,80 ± 0,08	1	0,86 ± 0,09	0,69 ± 0,07
Cu	0,80 ± 0,08	0,62 ± 0,06	0,63 ± 0,08	0,64 ± 0,06	0,65 ± 0,06	0,71 ± 0,07	1,38 ± 0,14	1,24 ± 0,12	1,24 ± 0,12	1,23 ± 0,13	1,23 ± 0,12	1,26 ± 0,13	8,5 ± 1,7	8,0	0,87 ± 0,04	1,13 ± 0,05	1	0,99 ± 0,05	0,98 ± 0,05	1,35 ± 0,05	1,26 ± 0,013	1	0,96 ± 0,10	0,70 ± 0,07
Nb	0,78 ± 0,08	0,79 ± 0,08	0,79 ± 0,08	0,78 ± 0,08	0,78 ± 0,08	0,78 ± 0,08	1,35 ± 0,14	1,25 ± 0,12	1,15 ± 0,12	1,12 ± 0,11	1,12 ± 0,11	1,20 ± 0,12	10,1 ± 1,0	10,7	0,85 ± 0,05	1,06 ± 0,05	1	0,95 ± 0,05	1,01 ± 0,05	1,33 ± 0,13	1,33 ± 0,11	1	0,82 ± 0,08	0,76 ± 0,08
Th^{232}	0,46 ± 0,05	0,43 ± 0,04	0,44 ± [illegible]	0,41 ± 0,04	0,42 ± 0,04	0,43 ± 0,04	0,65 ± 0,07	0,61 ± 0,06	0,60 ± 0,06	0,54 ± 0,05	0,57 ± 0,06	0,59 ± 0,06	37,5 ± 7,5	26,5	1,12 ± 0,17	1,10 ± 0,17	1	0,92 ± 0,14	0,98 ± 0,15					
U^{238}	0,48 ± 0,05	0,48 ± 0,05	0,49 ± 0,05	0,44 ± 0,04	0,44 ± 0,04	0,47 ± 0,05	0,66 ± 0,07	0,66 ± 0,07	0,67 ± 0,07	0,62 ± 0,06	0,60 ± 0,06	0,64 ± 0,06	33,18 ± 6,6	28,5	1,17 ± 0,18	0,93 ± 0,14	1	1,04 ± 0,16	1,23 ± 0,18					

PHENOMENOLOGY OF QUADRUPOLE EXCITATIONS IN EVEN-EVEN NUCLEI

N.S. Rabotnov, A.A. Seregin

(Submitted to Jadernaja Fizika)

The authors discuss the choice of an operator for the potential energy of quadrupole surface oscillations of even-even nuclei, which depends on both deformation variables. They propose a method for exact numerical solution of the Schroedinger collective-model equation with selected potential; the method affords adequate accuracy in the deformationally transitional region, where the approximations so far used are unsatisfactory. The results obtained make it possible to trace the conversion of the equidistant vibrational spectrum of a spherical nucleus to the rotational-oscillatory spectrum of strongly deformed nuclei.

EFFECT OF DISCRETE STRUCTURE OF A SINGLE-PARTICLE SPECTRUM ON THE THERMODYNAMIC FUNCTIONS OF NUCLEI

A.V. Ignatyuk, Yu.N. Shubin

(Submitted to Jadernaja Fizika)

The authors calculate the thermodynamic characteristics of excited nuclear states using a single-particle spectrum of Nilsson potential. They discuss the effect of pair correlations on the excitation energy dependence of the thermodynamic functions of nuclei. The results of the calculations describe fairly well the experimental data on the density of excited nuclear states over a broad range of mass numbers. Table 1 compares the experimental [1] and calculated entropy values for a number of nuclei.

[1] A.V. Malyshev, Zh. eksp. teor. Fiz. 45 (1963) 316

Table 1

Element	A	B_n MeV	a MeV^{-1}	$\delta_{expt.}$ MeV	$S_{expt.}$	$S_{theor.}$	$E^{cond.}$ MeV	$T_{crit.}$ MeV
Cr	54	9,72	7,40	2,81	14,3	14,9	4,92	0,74
Fe	58	10,05	6,75	3,11	15,8	16,0	4,45	0,73
Ni	62	10,59	7,55	3,28	14,9	16,0	2,60	0,68
Zn	68	10,20	9,05	3,08	16,2	16,4	2,54	0,72
Sr	88	11,09	9,40	2,93	17,5	17,0	0,68	0,73
Zr	92	8,63	11,4	2,13	17,2	17,2	2,69	0,71
Cd	112	9,05	17,6	2,79	21,0	19,2	3,27	0,67
Cd	114	9,06	17,8	2,87	21,0	19,4	4,72	0,66
Sn	116	9,50	15,3	2,48	20,7	18,5	2,56	0,64
Sn	118	9,36	15,6	2,82	20,2	18,7	3,86	0,64
Sn	120	9,11	14,3	2,81	19,0	18,6	4,57	0,63
Te	124	9,42	17,2	2,68	21,5	21,1	7,15	0,65
Te	126	9,10	16,6	2,65	21,1	20,9	6,90	0,63
Nd	144	7,81	16,9	2,36	19,2	20,8	3,74	0,55
Nd	146	7,58	18,6	2,19	20,0	21,6	4,45	0,54
Sm	148	8,12	20,0	2,39	21,4	23,0	4,42	0,55
Sm	150	8,01	23,3	2,72	22,2	23,2	4,67	0,54

B_n is the neutron binding energy, $\delta_{expt.}$ is the pairing energy used in determining the effective excitation energy, $U^* = B_n - \delta_{expt.}$ [1],

$S_{expt.}$ is the entropy value found from the experimental data on the density of neutron resonances, $S_{expt.} = 2\sqrt{aU^*}$,

$S_{theor.}$ is the calculated value using a pairing model,

$E_{cond.}$ is the calculated value for the condensation energy and

$T_{crit.}$ is the critical temperature.

DENSITY OF EXCITED STATES OF ODD NUCLEI

A.V. Ignatyuk

(Submitted to Jadernaja Fizika)

The author studies the possibility of taking into account the influence of an unpaired particle on the thermodynamic characteristics of the nucleus in the model involving pairing at non-zero temperature. For conversion to the simple model of non-interacting particles above the phase transition point it is necessary to introduce the effective energy of excitation:

$$U^* = U - E_{cond.}$$

Fig. 1 gives the results of calculations of the condensation energy $E_{cond.}$ for the simple and neutron components with a single-particle spectrum of the Nilsson model.

In analysing experimental data on the density of excited nuclear states the expression normally used for the effective excitation energy is [1]

$$U^* = U - \delta$$

Where $\delta = 0$ for the odd component and is equal to the pairing energy for the even component. The value of U obtained in this way does not correspond to that predicted by theory since δ differs appreciably from the condensation energy. From Fig. 1 it can be seen that δ corresponds rather to the difference between the condensation energies of the even and odd systems. Thus the way in which the experimental data on the level density parameter **a** are at present processed [1] does not correspond to a conversion to the parameter a of non-interacting particles but simply combines the families of curves of the parameter a for odd, even-even and odd-odd nuclei.

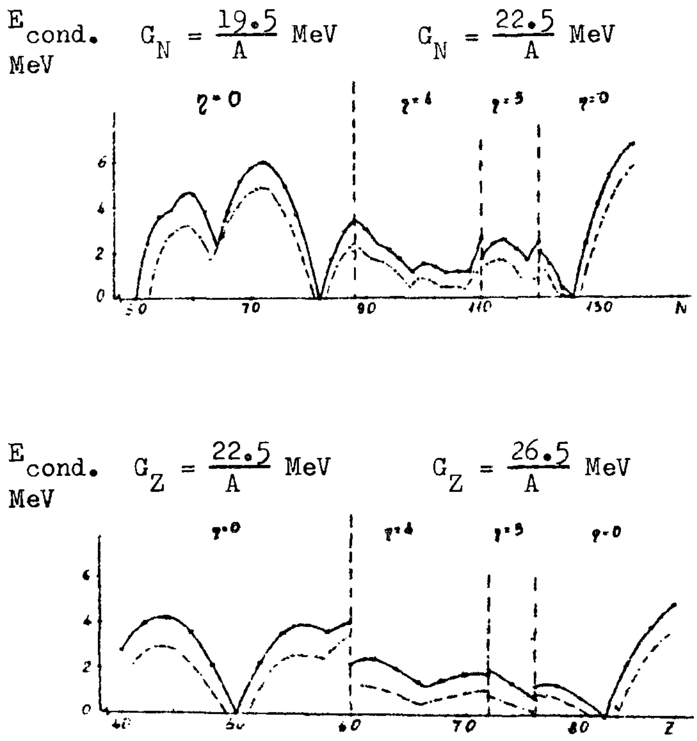

Fig. 1 Condensation energy for even *——* and odd ——·—— number of nucleons (η represents the deformation of the Nilsson potential).

[1] T. Ericson, Adv. in Phys., 9 425 (1960).

[2] A.V. Malyshev, Zh. eksp. teor. Fiz. 45 316 (1963).

[3] A. Gilbert, A. Cameron, Can. J. Phys., 43 1446 (1965).

[4] E. Erba et al., Nuovo Cim., 22 1256 (1961).

THERMODYNAMIC DESCRIPTION OF THE ENERGY SPECTRA OF ATOMIC NUCLEI

Yu.V. Sokolov, V.S. Stavinsky

Using the existing spectroscopic data the authors attempt to construct the thermodynamics of atomic nuclei from the (p,p') and (α,p) reactions. They analyse the functions of the state,

$$Z(\beta) = \sum_{k=0}^{\infty} \Omega_k e^{-\beta E_k} \quad (1)$$

Since experimental conditions do not furnish a complete energy spectrum (the number of levels observed is always finite) or the statistical weights of each level, and since some of the levels may be lost, the authors assessed the effect of different factors on a system with an equidistant spectrum in a thermostat.

In particular they assessed the way in which thermodynamic functions are affected by a spectral discontinuity at the k-th level, the loss of every n-th level in the spectrum and various types of degeneracy.

In the analysis of experimental spectra the effect of spectral discontinuity and loss of levels on the thermodynamic characteristics is taken into account using an independent Fermi particle model. It is shown that for nuclei of ^{41}Ca, ^{51}Cr, ^{55}Fe, ^{58}Fe, ^{59}Ni and ^{61}Ni the proportion of levels lost is about 10% and the remaining levels are sufficient to calculate $Z(\beta)$, if the temperature is not greater than 0.5 MeV.

In order to describe reasonably accurately the statistical properties of nuclei in the range of temperaturesobserved (T ~ 1 MeV) according to estimates made using an independent Fermi particle model, it is necessary to know the spectra of excited states over a wider energy range up to and including 20 MeV.

DENSITY OF LEVELS OF ATOMIC NUCLEI

Yu.N. Shubin

(Presented to the Anglo-Soviet Seminar on "Nuclear Constants for Reactor Computations", Dubna, 18-22 June 1968 (ASS-68/4))

The authors discuss the present state and future prospects of the statistical method for describing the density of nuclear levels, which determine the mean widths of various processes (radiation mean width, neutron mean width and fission mean width). They show that use of a model postulating virtually non-interacting particles and employing phenomenological means to take account of residual interaction (pairing) provides a satisfactory description of the available experimental data; by taking account of the detailed correlation between the fundamental parameter of level density theory (paramater a) and the shell structure, one can calculate this value with near-experimental accuracy in all cases of practical interest, including the fission fragment region. The authors propose a method for precise consideration of the thermodynamic properties of nuclei taking into account the discrete, degenerate spectrum of the shell model (Nilsson scheme) and present the corresponding results of numerical calculations both for a system of non-interacting particles and in a model taking into account pair correlations of the superconducting type.

EQUATION OF STATE OF AN INSULATED FERMI GAS

V.S. Stavinsky, Yu.N. Shubin

The authors study the equation of state of a Fermi gas in thermal insulation and show that if the number of particles is small, then at comparatively low excitation energies the equation of state of such a system may differ appreciably from the equation of state of a Fermi gas immersed in a thermostat.

ACTIVATION ANALYSIS WITH CHARGED PARTICLES - THE UNDERLYING NUCLEAR PHYSICS PRINCIPLES

N.N. Krasnov

The authors have obtained the basic formulas for the determination of impurities by activation analysis with charged particles. The formulas are based on use of the concept of isotope yield and an approximate expression for the path length of charged particles in matter [1].

When a material (M) contains an element (i) in the form of one of the components or as a homogeneous admixture, the activity of the isotope (k) formed from this element is given by the following formula:

$$^{k}N_{im} = {}^{k}B_i \eta_{im} \mathfrak{J} \frac{P_m}{P_i} \left(\frac{1 - e^{-\lambda_k t}}{\lambda_k} \right) \qquad (1)$$

where $^{k}N_{im}$ (in disintegrations per second) is the activity of the isotope (k) on completion of irradiation;

$^{k}B_i$ (in disintegrations per second per microampere-hour) is the yield of the isotope (k) when a thick target composed entirely of element (i) is irradiated;

η_{im} is the quantity of element (i) in the material (M) in terms of weight per cent;

P_M and P_i are coefficients proportional to the path length of particles in the material (M) and element (i);

$\mathfrak{J}$ (in microamperes) is the beam current;

t (in hours) is the irradiation time; and

λ_k (in hours) is the decay constant of isotope (k).

The values of the coefficients P for various elements are given in the table; they were calculated according to the formula:

$$P = \frac{A}{Z_A} I_A^{\frac{1}{4}} \qquad (2)$$

where A and Z_A are the mass number and relative charge of the irradiated element; and

I_A (in keV) is the effective ionization potential of the irradiated element.

Where the irradiated material consists of a number of elements, the coefficient P_Σ is determined by a method similar to the Bragg rule:

$$\frac{1}{P_\Sigma} = \frac{m_1}{P_1} + \frac{m_2}{P_2} + \dots + \frac{m_S}{P_S} \qquad (3)$$

where P_1 P_2 ... P_S are coefficients of the individual components; and

m_1 m_2 ... m_S are the quantities of the individual components as fractions of the total weight.

Formula (1) makes it possible to determine the amount of admixture η_{im} by the absolute method if the value of the isotope yield ${}^kB_i$ is known.

To determine impurities by the relative method, i.e. by comparison with a standard irradiated under exactly the same conditions as the material studied, the authors derived the following formula:

$$\eta_{im} = \eta_{i3} \frac{{}^kN_{im} P_3}{N_{i3} P_M} \qquad (4)$$

where η_{i3} is the quantity of the element (i) in the standard ($_3$) in terms of weight per cent;

${}^kN_{i3}$ is the activity of the isotope (k) in the irradiated standard; and

P_3 is a coefficient proportional to the path length of particles in the substance of which the standard is composed.

If experimental data on isotope yields are available, absolute determination of impurities is possible even when a single isotope is formed from the various elements making up the impurity. For example in the case of two elements (i) and (ell), from which a single isotope (k) is formed, formula (1) takes the following form:

$${}^kN_{(i+\ell)} = ({}^kB_i \eta_{im} \frac{1}{P_i} + {}^kB_\ell \eta_{\ell m} \frac{1}{P_\ell}) P_m \mathfrak{I} (\frac{1-e^{-\lambda_k t}}{\lambda_k}) \qquad (5)$$

By irradiating the material under investigation twice (at different yield values) we obtain a system of two equations with two unknowns (η_{im} and $\eta_{\ell m}$) which can be determined without difficulty.

In all the cases described above it was assumed that the thickness of the irradiated samples and standards exceeded the particle path length.

[1] M.Z. Maksimov, Zh. eksp. teor. Fiz. 37 (1959) 127.

Table 1

Values of coefficients $P = \frac{A}{Z_A} (I_A)^{\frac{1}{4}}$ for various elements

H	0,364	Ca	1,391	Y	1,832	Ce	2,126	Ir	2,345
He	0,833	Sc	1,502	Zr	1,844	Pr	2,111	Pt	2,357
Li	1,066	Ti	1,541	Nb	1,842	Nd	2,132	Au	2,356
Be	1,115	V	1,588	Mo	1,868	Pm	2,117	Hg	2,377
B	1,120	Cr	1,562	Tc	1,892	Sm	2,167	Tl	2,399
C	1,078	Mn	1,599	Ru	1,898	Eu	2,163	Pb	2,409
N	1,114	Fe	1,576	Rh	1,899	Gd	2,211	Bi	2,408
O	1,147	Co	1,615	Pd	1,930	Tb	2,209	Po	2,395
F	1,243	Ni	1,565	Ag	1,925	Dy	2,223	At	2,376
Ne	1,214	Cu	1,648	Cd	1,970	Ho	2,240	Rn	2,489
Na	1,231	Zn	1,650	In	1,985	Er	2,245	Fr	2,478
Mg	1,265	Ga	1,716	Sn	2,020	Tu	2,243	Ra	2,490
Al	1,324	Ge	1,743	Sb	2,041	Yb	2,272	Ac	2,479
Si	1,298	As	1,758	Te	2,106	Lu	2,273	Th	2,512
P	1,358	Se	1,809	J	2,065	Hf	2,295	Pa	2,481
S	1,330	Br	1,790	Xe	2,105	Ta	2,300	U	2,534
Cl	1,402	Kr	1,837	Cs	2,102	W	2,313	Np	2,502
Ar	1,509	Rb	1,835	Ba	2,141	Re	2,318	Pu	2,535
K	1,414	Sr	1,843	La	2,136	Os	2,344		

^{13}N, ^{11}C AND ^{18}F YIELDS FOR THE DETERMINATION OF CARBON AND OXYGEN IMPURITIES BY ACTIVATION ANALYSIS WITH CHARGED PARTICLES (p, d, ^{3}He, α)

N.N. Krasnov, P.P. Dmitriev, Z.P. Dmitrieva,
I.O. Konstantinov and G.A. Molin

The authors obtained experimental data for the dependence of ^{13}N, ^{11}C and ^{18}F yield on the bombarding particle energy when thick carbon and oxygen targets are exposed to protons, deuterons, ^{3}He ions and alpha particles. The samples were irradiated in the external beam of the 1.5-m cyclotron at the Physics and Power Engineering Institute of the USSR State Committee on the Utilization of Atomic Energy, which is capable of accelerating protons and deuterons to ~22 MeV, ^{3}He ions to ~30 MeV and alpha particles to ~44 MeV. The particle energy was varied by means of retarding foils. The total error in the determination of yield is ± 10%. Yield is given in disintegrations per second per microampere-hour (disintegrations/sec.μA.hr). On the basis of the data obtained it can be concluded that all four types of particles ensure high isotope yields and consequently high sensitivity in activation analysis.

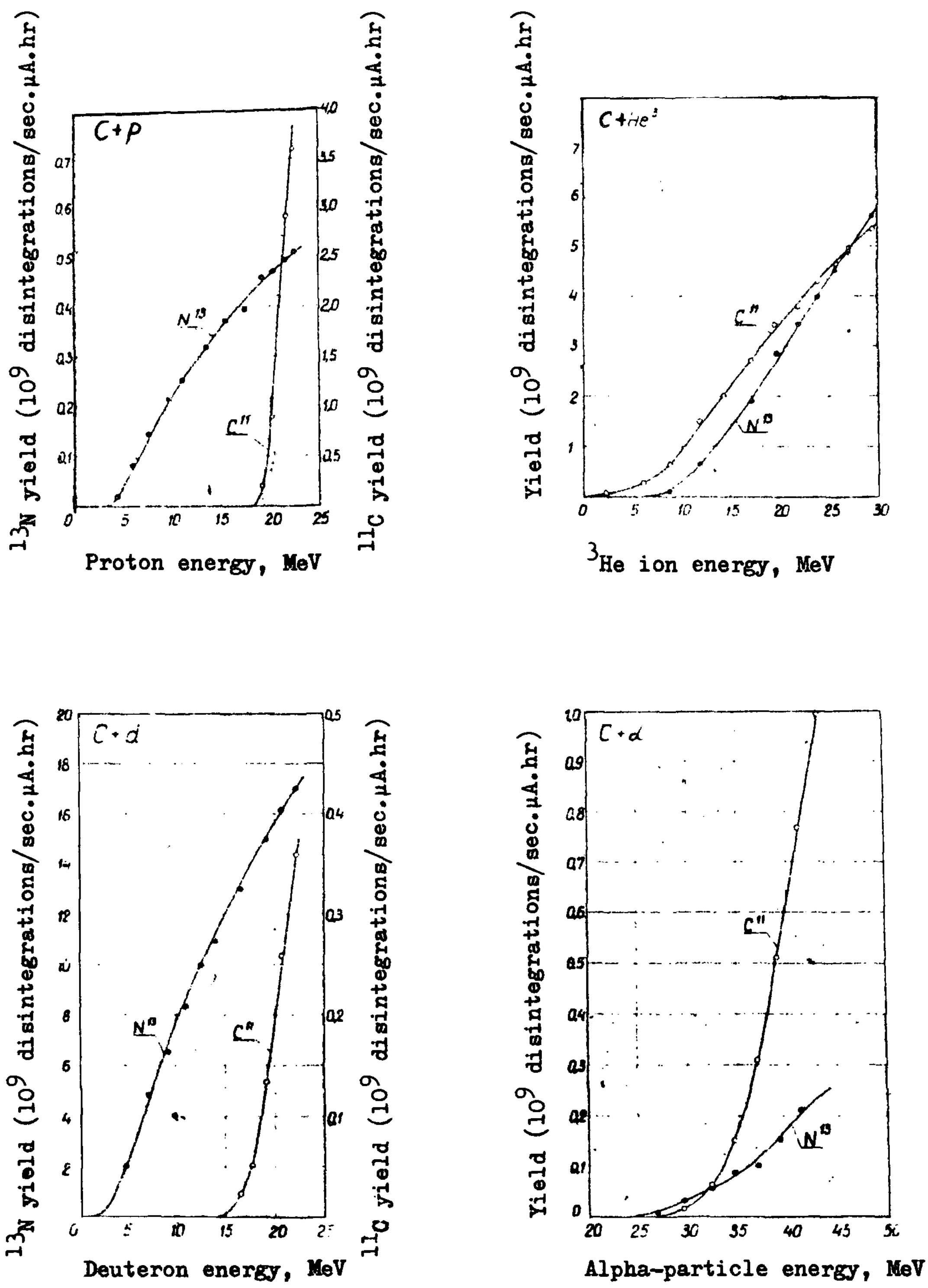

Fig. 1 ^{13}N and ^{11}C yields when carbon is exposed to protons, deuterons, ^{3}He ions and alpha particles.

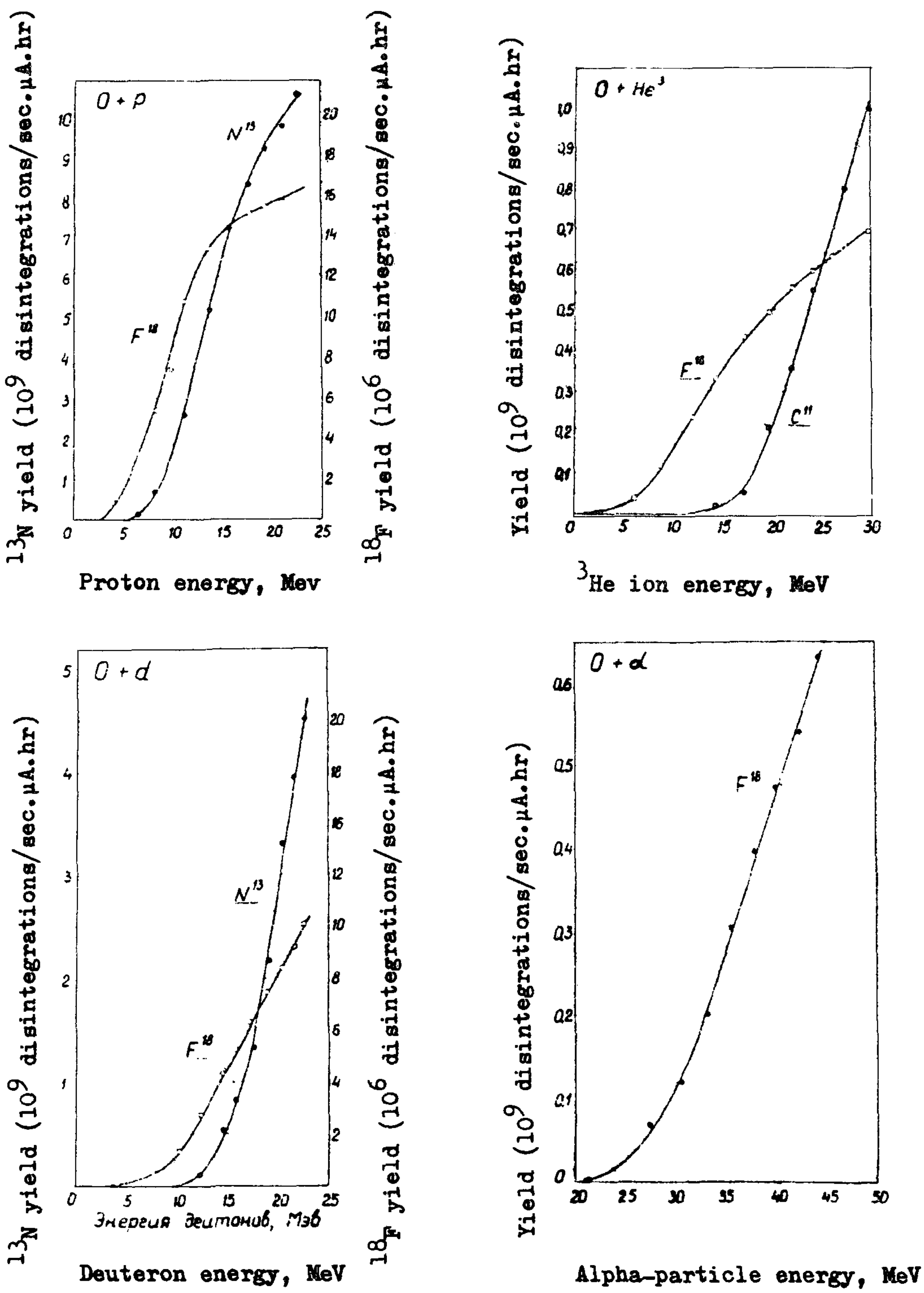

Fig. 2 ^{13}N, ^{11}C and ^{18}F yields when oxygen is exposed to protons, deuterons, ^{3}He ions and alpha particles.

CYCLOTRON PRODUCTION OF ^{151}Gd AND ^{153}Gd

N.A. Konyakhin, I.O. Konstantinov, P.P. Dmitriev,
N.N. Krasnov, V.M. Tuev

(Submitted to Atomnaja Energija)

The cyclotron at the Institute of Physics and Power Engineering has been equipped with a special target of pure metallic europium for the production of ^{151}Gd and ^{153}Gd by the (p,n) and (d,2n) reactions. The physical yield for such a target is 30% greater than with the Eu_2O_3 targets used by other investigators [1].

By irradiating thin foils of metallic europium sandwiched in between layers of copper foil in the manner described in [2], the authors have obtained the excitation functions for the nuclear reactions $^{151}Eu(d,2n)^{151}Gd$ and $^{153}Eu(d,2n)^{153}Gd$, together with the corresponding yield curves. The cross-section and yield values, which are subject to errors of ± 20%, are shown in Table I. The excitation functions and yield curves are shown in Figs 1 and 2.

Table I

Cross-sections of (d,2n) reactions

Deuteron energy (MeV)	Reaction cross-section, mb	
	$^{151}Eu(d,2n)^{151}Gd$	$^{153}Eu(d,2n)^{153}Gd$
21,2	115	117
19,5	148	144
18,1	168	187
16,7	235	233
15,3	300	295
13,6	296	305
11,8	226	260
9,8	128	180
7,4	46	68
4,1	5	3

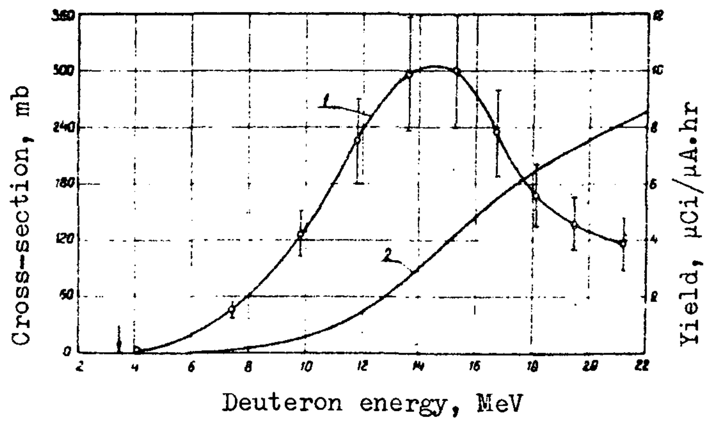

Fig. 1 Excitation function of the $^{151}Eu(d,2n)^{151}Gd$ reaction [1] and ^{151}Gd yield curve for a thick target

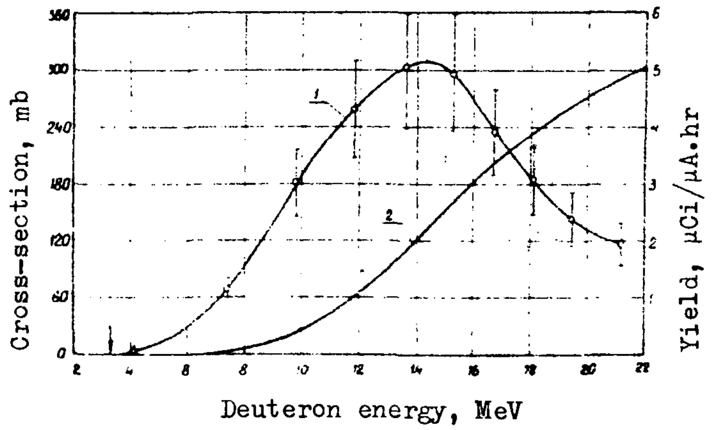

Fig. 2 Excitation function of the $^{153}Eu(d,2n)^{153}Gd$ reaction [1] and ^{153}Gd yield curve for a thick target

[1] S. Bjornholm, P.H. Dam, H. Nordby, N.O. Roy Poulsen, Nucl. Instr. and Methods 5 (1959) 196.

[2] P.P. Dmitriev, I.O. Konstantinov, N.N. Krasnov, Atomnaja Energija 22 (1967) 310.

PROPAGATION OF RESONANCE NEUTRONS IN HOMOGENEOUS MEDIA: THEORY AND SPECIAL FUNCTIONS

L.P. Abagyan, F.F. Mikhailus,
M.N. Nikolaev, V.V. Orlov

(Presented at the Anglo-Soviet Seminar on "Nuclear Constants for Reactor Computations", Dubna, 18-22 June 1968 (ASS-68/23))

In fast reactors resonance effects have a marked influence not only on the size of the absorption cross-section but also the moderating capacity of the medium and its diffusion characteristics.

This fact, together with the complexity and multiplicity of forms of neutron spectra in fast reactors, has necessitated the formulation of a detailed theory for neutron propagation in media with resonance cross-sections, based on consideration of a rigorous kinetic equation (since in fast reactor computations it is often impossible to confine oneself to the diffusion approximation).

This theory is set out in the first part of this work. It results in a kinetic equation for neutron flux averaged over a large number of resonances in which the cross-sections smoothed out in a given manner over the resonances figure as neutron-physics constants of the medium.

The authors also discuss various approximations in which these cross-sections can be expressed in the form of more or less simple functions of resonance parameters. They show that such cross-sections can be obtained for a wide class of cases provided one has some means of establishing the factors determining resonance self-screening of the cross-sections, which are functions of three parameters, α, ξ, φ.

$$\alpha = \sigma_{ro} / (\sigma_p + \tilde{\sigma})$$

where $\sigma_{ro} = 4\pi\bar{\lambda}^2 g \dfrac{\Gamma_n^0}{\Gamma}$,

σ_p is the potential scattering cross-section and

$\tilde{\sigma}$ is the aggregate mean total cross-section of all other components of the medium, related to a single atom of the given element with resonance cross-section.

$$\xi = \Gamma/\Delta,$$

where $\Delta = 2\sqrt{\dfrac{E_o kT}{A}}$

$\cos\varphi$, where φ is the phase of potential scattering coherent with resonance scattering.

The second part of the work describes how these coefficients are determined and computed. It also contains information on use of the results of the computations, these results being presented in both graph and tabular form.

SUB-GROUP SYSTEM OF CONSTANTS

M.N. Nikolaev, F.V. Khokhlov

(Presented at the Anglo-Soviet Seminar on "Nuclear Constants for Reactor Computations", Dubna, 18-22 June 1968 (ASS-68/10))

The authors describe a method of calculating sub-group constants on the basis of information concerning the resonance structure of the cross-section set out in the form of the self-screening coefficients presented in [1].

Sub-group constants are adduced for those elements and those groups for which self-screening coefficients are given, i.e. in those cases where resonance effects are considerable.

The sub-group constants obtained may be used not only for the sub-group method.

Sub-group representation of a system of group constants make it possible to determine the macroscopic constants of the system without recourse to interpolation in regard to the "dilution cross-section" and temperature (if there is temperature dependence), which makes the group constants system described in [1] more convenient to use.

[1] L.P. Abagyan, N.O. Bazazyants, I.I. Bondarenko, M.N. Nikolaev "Group constants for nuclear reactor computations" (in Russian) Moscow, Atomizdat, 1964.

MEASUREMENT OF THE STRUCTURE OF TOTAL NEUTRON CROSS-SECTIONS

V.V. Filippov, M.N. Nikolaev

(Presented at the Anglo-Soviet Seminar for "Nuclear Constants for Reactor Computations", Dubna, 18-22 June 1968. (ASS-68/17))

The authors processed the results of measurements of transmission functions for twenty elements from beryllium to uranium in the energy range from tens of keV to several MeV.

The transmission functions

$$T(t) = \int_{\Delta E} f(E) \exp(-\sigma_{tot}(E) n t) dE \qquad (1)$$

were measured up to attenuation factors of 10^{-3} to 10^{-4}; the divergence from the exponential law was a measure of the structure of the total cross-section in the neutron energy band studied ΔE_n. In order to determine the characteristics of the strucutre the measured transmission functions $T(t)$ were described as a superposition of weighted exponents using the least squares method:

$$T(t) = \sum_{i=1}^{n} a_i \exp(-\sigma_{tot}^{i} n t) \qquad (2)$$

As a rule it was sufficient in equation (2) to take two exponents; in only a few cases was it necessary to take into account the contributions of three exponents.

The total cross-section structure characteristics found in this manner a_i and σ_i are parameters of the distribution function of the total cross-section, given in histogram form:

$$\frac{dP(\sigma_{tot})}{d\sigma_{tot}} = \sum_{i=1}^{n} a_i \delta(\sigma_{tot} - \sigma_{tot}^{i})$$

MEAN CHARACTERISTICS OF THE CAPTURE-TO-FISSION PROBABILITY RATIOS IN THE RESONANCE AND EPI-RESONANCE REGION

L.P. Abagyan, N.S. Rabotnov, L.N. Usachev

(Presented at the Anglo-Soviet Seminar for "Nuclear Constants for Reactor Computations", Dubna, 18-22 June 1968. (ASS-68/2))

The authors discuss the influence of fluctuations in partial widths relative to the mean values on the (varyingly averaged) probability ratios of radiative capture and fission. They investigate the values $\alpha = \langle\sigma_\gamma\rangle/\langle\sigma_f\rangle$, $\alpha_\eta = \langle\nu\rangle/\langle\eta\rangle - 1$, $\langle\alpha\rangle = \langle\sigma_\gamma/\sigma_f\rangle$ and $\bar{\alpha} = \bar{\Gamma}_\gamma/\bar{\Gamma}_f$ and the relation between them and show that there is a system of inequalities $\langle\alpha\rangle > \alpha_\eta > \alpha > \bar{\alpha}$. On the basis of the known resonance parameters of ^{239}Pu they calculate the energy dependence of $\alpha(E)$ in the range $10^2 - 3 \times 10^4$ eV taking into account these effects and also the effect of fluctuation of the mean fission and neutron widths when the neutron energy is varied.

CALCULATION OF BREMSSTRAHLUNG ON THICK TARGETS

A.S. Soldatov, G.N. Smirenkin

(Presented at the Anglo-Soviet Seminar on "Nuclear Constants for Reactor Computations", Dubna, 18-22 June 1968 (ASS-68/2))

The gamma spectra of forward Bremsstrahlung for photon energies $E\gamma$ = (4 - 10) MeV and limiting Bremsstrahlung spectrum energies E_{max} = (4.5 - 10) MeV from a tungsten target of thickness t = 0.3 of the radiation length (1 mm) were calculated in the manner proposed by Lowson [1] for targets with low Z and $t < 0.15$ of the radiation length. The desired spectrum σ^{thick}_{Brems} is represented as the sum of the spectra from the layers of the target taken with particular weights $W_n = \ell_n\, 950\, t_n - \ell_n\, 950\, t_{n-1}$ (n is the number of the target layers, t_n is the aggregate thickness of n layers of the target in radiation lengths).

$$\sigma_{Brems}^{thick} = \sum_{1}^{N} W_n \; \sigma_{Brems} \; (T_n, E_\gamma),$$

where N is the total number of target layers,

σ_{Brems} is the Bremsstrahlung spectrum integrated over all photon emission angles and

T_n is the kinetic energy of electrons which have reached the n-th layer, which depends on t_n.

In the calculation it was assumed that $T_n = T_o - (- \frac{dT}{dt})_{ion} t$,

where T_o is the initial kinetic energy of the electrons and

$(- \frac{dT}{dt})_{ion}$ represents the ionization losses of energy by an electron which, for Eγ = (4 - 10) MeV, are taken to be equal to $7.75 \frac{\text{MeV}}{\text{Rad. length}}$.

Using the method described, calculations were carried out for tungsten target thicknesses t = 3 mm, 0.25 mm and 0.125 mm and E_{max} = 9.65 MeV and 4.5 MeV, for which there are experimental data on the form of the photon spectra [2]. The agreement between the calculated and experimental results is fully satisfactory up to Eγ = 2.0 MeV. Table 1 shows the values of $E\gamma \cdot \sigma_{Brems}^{thick}$ for tungsten targets with t = 1 mm in relative units.

[1] Lowson, J., Nucleonics, 10 61 (1952).

[2] Starfelt, Koch, Phys. Rev., 102 1958 (1956).

E_{max}, MeV

Eγ MeV	4.50	4.75	5.00	5.25	5.50	5.75	6.00	6.25	6.50	6.75	7.00	7.25	7.50	7.75	8.00	8.25	8.50	8.75	9.00	9.25	9.50	9.75	10.00
4.00	3,163	4,281	5,247	6,198	6,881	7,788	8,490	9,181	9,311	10,07	10,88	11,09	11,40	12,21	12,60	13,06	13,50	13,61	13,94	14,23	14,51	14,77	15,02
4.25	1,900	3,136	4,227	5,200	6,096	6,918	7,640	8,644	9,083	9,602	10,25	10,70	11,21	11,60	12,05	12,49	12,70	13,14	13,46	13,75	14,02	14,31	14,67
4.50	0,444	1,884	3,115	4,196	5,167	6,041	6,842	7,418	8,320	8,997	9,601	10,18	10,63	11,09	11,51	11,91	12,28	12,61	12,96	13,24	13,57	13,85	14,12
4.75		0,637	1,867	3,098	4,160	5,104	6,000	6,814	7,561	8,268	8,923	9,517	10,08	10,53	10,98	11,39	11,78	12,15	12,49	12,88	13,18	13,42	13,69
5.00			0,481	1,893	3,079	4,144	5,104	5,978	6,771	7,511	8,203	8,835	9,443	9,965	10,46	10,88	11,20	11,67	12,03	12,41	12,69	12,99	13,24
5.25				0,425	1,844	3,056	4,125	5,078	5,961	6,755	7,466	8,151	8,796	9,375	9,801	10,36	10,79	11,18	11,67	11,92	12,25	12,51	12,86
5.50					0,480	1,821	3,040	4,106	5,083	5,918	6,690	7,424	8,109	8,742	9,314	9,825	10,29	10,72	11,11	11,48	11,82	12,15	12,46
5.75						0,416	1,818	3,027	4,088	5,034	5,888	6,660	7,391	8,044	8,695	9,268	9,765	10,22	10,64	11,03	11,38	11,74	12,06
6.00							0,527	1,808	3,016	4,073	4,015	6,848	6,644	7,399	8,027	8,552	9,074	9,718	10,16	10,37	10,91	11,32	11,65
6.25								0,407	1,709	3,002	4,058	4,997	5,811	6,617	7,318	7,998	8,614	9,171	9,665	10,11	10,52	10,90	11,25
6.50									0,449	1,790	2,992	4,018	4,948	5,829	6,505	7,304	7,868	8,570	9,134	9,620	10,06	10,46	10,85
6.75										0,399	1,723	2,988	4,000	4,867	5,848	6,578	7,200	7,915	8,540	9,096	9,580	10,01	10,41
7.00											0,396	1,776	2,978	4,002	4,956	5,793	6,556	7,259	7,910	8,510	9,064	9,544	9,977
7.25												0,393	1,769	2,964	4,012	4,948	5,770	6,539	7,239	7,888	8,493	9,043	9,511
7.50													0,390	1,763	2,956	4,003	4,931	5,765	6,524	7,221	7,867	8,449	9,008
7.75														0,383	1,787	2,949	3,994	4,921	5,755	6,510	7,205	7,848	8,448
8.00															0,385	1,762	2,942	3,986	4,911	5,762	6,487	7,180	7,831
8.25																0,383	1,747	2,906	3,978	4,902	5,712	6,485	7,176
8.50																	0,380	1,742	2,925	3,971	4,894	5,722	6,474
8.75																		0,378	1,741	2,924	3,866	4,886	5,719
9.00																			0,376	1,735	2,919	3,958	4,879
9.25																				0,375	1,729	2,919	3,958
9.50																					0,373	1,725	2,909
9.75																						0,371	1,721
10.00																							0,369

TWO-LEVEL ANALYSIS OF THE FISSION CROSS-SECTION OF PLUTONIUM-239 IN THE RESONANCE REGION

A.A. Lukyanov, A.V. Ignatyuk, V.P. Lunev

(Presented at the Anglo-Soviet Seminar on "Nuclear Constants for Reactor Computations", Dubna, 18-22 June 1968. (ASS-68/3))

The marked influence of interference effects on the energy structure of the plutonium-239 cross-section in the resonance region is responsible for the wide use made of multilevel systems of calculation for purposes of analysis. As a rule, the computational systems are based on use of the results of R-matrix theory, which makes it possible to find parameters for the observed cross-sections using a set of energy-dependent parameters; however, the number of these parameters is normally very large, which makes the task of practical analysis very cumbersome, and, what is more, ambiguous. For this reason multilevel computations are carried out using certain simplifying assumptions regarding the resonance parameters. In most work these assumptions relate either to the number of fission channels (which is assumed to be small) or to the energy dependence (the cross-section being represented as the sum of single-level contributions and a particular cross-section value - constant as between each pair of levels - corresponding to interference effects). In this work the authors use a two-level description of the energy dependence of the cross-section between two observed maxima with a given value of total momentum J. The contribution of the remaining levels is taken into account approximately. In addition to the ordinary parameters of single-level analysis - the resonance widths for the individual channels Γ_{λ_c} and the position of the level E_λ - the authors determine the so-called "transverse fission width" $\Gamma_{\lambda\lambda'f}$, which represents the sum of the products of the fission width amplitudes of the two levels in question in each channel available for fission. The corresponding value for radiation channels is assumed to be zero.

The programme for finding the parameters uses the least-squares method. The analysis that is made of the experimental data presented in other papers points to the advantages of a two-level description by comparison with other multilevel systems, especially in the vicinity of the interference minima region.

EFFECT OF FLUCTUATION IN PARTIAL WIDTH ON THE COMPETITION BETWEEN FISSION AND INELASTIC SCATTERING

N.S. Rabotnov

(Submitted to Jadernaja Fizika)

If account is taken of the fluctuation in fission and neutron widths relative to the mean values, this may in certain cases have a qualitative effect on the results of analysis of the energy dependence of the fission cross-section in threshold elements. In the sub-threshold region, near the inelastic scattering level, the following approximate relationships hold good:

$$\left\langle \frac{\Gamma_n \Gamma_f}{\Gamma_n + \Gamma_{n'}} \right\rangle = \frac{\bar{\Gamma}_f}{1 + \sqrt{r}} \; ; \; \left\langle \frac{\Gamma_n \Gamma_{n'}}{\Gamma_n + \Gamma_{n'}} \right\rangle = \frac{r\,\bar{\Gamma}_n}{(1 + \sqrt{r})^2} \; ; \quad r = \frac{\bar{\Gamma}_{n'}}{\bar{\Gamma}_n}$$

In consequence, at low values of r inelastic scattering has a much more marked competitive effect on the fission cross-section than should be expected from the observed inelastic scattering excitation functions.

$\bar{\nu}$ IN THE SPONTANEOUS FISSION OF ^{242}Pu

L.I. Prokhorova, G.N. Smirenkin, Yu.M. Turchin

(Submitted to Atomnaja Energija)

The values published more than ten years ago for the mean number of prompt neutrons $\bar{\nu}$ per spontaneous fission of ^{242}Pu differ appreciably from each other:

2.11 ± 0.09 [1] and 2.43 ± 0.16 [2]

A knowledge of the value of $\bar{\nu}$ for one of the heaviest plutonium isotopes is of major importance in investigating the dependence of $\bar{\nu}$ on the atomic weight A. The idea that $\bar{\nu}$ is linearly dependent on A, as proposed in [2], has been fairly widely accepted, but calculations of $\bar{\nu}$ based on the fission-energy balance [3] reveal a more complex dependence of $\bar{\nu}$ on the A and Z of the fissioning nucleus.

For measuring $\bar{\nu}$ in the spontaneous fission of ^{242}Pu the authors employ a pulse coincidence counting technique using a neutron detector (12 counters with ^{3}He in a paraffin block) and an ionizing chamber placed inside the detector to record fission involving the substance under investigation.

The $\bar{\nu}$ value for ^{242}Pu was measured in relation to that for the spontaneous fission of ^{244}Cm.

The ratio of $\bar{\nu}$ for ^{242}Pu to that for ^{244}Cm, as measured in this experiment, was 0.737 ± 0.014. Taking the $\bar{\nu}$ of ^{244}Cm to be 2.71 ± 0.04 [4] we obtain for ^{242}Pu $\bar{\nu}$ = 2.13 ± 0.05.

Thus the results of this work support the data reported in [1] and the consequences of the calculations in [3] regarding the dependence of $\bar{\nu}$ on A.

[1] D.A. Hicks, J. Ise, Jr., R.V. Pyle, Phys. Rev. 101 (1956) 1016.

[2] W.W.T. Crane, G.H. Higgins, H.R. Bowman, Phys. Rev. 101 (1956) 1804.

[3] I.I. Bondarenko, B.D. Kuzminov, L.S. Kutsaeva, L.I. Prokhorova, G.N. Smirenkin, Paper presented to the Second United Nations International Conference on the Peaceful Uses of Atomic Energy 15 (1958) 353.

[4] V.I. Bolshov, L.I. Prokhorova, V.N. Okolovich, G.N. Smirenkin, Atomnaja Energija 17 (1964) 28.

FISSION CROSS-SECTION OF ^{209}Bi, ^{235}U, ^{238}U, ^{237}Np AND ^{239}Pu FOR 1-9 GeV PROTONS

E.S. Matusevich, V.I. Regushevsky

The fission cross-sections σ_f were measured on the beam of the Joint Institute for Nuclear Research's proton-synchrotron using **glass detectors.**

	Cross-section in barns					Relative units
Ep, GeV	^{209}Bi	^{238}U	^{235}U	^{237}Np	^{239}Pu	^{233}U
1,0	0,26±0,03	0,70±0,07	0,76±0,08	1,12±0,12	1,14±0,12	1,0
2,0	0,24±0,03	0,71±0,07	0,71±0,07	0,93±0,10	0,91±0,10	0,78
5,0	0,26±0,03	0,58±0,06	0,59±0,06	0,80±0,08	0,69±0,07	0,67
9,0	0,25±0,03	0,55±0,06	0.60±0,06	0,79±0,08	0,68±0,07	0,65

STATISTICAL DESCRIPTION OF FISSION PRODUCT YIELDS

A.V. Ignatyuk

(Submitted to Jadernaja Fizika)

The shell correction method developed recently [1] seems sufficiently reliable not only for calculating the energy of nuclei with non-equilibrium deformation but also for the purpose of extrapolation to the region of strongly deformed nuclei. Calculations of the density of excited states of nuclei in the superfluid nucleus model using the single-particle spectrum of the shell model [2] can be used to investigate the dependence of the density of the excited states of nuclei on their deformation. Use of these methods of calculation to investigate the fission-fragment mass region makes it possible to adhere to a purely statistical approach [3] in describing the basic characteristics of fission fragment yields. The mass and charge yields and distribution of the mean kinetic energies of fragments of a given mass were calculated for ^{236}U (Fig. 1).

[1] V.N. Strutinsky, Nucl. Phys. A 95 (1967) 420.

[2] A.V. Ignatyuk, Yu.N. Shubin, Report to the Eighteenth Conference on Nuclear Spectroscopy, Riga (1968).

[3] P. Fong, Phys. Rev. 102 (1956) 434.

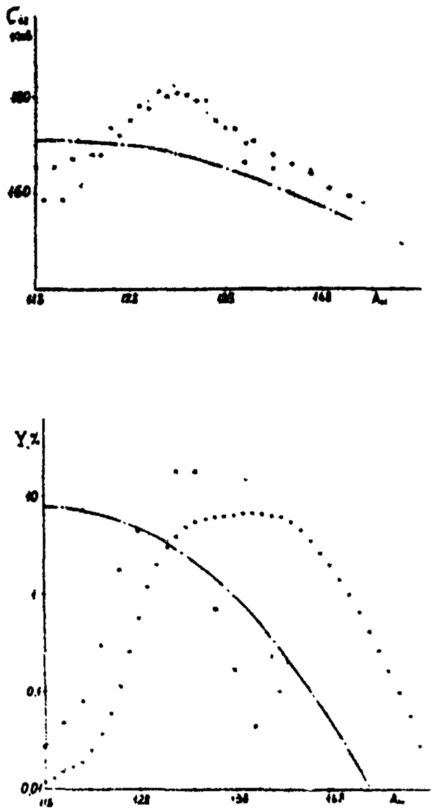

Fig. 1 Mean kinetic energies and mass yield of ^{236}U

—— • —— Liquid-drop calculations

x x x Calculations taking into account the effect of shell structure on the energy and density of excited states of fragments

• • • Experimental data on the thermal fission of ^{235}U (n,f)

ANGULAR ANISOTROPY OF NEUTRON-INDUCED FISSION OF ^{238}U NEAR THE THRESHOLD

G.N. Smirenkin, Kh.D. Androsenko

(Submitted to Pisma Zh. eksp. teor. Fiz.)

The authors present the results of detailed studies of the angular distribution of ^{238}U fission fragments resulting from fission induced by 0.8-3.4 MeV neutrons. The fragments were recorded by means of the fission-track technique (glass detectors).

The experimental data are given in compact form in Fig.1. This figure demonstrates the good agreement between the experimental results and the formula used in the Strutinsky-Halpern statistical theory

$$W(\vartheta) \sim \mathrm{Sin}^{-3}\vartheta \int_0^{p\mathrm{Sin}^2\vartheta} x^{\frac{1}{2}} e^{-x}\, I_0(x)dx = \mathrm{Sin}^{-3}\vartheta\ \varphi(p\mathrm{Sin}^2\vartheta) \qquad (1)$$

where $p = \frac{\bar{I}^2}{2\varkappa_0^2}$ ($\varkappa_0^2$ denotes the distribution width of $\varkappa$, $F(\varkappa) \sim e^{-\frac{\varkappa^2}{2\varkappa_0^2}}$

The way in which the experimental data are presented in Fig.1 makes use of the fact that the ratio

$$\frac{W(0^o)}{W(\vartheta)} = \frac{2(p\mathrm{Sin}^2\vartheta)^{3/2}}{3\varphi(p\mathrm{Sin}^2\vartheta)}$$

depends on the single parameter $x = p\cdot\mathrm{Sin}^2\vartheta$.

Investigation of 18 angular distributions (for the most part in the region where there is a precipitous drop in the fission cross-section σ_f) revealed the exceptional stability of the form $W(\vartheta,E)$ and its correspondence to the statistical distribution $F(\varkappa)$ not only around the threshold but in the sub-barrier energy region. The fission behaviour of ^{238}U below the threshold at 0.5-0.7 MeV is consistent with a large number of channels taking part in the fission. This effect, which is surprising from the point of view of generally accepted concepts, is susceptible of explanation in the light of the new concept of a "two-peaked" barrier [2].

[1] V.M. Strutinsky, I. Halpern, Report to the Second Geneva Conference P/1513 (1958).

[2] V.M. Strutinsky, Nucl. Phys. A 95 (1967) 420.

[3] Neutron Cross-Sections, BNL-325, Suppl. 2.

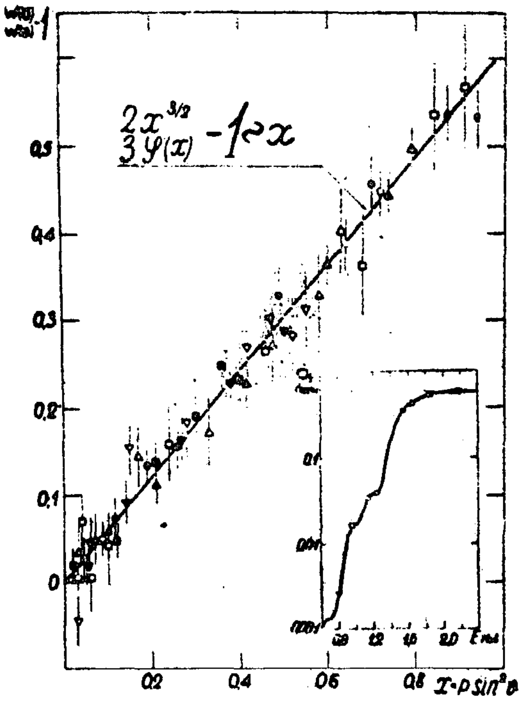

Fig. 1 Comparison of experimental data on W(ϑ) with formula (1) dreived from the statistical theory of angular distributions of fission fragments. The insert shows the energy dependence of the neutron-induced fission cross-section $\sigma_f(E)$ of ^{238}U [3]

Legend:

▽	0.8 MeV	□	0.95 MeV	△	1.15 MeV
O	1.25 MeV	●	1.55 MeV	▲	1.65 MeV
■	1.85 MeV	▼	2.2 MeV		

I.V. Kurchatov Atomic Energy Institute*

s AND p LEVELS OF ^{120}Sn

G.V. Muradyan, Yu.G. Shchepkin,
Yu.V. Adamchuk, M.G. Arutyunov

(Presented at the Anglo-Soviet Seminar on Nuclear Constants for Reactor Computations, Dubna, 18-22 June 1968 (Paper No. ASS-68/14))

The authors report on measurements on the identification and determination of the parameters of s and p levels of ^{120}Sn. The levels were identified by the moving-sample method [1]. The level parameters were determined from measurements of total cross-sections, capture cross-sections and self-indication. It may be noted that previous investigations of ^{120}Sn [2] with a resolution approximately four times worse than in the present work resulted in a value of $S_0 \approx 0.1 \times 10^4$, which is approximately ten times less than the value predicted by the optical model.

Since, generally speaking, tin isotopes fall outside the scheme of the optical model, these discrepancies could be explained on the assumption that by virtue of some specific property of these nuclei, for example the presence of proton magic, the imaginary part of the optic potential for certain tin isotopes is anomalously small.

Another, more verisimilitudinous explanation of the experimental data on the S_0 strength function, which has been advanced by Feshbach, Block and Shakin [3], consists in the assumption that in the formation of a compound nucleus a large role is played by incoming three-quasi-particle states. The probability of the appearance of three-quasi-particle states varies non-monotonously from nucleus to nucleus, so that the strength function may also be non-monotonous. The question arises whether it is possible to provide experimental refutation or support for any of these explanations.

This can be done by determining together with the S_0 strength function the S_1 strength function, which corresponds to a neutron p-wave. If, for example, we assume that in the case of tin the imaginary part of the optic potential is for some reason or other lowered, then in this region of atomic

---

* Edited by Yu.V. Adamchuk.

weights it is not only the S_0 value which should be low but also the the S_1 value. If experiments show that for a given nucleus S_0 is lowered but S_1 is not lowered, then the assumption that the imaginary part of the optic potential is small does not hold good.

In order to measure the S_1 strength function it is necessary to identify the levels excited by neutrons with $\ell = 0$ and $\ell = 1$ (s and p levels).

These measurements were performed on the Institute's linear electron accelerator by the time-of-flight method. The duration of the accelerator pulse was 0.2 μsec, the pulse current 0.5 A, the pulse frequency 244 Hz and the energy of the accelerated electrons 25 MeV. The samples used in all measurements were enriched to more than 97% in ^{120}Sn.

Identification of the s and p levels was performed on an orbital angular momentum selector [1]. Neutron capture in a sample of the substance studied was recorded by means of a detector placed at a distance of 37 m from the accelerator target. The sample velocity was 35 m/sec. The detector consists of 2 NaI(Tl) crystals 200 x 100 mm in diameter shielded on the side of the sample by a 3.5-cm thickness of ^{10}B.

The external shielding made it possible to reduce the background considerably and so increase the range of measurements up to about 4 keV. Reduction of neutron background is particularly important when carrying out measurements to identify levels by the orbital angular momentum method owing to the necessity of using thick samples in the detector and for transmission.

The optimum choice of sample thickness for transmission $n_T = 0.0487$ at./b and in the detector $n_D = 0.014$ at./b was determined on the basis of those weak resonances (365.2 eV and 1288 eV) for which it is still possible to carry out an identification in terms of ℓ with an acceptable measurement time.

In order to identify the level it is necessary to compare $\Delta A_{theor.}$ with $(\Delta A_{expt.} + \delta)$, where δ is the corresponding error. Here $\Delta A_{expt.}$ is the experimentally obtained difference between the areas $\sum_i N_i^+{}_{expt.}$ and $\sum_i N_i^-{}_{expt.}$ (or the difference between the number of counts as a function of channel number). The signs (−) and (+) correspond to series of measurements obtained when the sample is moved in the same direction as the neutron beam, (−) and in the opposite direction (+). $\Delta A_{theor.}$ is the value that may be theoretically expected for such difference, calculated on a computer with known level parameters and taking into account the Doppler effect and interference between potential and resonance scattering.

Obviously $\Delta A^{p}_{theor.} = 0$ for the p level and $\Delta A^{s}_{theor.} \neq 0$ for the s level. The error δ restricts the accuracy of the identification, resulting in a number of cases in an ambiguous determination of the orbital angular momentum of the bombarding neutrons. On the basis of δ it is possible to estimate the probability φ_s and φ_p of the level being s and p respectively. These probabilities are shown in Table 1.

Measurements of the total cross-section were carried out for a flight length of 109 m with a resolution of 3.8 nsec/m [4]. The samples used were 70 mm in diameter and the number of atoms was 0.0191 at./b, 0.0841 at./b and 0.1119 at./b.

The data from the analyser in the form of the number of counts as a function of channel number were printed out on punch cards and fed into a computer. Analysis was in two stages. At the first stage the data were corrected for counting losses resulting from the dead time of the recording apparatus. This error was less than 10%. The background was then subtracted and the resonance transmission calculated:

$$\exp\ (- n\sigma_t + n\sigma_{pot.}).$$

At the second stage energy intervals were selected for each resonance, within the limits of which the trough areas were calculated. The interval boundaries, the resonance energy and the trough areas were fed into the computer for the purpose of calculating the dependence $g\Gamma_n = f(\Gamma)$ (Γ being the total width of the level, g a statistical spin factor). This dependence was found by matching the theoretical area to the experimental, by means of varying $g\Gamma_n$ and Γ. The theoretical area was calculated on the basis of the Breit-Wigner formula, taking into account Doppler effect, the interference between the resonance and potential scattering and the neutron spectrometer resolution function. In order to find the errors in Γ and $g\Gamma_n$ the dependence $g\Gamma_n = f^*(\Gamma)$ was calculated simultaneously for a deflected value of the experimental area.

Measurement of the total cross-sections with a sufficiently large amount of the isotope ^{120}Sn made it possible to identify strong levels by their shape. The resonances at 9017 eV, 3128 eV and 951.2 eV were identified as s levels and the level at 1720 eV as a p level, which agrees with the results of identification on the orbital angular momentum selector.

The capture cross-section and self-indication measurements were carried out on a neutron spectrometer with a path length of 37 m and resolution of 12 nsec/m [5]. For recording the capture gamma rays the same detector was used as for identification of levels. The samples used in the measurements were 70 mm in diameter with $n_T = n_D = 0.00072$ at./b, 0.014 at./b and 0.0191 at./b.

The capture and self-indication curves were analysed using the known curves showing the dependence of area on level parameters, disregarding interference and resolution. The successive approximations method was used to include a correction to take account of capture subsequent to scattering.

Detector efficiency and neutron flux were calibrated over the parameters of a number of levels, determined from the total cross-section and self-indication measurements. The results of calibration show that the maximum variation in detector efficiency in the event of a transition from one resonance to another does not exceed ± 20%. This indeterminacy introduces a basic error into the capture measurements. In the self-indication measurements the main source of error is the statistical error (5 to 10%). For purposes of isotope identification, the total cross-sections and capture cross-sections of the remaining tin isotopes were measured.

To determine the level parameters the results of measurements of σ_t, σ_γ and σ_{tD} were analysed simultaneously. Fig. 1 gives an example of the determination of $g\Gamma_n$ and Γ. The parameters of 20 neutron resonances determined in this manner are shown in Table 1.

The energy region where a substantial percentage of the observed levels was identified comprises 4.3 keV. The majority of levels in this region are p levels and only two levels were identified with 100% probability as s levels. The p level at 1720 eV was found to have the compound nucleus spin I = 1. The radiation width Γ_γ was determined for five levels. The deviation $\Gamma_{\gamma i}$ from the mean value $\bar{\Gamma}_\gamma = 124 + 30$ lies for the most part within the error limits except for $\Gamma_\gamma = 202 + 20$ for the p level at 427.2 eV. Owing to the small number of levels and the large error in Γ_γ it is not possible to make a correct statistical analysis of the radiation widths.

The $g\Gamma_n$ values and the results of identification of levels of orbital angular momentum were used to calculate the strength functions S_0 and S_1.

Table 1

E_0 (eV)	$g\Gamma_n$ (meV)	$\Delta g\Gamma_n$ %	Γ_γ (meV)	$\Delta\Gamma_\gamma$ %	J	φ_p	φ_s	l
67,32	0,035	30						
I50,0	0,045	20						
365,2	3,04	5	I27	20		0,94	0,06	I
427,2	II,I	6	202	I3		I,0	0	I
922,6	22	20			(2)	I,0	0	I
95I,8	I00	I0	76	30	I	0	I,0	0
I288	I7,0	6	I22	25		0,65	0,35	I
I424	35	40				0,95	0,05	I
I720	I87	8	85	30	I	I,0	0	I
2837	45	28				0,65	0,35	I
3I28	780	I3			I	0	I,0	0
3859	I00	25				0,63	0,37	(I)
4273	30	50				0,5	0,5	-
4379	800	20				I,0	0	I
5035	II0	35						
5080	400	25						
7335	I80	35						
7497	70	50						
8I57	900	30						
90I7	6560	5				0	I,0	0
9587	3I00	25						

The calculation was carried out taking into account the probability of the levels being s or p.

If the energy interval ΔE in which S_0 is determined is taken as 4.3 keV, then

$$S_0 = \frac{\Sigma(g\Gamma_n^0\ \varphi_s)}{\Delta E} = (0.043 {+0.06 \atop -0.02}) \times 10^{-4}$$

If ΔE is taken as equal to 10 keV and only 100% s levels are used, then for S_0 we get $(0.09 {+0.15 \atop -0.05}) \times 10^{-4}$. From these data we can conclude that

$$S_0^{expt.} = (0.07 {+0.12 \atop -0.04}) \times 10^{-4}$$

Fig. 1 Determination of parameters of the 427.2 eV level from measurements of total cross-section and self-indication.

a, a', a" – total cross-section n_T = 0.1119 at./b, 0.084 at./b, 0.014 at./b

b, b', b" – self-indication $n_D = n_T$ = 0.072 at./b, 0.014 at./b, 0.01915 at./b

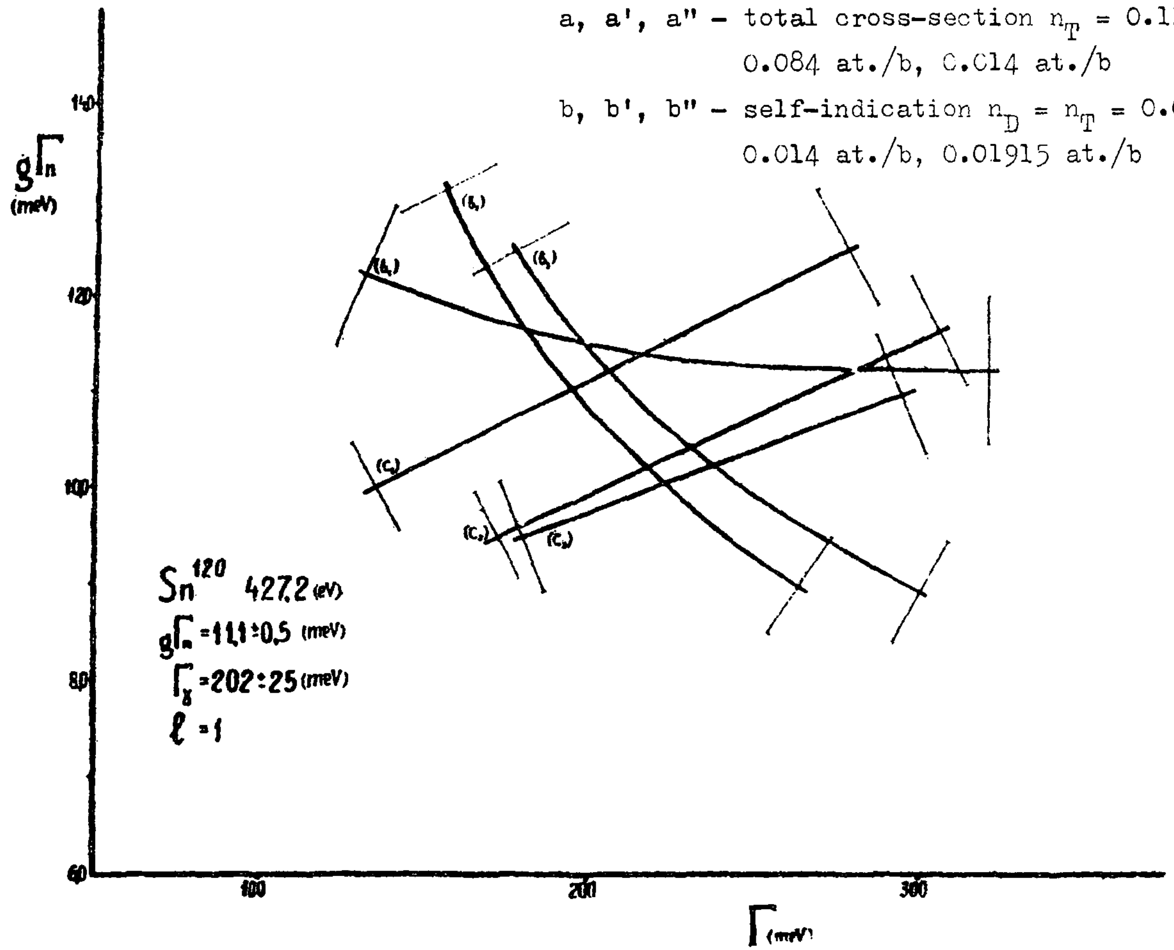

An important result of this work is the determination of the strength function for a neutron p-wave (S_1). The calculation was performed using a formula which takes into account the probability Φ_p. The value obtained, $S_1^{expt.} = (3.7 \begin{smallmatrix}+1.8\\-0.9\end{smallmatrix}) \times 10^{-4}$, is in good agreement with the value 3.10, calculated using the optical model. The errors in $S_0^{expt.}$ and $S_1^{expt.}$ were calculated in similar manner [6].

From the fact that $S_0^{expt.}$ is much less than the value predicted by the optical model while $S_1^{expt.}$ agrees with the conclusions furnished by that model, it follows that the interaction of s and p neutrons with this nucleus cannot be described using a single optic potential and that the incoming states have a marked effect on the formation of the compound nucleus ^{121}Sn.

REFERENCES

[1] G.V. Muradyan, Yu.V. Adamchuk, S.S. Moskalev, Pribory Teh. Eksp. (Instruments and Experimental Techniques) 6 (1966) 43.
T. Fuketa, I.A. Harvey, F.A. Khan, ORNL-3425, page 36.

[2] Yu.V. Adamchuk, S.S. Moskalev, G.V. Muradyan, Jadernaja Fizika 3 (1966) 801.

[3] C.M. Shakin, Annals of Physics 22 (1963) 54 and 373.
B. Block and H. Feshbach, Annals of Physics 23 (1963) 47.

[4] G.V. Muradyan, Yu.V. Adamchuk, Yu.G. Shchepkin, Pribory Teh. Eksp. (1968).

[5] G.V. Muradyan, Yu.V. Adamchuk, S.S. Moskalev, Pribory Teh. Eksp. 6 (1966) 43.

[6] H.V. Muradyan, Yu.V. Adamchuk, Nucl. Phys. 68 (1965) 549
G.V. Muradyan, Yu.V. Adamchuk, Nuclear Data for Reactors (Proc. Conf. Paris, 1966), I, IAEA, Vienna (1967) 79.

NEUTRON CROSS-SECTIONS OF ^{117}Sn

Yu.V. Adamchuk, V.S. Zenkevich, S.S. Moskalev,
G.V. Muradyan, Yu.G. Shchepkin

(Presented at the Anglo-Soviet Seminar on
"Nuclear Constants for Reactor Computations",
Dubna, 18-22 June 1968.
(Paper No. ASS-68/12))

The authors have investigated the total cross-section and the capture and scattering cross-sections of ^{117}Sn. These measurements together made it possible to determine not only the position of the levels (E_o) and the parameters $g\Gamma n$, obtained previously from measurements of σ_t [1], but also the spins and radiation widths of a number of levels. Moreover, these measurements were carried out with approximately four times better resolution than was used in Ref. [1] so that it was possible to increase the number of levels found by about 150% and subject them to statistical analysis.

The measurements were carried out on the Institute's linear electron accelerator using the time-of-flight method. The length of the accelerator electronpulse was 0.2 μsec, the pulse current 0.5 A, the pulse frequency 122 Hz and the energy of the accelerated electrons 25 MeV.

The samples used in all measurements were enriched to 88% in ^{117}Sn. The total cross-section was measured over a flight length of 109 m with a resolution of 3.8 nsec/m. The neutrons were detected by means of a ^{10}B sample and eight NaI (Tl) crystals 150 mm in diameter using the $^{10}B\ (n,\gamma)$ reaction, the detector efficiency at 1 keV being about 25%. The ^{117}Sn sample 70 mm in diameter with $n = 1.45 \times 10^{-2}$ atoms of ^{117}Sn per barn was placed at a distance of 37 m from the accelerator target.

Capture and self-indication were measured over a flight length of 37 m with a resolution of 12 nsec/m. The detector was formed by two NaI (Tl) detectors 150 mm in diameter, shielded by ^{6}LiH. The number of ^{117}Sn atoms in a sample 70 mm in diameter placed in the detector (n_D) was 0.713×10^{-2} per barn for the study of capture. Taking also self-indication into account, the number of ^{117}Sn atoms present in a sample for transmisstion (n_t) was 0.728×10^{-2} per barn. The results of the total neutron cross-section, radiative capture and self-indication measurements have been analysed in the foregoing article in this Bulletin ("s and p levels of ^{120}Sn"). Scattering was measured over a flight length of 15 m [2]. A sample with $n = 0.296 \times 10^{-2}$

atoms of ^{117}Sn per barn, elliptical in form and with a surface area of 138 cm^2, was placed at an angle of 45^o 25 cm from the surface of a neutron source (the moderator surrounding the accelerator's uranium target) and the neutron detector 15 m away from the sample. The scattering angle was 90^o. The energy indeterminacy in these measurements was added to indeterminacies in measurement of the time of flight (0.4 μsec), indeterminacies in the flight length (2 cm) and indeterminacies in the scattering angle (±25%), resulting in an indeterminacy in the amount of energy lost by the neutron in the event of scattering. Above 0.5 keV the energy indeterminacy is mainly due to the indeterminacy in respect of time (25 nsec/m) while below 0.3 keV it is due mainly to the indeterminacy in regard to the scattering angle ($\Delta E = 0.015E$).

All measurements (σ_t, σ_γ, σ_{tD}, σ_s) were made on the 2048-channel time analyser using a channel width of 0.25 μsec. Each series of measurements was repeated three to four times. For isotopic identification of the levels the authors also measured the total cross-sections and the capture cross-sections of the remaining tin isotopes.

In order to calculate the absolute probability of neutron scattering on the sample of tin-117 in question, they also carried out measurements with a lead sample of thickness 0.569×10^{-2} at./b. The geometry for measuring scattering from the lead sample and the arrangement of sample, detector and neutron source were absolutely identical to those adopted for ^{117}Sn. Knowing the quantitative ratio of neutrons scattered on ^{117}Sn and Pb and taking the scattering cross-section of lead to be 11.28 + 0.06 barn [3], it was possible to determine the absolute neutron scattering probability on the sample of ^{117}Sn.

The function $g\Gamma_n = fg(\Gamma)$ was calculated on a computer by matching a theoretical area to the experimental by varying Γ, Γ_n and g (g = 1/4 or 3/4). The theoretical area was calculated over the given energy range on the basis of Breit-Wigner's formula, taking into account the Doppler effect, potential scattering and interference between resonance and potential scattering. Account was taken of the fact that the scattered neutrons come from various depths in the sample and that an ejected neutron may undergo radiative capture. This last effect is clearly seen in the area of good resolution.

Fig. 1 shows the energy-dependence of the scattering probability on the sample in question (the discontinuities corresponding to the omitted resonances of ^{116}Sn and ^{118}Sn). For the resonance at 38.80 eV the trough to the right of the resonance displays the effect of absorption subsequent to scattering. The distance between the trough and the resonance precisely corresponds to the drop in energy in the event of scattering at an angle of 90°. The magnitude of this correction (to Γn) for the different ^{117}Sn levels does not exceed 20%. To take interference and potential scattering into account it is necessary to know the potential scattering cross-section. This was determined from similar measurements of ^{117}Sn scattering in the inter-resonance region. The value obtained $\sigma_{pot.} = 4.75 + 0.04$ barns agrees within the error limits with the data in Ref. [4].

From the experimental data in the region where there is no loss of levels ($\Delta E = 1$ keV) the authors determined the value of the strength function S_o:

$$S_o = \frac{\overline{2g\Gamma n^o}}{2\overline{D}} = \frac{1.4 \times 10^{-3} \times 22}{2 \times 1000} = (0.16 \begin{smallmatrix}+0.03\\-0.02\end{smallmatrix}) \times 10^{-4}$$

The errors in S_o were calculated similarly [5]. The value of $S_{o\ expt.}$ is approximately four times less than the value of $S_{o\ theor.}$ predicted by the optical model, which can obviously be explained by the effect of incoming states when a compound nucleus is formed. The small number of levels for which spins (I) have been determined makes it impossible to perform a statistical analysis, for example to investigate the dependence of level density on spin. Some degree of spin dependence of the levels found can be seen in the mean radiation width:

$$\overline{\Gamma}_\gamma (I = 0) = 60 \pm 15 \text{ meV}; \quad \overline{\Gamma}_\gamma (I = 1) = 85 \pm 20 \text{ meV}$$

Despite the fact that the strength functions for different spin systems include large errors, the values obtained are close to one another:

$$S_o (I = 0) = (0.2 \begin{smallmatrix}+0.2\\-0.1\end{smallmatrix}) \times 10^{-4}; \quad S_o (I = 1) = (0.25 \begin{smallmatrix}+0.25\\-0.1\end{smallmatrix}) \times 10^{-4}$$

It will be noted that in the calculations of $g\Gamma n = fg (\Gamma)$ no account was taken of the resolution of the neutron spectrometer or multiple scattering. The error resulting from failure to take resolution into account was reduced to a negligibly small level by the choice of a sufficiently wide energy range within which the area is obtained. The error resulting from multiple scattering is estimated not to exceed 10%.

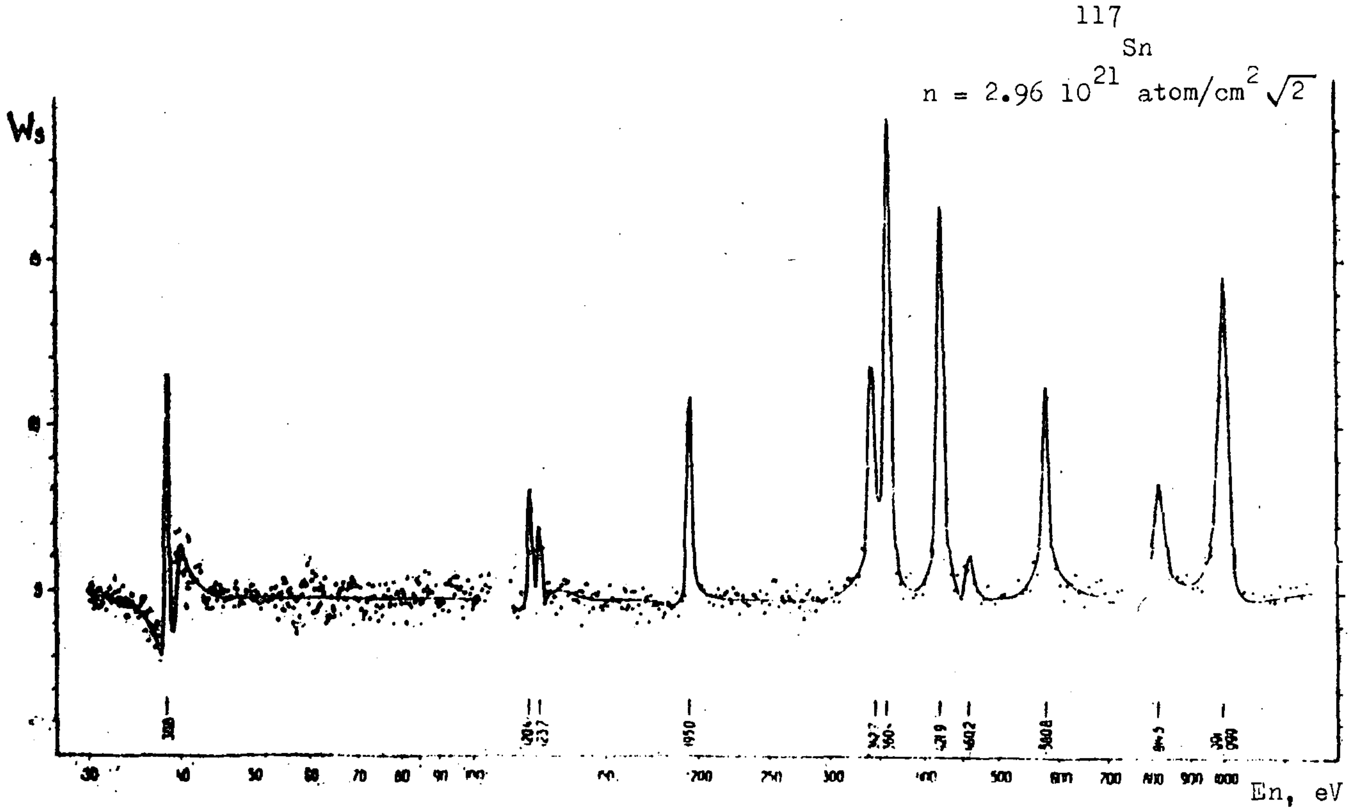

Fig. 1 Energy dependence of scattering probability

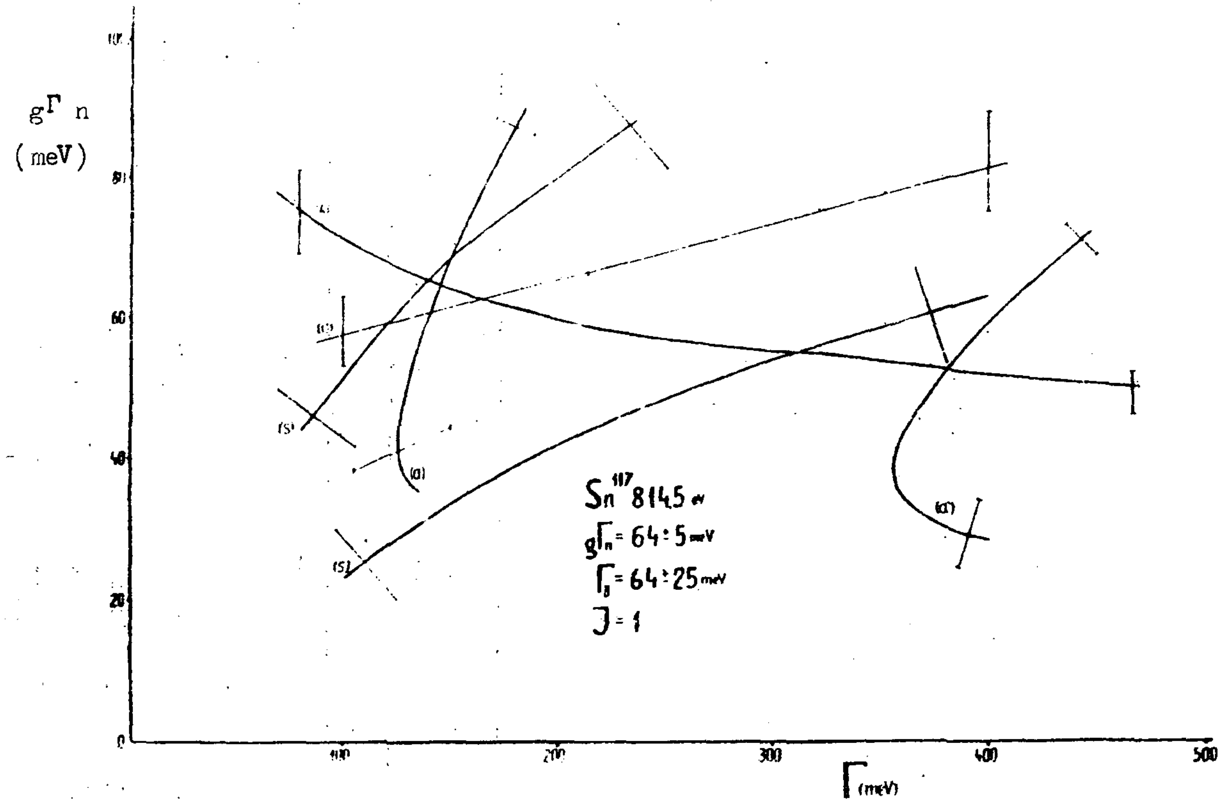

Fig. 2 Determination of parameters of the 814.5 eV level from measurements of the total cross-section, scattering cross-section, capture and self-indication. The relation $g\Gamma n = (f)\Gamma$ is calculated from the total cross-section (curve b), from capture with $g = 3/4$ and $g = 1/4$ (curve c), from self-indication (curve b) and from scattering with $g = 3/4$ or $g = 1/4$ (curve S).

To determine the level parameters the authors simultaneously analysed the results of the measurement of σ_t, σ_γ, σ_{tD} and σ_s. Fig. 2 gives as an example the way in which Γn, $\Gamma\gamma$ and g are determined from the results of these four measurements. Table 1 gives the parameters of the levels found. It will be noted that in Ref. [1] 24 levels were found. The authors found 32 new levels, thanks to the measurements of σ_t with a resolution four times better than was used in Ref. [1] to measure capture.

REFERENCES

[1] T. Fuketa, F.A. Khan, I.A. Harvey ORNL-3425.

[2] V.F. Gerasimov, V.S. Zenkevich, S.S. Moskalev, Pribory Teh. Eksp. (Instruments and Experimental Techniques) (1968).

[3] Rayburn, Nucl. Phys. 61, (1965) 381.

[4] I.A. Harvey, T. Fuketa, WASH-1048 p. 70.

[5] H.V. Muradyan and Yu.V. Adamchuk, Nucl. Phys. 68 (1965) 381.

Table 1

E_0 (eV)	ΔE_0 (eV)	I	$2g\Gamma_n$ (meV)	$\Delta(2g\Gamma n)$ %	$2g\Gamma n^0$ (meV)	Γ_γ (meV)	$\Delta\Gamma_\gamma$ (meV)
1	2	3	4	5	6	7	8
I,32	-	-	0,0002	I0	0,000I7	-	-
34,05	0,05	-	0,032	30	0,0059	-	-
35,80	0,05	I	6	30	0,9[illegible]	90	25
74,45	0,2	-	0,05	40	0,0058	-	-
I20,4	0,3	I	I2	8	I,09	72	I7
I23,7	0,3	0	4,4	5	0,396	76	I6
I48,0	0,3	-	0,I4	40	0,0I2	-	-
I66,2	0,4	-	0,32	30	0,025	-	-
I95,9	0,5	I	28	I5	2,0	-	-
200,7	0,6	-	I,I	30	0,078	-	-
22I,4	0,6	-	0,5	25	0,034	-	-
275,6	0,8	-	0,34	25	0,02I	-	-
296,7	I	-	I	40	0,058	-	-
342,7	I	0	33	I0	I,78	54	26
360,0	I	-	24	30	I,3	-	-
40I,2	I	-	7,4	I5	0,37	-	-

I	2	3	4	5	6	7	8
42I,9	I	I	II0	25	5,4	I30	60
460,2	I	0	26	I0	I,2I	62	29
527,I	I		0,I5	25	0,0065		
534,0	I		2,8	30	0,I2		
557,8	I		I,4	25	0,059		
580,8	I	0	56	I0	2,32	50	25
647,9	I		4	50	0,I6		
659,6	I		4	50	0,I6		
687,4	I		2,8	40	0,II		
706,5	I		4,6	30	0,I7		
79I,3	I		I3,6	I0	0,484		
8I4,5	2	I	I28	9	4,49	64	25
867,2	2		2I	20	0,7I		
882,3	2		5,6	35	0,I9		
94I,5	2		40	I0	I,3		
99I	2		400	I5	I2,7		
999	2		I80	I5	5,7		
II67	2		24	20	0,7		
II9I	3		I6	50	0,46		
II23	3		24	50	0,69		
I280	3		24	40	0,67		
I3I8	3		3,2	50	0,088		
I36I	3	I	I84	8	4,98	65	20
I443	3		8,2	30	0,22		
I493	4		I48	8	3,83		
I552	4		I0	60	0,25		
I630	4		70	30	I,7		
I674	4		I00	40	2,4		
I754	4		I20	25	2,86		
I8I2	5		50	60	I,2		
I87I	5		80	60	I,9		
I903	6		80	25	I,83		
20I3	6		400	20	8,9I		
2084	6		450	20	9,8		
2I60	6		70	40	I,5		
2I98	6		70	40	I,5		
2262	7		I00	20	2,09		
2320	7		75	25	I,56		
2587	8		480	20	9,43		
2978	I0		580	25	I0,6		

NEUTRON-SPECTROSCOPE INVESTIGATION OF SEPARATED SILVER ISOTOPES

G.V. Muradyan, Yu.V. Adamchuk

(Presented at the Paris Conference on Nuclear Data (1966))

(Table corrected in accordance with measurements carried out in 1968).

The results of study of radiative capture on the silver isotopes ^{107}Ag and ^{109}Ag up to ~ 100 eV have eliminated a discrepancy in the theory of level spacings. The measurements that had been made of the total neutron cross-sections of a natural mixture of silver on the Columbia University synchro-cyclotron (USA) with the best resolution available at the present time (0.5 nsec/m) [1] had lead to an unexpected result: small spacings between silver levels are encountered less frequently than one would obtain from Wigner distribution in the event that several level systems are superposed (in the present case more than four systems). This conclusion leads to consequences which entail a radical review of the present-day theory of the nucleus.

The results obtained by the authors of this article have shown that the observed absence of small spacings between the levels is illusory and is explained by the fusion of the levels of various isotopes within the limits of their widths and resolution so that measurement of a natural mixture made it impossible for the authors of Ref. [1] to identify these cases as cases of twin levels. Measurement of separated isotopes enabled the authors of the present article to demonstrate about twenty new levels. The experimental conditions are described in foregoing articles in this Bulletin (see articles on ^{120}Sm and ^{117}Sm).

Table 1 gives the isotopic identification of silver levels. It also gives the parameters of the levels of ^{107}Ag and ^{109}Ag, mainly taken from Ref. [1]. An asterisk denotes those levels first discovered in the present work and levels for which the values of $2g\Gamma_n^o$ have been clarified. The value of $2g\Gamma_n^o$ for the newly discovered levels of ^{107}Ag and ^{109}Ag was determined on the assumption Γ_γ = 140 meV.

Fig. 1 shows the level spacing distribution as given in Ref. [1] and a histogram of the sum of the level spacings for ^{107}Ag and ^{109}Ag (i.e. $^{107}Ag + ^{109}Ag$), plotted from the results presented in the present article.

Fig. 1B shows that the experimental distributions are in good agreement with Wigner distribution in the event of a number of level systems being superposed, especially if account is taken of possible losses of levels owing to the superposition of levels with different spin systems for one and the same isotope.

Thus the discrepancy noted in Ref. [1] between the experimental distribution of silver levels and the theoretical distribution obtained from the superposition of a number of independent systems of levels disappears.

The considerable number of cases where ^{107}Ag and ^{109}Ag levels can be seen to coincide suggests that there is a possible correlation between the positions of the levels of these isotopes. The authors have undertaken an analysis to determine this and have found that there is no correlation between ^{107}Ag and ^{109}Ag levels within the limits of the statistical accuracy obtained.

The values of the S_0 and S_1 strength functions for silver isotopes (in units of 10^4) were found to be as follows:

$$S_0 = 0.43^{+0.17}_{-0.12} \qquad S_1 = 1.9^{+1.3}_{-0.6} \qquad \text{for } ^{107}Ag$$

$$S_0 = 0.83^{+0.23}_{-0.19} \qquad S_1 = 1.4^{+1.1}_{-0.5} \qquad \text{for } ^{109}Ag$$

Table I

Isotopic identification and parameters
of resonance levels of silver

	^{107}Ag			^{109}Ag		
	E_o, eV	$2g\Gamma n^o$, meV	Remarks	E_o, eV	$2g\Gamma n^o$, meV	Remarks
I	I6,30	I,48 ±0,06		5,20	8,I6 ±0,06	
2	4I,50	I,32 ±0,I6		30,50	2,00 ±0,I8	
3	44,80	0,27 ±0,04		32,63	0,00I9±0,0004	*
4	5I,40	4,48 ±0,40		40,20	I,36 ±0,I6	
5	83,50	0,0030±0,0007		55,70	2,56 ±0,20	
6	I07,6	0,00I9±0,0004	*	70,80	4,76 ±0,44	
7	II0,88	0,008 ±0,00I		87,67	I,00 ±0,08	
8	I28,04	0,008 ±0,004		9I,50	0,005 ±0,00I	
9	I44,20	0,76 ±0,08		I06,29	0,0I2 ±0,004	
I0	I54,7	0,0045±0,0009	*	II3,5	0,0054±0,00II	*
II	I62,40	0,02 ±0,0I		I33,90	I0,40 ±0,80	
I2	I67,I0	0,0I6 ±0,004		I39,70	0,I8 ±0,02	
I3	I7I,2	0,0065±0,00I3	*	I60	0,0079±0,00I6	*
I4	I73,I0	5,00 ±0,40		I69,80	0,028 ±0,008	
I5	I83,60	0,0I2 ±0,004		I72,8	6,I ±0,9	*
I6	202,50	I,I2 ±0,I2		I98,4	0,0II ±0,02	*
I7	2I8,20	0,0I2 ±0,0I2		209,60	2,48 ±0,20	
I8	25I,29	0,60 ±0,I6	*	25I,29	0,60 ±0,I2	*
I9	260	0,0I68±0,0034	*	258,89	0,I25 ±0,0I9	*
20	264,47	0,24 ±0,02		264,47	0,022 ±0,004	*
2I	270,5	0,0076±0,00I5	*	272,5	0,I2 ±0,0I	
22	3I0,92	I0,0 ±2,0		274,90	0,020 ±0,008	
23	329	0,0I8 ±0,004	*	283,90	0,0I6 ±0,008	
24	347,34	0,020 ±0,008		290,86	0,76 ±0,08	
25	356,20	0,020 ±0,008		293,00	0,020 ±0,008	
26	36I,83	I,80 ±0,08		300,64	0,08 ±0,02	
27	372	0,0I45±0,0030	*	3I6,40	I4,0 ±2,0	
28	382,I0	0,020 ±0,008		322,I0	0,020 ±0,008	
29	40I,70	0,024 ±0,0I2		327,80	0,40 ±0,06	
30	4I0,0I	0,0I6 ±0,008		340,4	0,0I0 ±0,002	*
3I	424	0,0073±0,00I5	*	360	0,074 ±0,0I5	*
32	444,60	I,80 ±0,20		387,00	3,32 ±0,I2	
33	46I,40	I,08 ±0,I2		39I,60	0,0I6 ±0,004	
34	466,80	4,60 ±I,20		398,00	I,52 ±0,08	

Table I (cont.)

35	472,2	0,72	±0,08		404,40	5,0	±0,2	
36	476,10	0,16	±0,02		423,40	0,88	±0,03	
37	479,54	0,12	±0,02		441,0	0,009	±0,002	*
38	515,47	4,4	±0,4		469,61	2,0	±0,8	
39	524,90	0,020	±0,008		487,72	1,16	±0,08	
40	532,20	0,07	±0,02		495,20	0,04	±0,02	
41	554,51	10,00	±1,00		500,60	10,0	±1,0	
42	576,67	3,04	±0,40		512,27	0,68	±0,08	
43	587,47	6,40	±0,60		526,60	0,04	±0,02	
44	605,06	0,10	±0,02		558	0,26	±0,05	*
45	625,59	0,64	±0,08		560,66	6,0	±0,8	
46	653,50	1,00	±0,08		565,43	8,0	±0,8	
47	674,50	3,00	±0,28		607,93	2,6	±0,2	
48	695,89	1,08	±0,12		622,17	5,6	±1,2	
49	703,51	0,26	±0,02		634,27	0,04	±0,02	
50	721,26	0,04	±0,01		648,21	0,04	±0,02	
51	734,70	0,04	±0,01		669,45	1,68	±0,20	
52	752,57	2,00	±0,50	*	681,50	0,16	±0,04	
53	784	0,21	±0,04	*	687,40	0,03	±0,02	
54	806	0,215	±0,040	*	713,87	0,07	±0,02	
55	813,0	0,24	±0,06		726,08	1,04	±0,12	
56	849	0,30	±0,05	*	730,39	0,07	±0,01	
57	882,33	4,00	±0,60		747,49	5,20	±0,40	
58	886,67	0,40	±0,12		752,6	2,0	±0,5	*
59	914,57	0,24	±0,04		784,7	11,6	±1,2	
60					803,80	1,8	±0,4	
61					831,39	0,20	±0,08	
62					849	0,090	±0,014	*
63					861,83	0,52	±0,08	
64					902,84	0,60	±0,12	

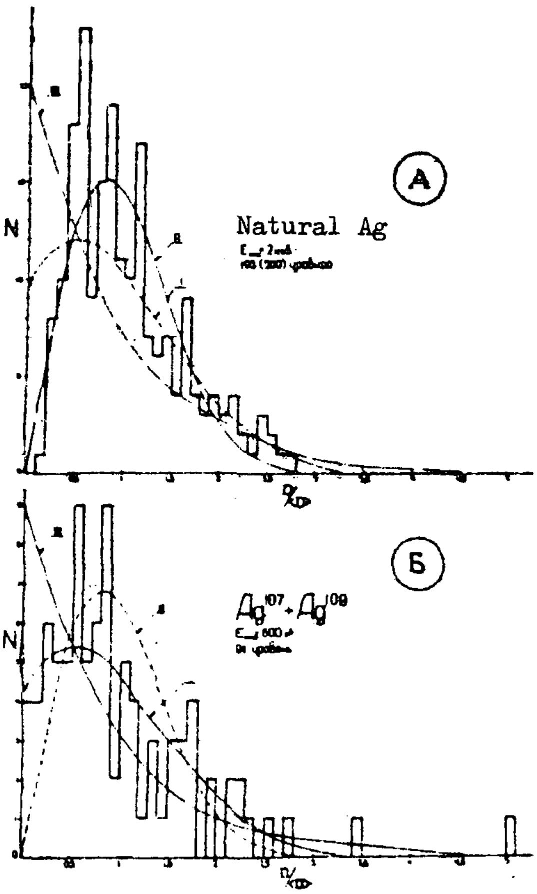

Fig. 1 (A) Level spacing distribution in natural mixture of silver isotopes, from Ref. [1].

(B) Level spacing distribution in $^{107}Ag + ^{109}Ag$ (present work).

Curve I - Wigner distribution for two systems of levels,
Curve II - Wigner distribution for one system of levels,
Curve III - random distribution.

So marked a divergence between the S_0 strength function values of nuclei with similar atomic weights does not fit within the framework of the optical model of the nucleus. A possible explanation for it is that incoming states play a large part in neutron capture by the nuclei of ^{107}Ag and ^{109}Ag.

REFERENCE

[1] J.B. Garg , J. Rainwater and W.W. Havens Jr.
Phys. Rev. 137 B547 (1965).

PARAMETERS OF NEUTRON RESONANCES OF SEPARATED ISOTOPES OF ANTIMONY

G.V. Muradyan, Yu.V. Adamchuk and Yu.G. Shchepkin

(Presented at the Anglo-Soviet Seminar on Nuclear Constants for Reactor Computations, Dubna, 18-22 June 1968 (Paper No. ASS-68/16 and subsequently submitted to Jadernaya Fizika))

Following the measurement of the radiative capture of silver isotopes [1] the authors undertook the study of transmission and radiative capture in separated isotopes of antimony ^{121}Sb and ^{123}Sb.

Antimony, like silver, has two even-odd isotopes which differ from each other in respect of two neutrons but are almost identical in respect of the proportions in which they are present in a natural mixture and the half-integral spin value.

By carrying out measurements with a fairly large amount (~ 400 g) of highly enriched (up to approximately 89.5%) separated isotopes of antimony, the authors were able to obtain qualitatively new data, show up a large number of levels not previously studied, effect a clear identification of levels by isotopes and so obtain reliable data on the statistical characteristics and strength functions of these isotopes.

The results of the measurements were analysed by the areas method taking into account interference between potential and resonance scattering [5]. The value of the neutron width $2\ g\Gamma_n$ was determined as was also for a number of resonances the full width Γ. The parameters of most levels were obtained on the basis of the results of measurements of transmission and radiative capture. For levels which do not show up in measurements of total cross-sections the value of $2\ g\Gamma_n$ was determined from the results of radiative capture measurements on the assumption that $\Gamma_\gamma = (100 \pm 10)$ mV.

The main source of errors in the parameters is the statistical error and the indeterminacy in regard to detector efficiency in the radiative capture measurements (~ 15%).

About 140 ^{121}Sb and 110 ^{123}Sb levels were investigated. The values of the parameters for antimony levels identified according to isotopes are shown in Table I together with the corresponding errors.

Fig. 1 shows the level spacing distribution of ^{121}Sb and ^{123}Sb, together with theoretical Wigner distributions (curve II is the Wigner distribution for one system of levels, curve I that for two systems of levels with identical mean spacings).

The experimental histograms are closer to the distribution for one system of levels (curve II), which contradicts what can be deduced from theory. However, as in the case of silver, this contradiction may be illusory. The fact is that for each isotope of Sb, two systems of levels show up, belonging to different spin states; these two systems happen to be superposed on each other and have approximately identical densities.

The histograms in Fig. 2≠ are very sensitive to any loss of levels. These losses are not due to the experimental loss of a level owing to its weakness, but are the result of the fusion of two levels within the limits of resolution and intrinsic width. On the basis of the actual resolution of the neutron spectrometer, and assuming for simplicity's sake that all spacings from zero to the mean spacing are equally probable, it can be shown that about 6% of the levels are lost as a result of fusion. Such a low rate of loss cannot be detected on a histogram showing the number of antomony isotope levels as a function of neutron energy. The histogram in Fig. 2, however, is highly sensitive to such losses of levels in the vicinity of $\frac{D}{\langle D \rangle} \sim 0$. If in the histogram in Fig. 2 we add to the region where fusion of levels takes place the lost 6% of levels, i.e. four spaces for ^{121}Sb and three spaces for ^{123}Sb, the experimental level spacing distribution will be closer to the distribution for two systems of levels*.

The anomalously large number of spaces at $\frac{D}{\langle D \rangle} \sim 0.5$ for the heavy isotope ^{123}Sb (see Fig. 2) merits attention. The authors observed precisely the same effect for the heavy isotope of silver ^{109}Ag.

The values of the S_0 and S_1 strength functions for ^{121}Sb and ^{123}Sb were found to be as follows:

$S_0 = (0.29^{+0.05}_{-0.04}) \times 10^{-4}$; $S_1 = (1.1^{+1.5}_{-0.5}) \times 10^{-4}$ for ^{121}Sb

$S_0 = (0.22^{+0.08}_{-0.05}) \times 10^{-4}$; $S_1 = (2^{+2}_{-1}) \times 10^{-4}$ for ^{123}Sb

---

≠ Translator's Note: Fig. 2 is missing from the original Russian text.

* After completion of the work reported here the authors obtained the results of measurements on Sb [2] which confirmed their suppositions.

The errors in the S values were calculated taking into account fluctuations in the reduced neutron widths and level spacings [3].

Such low values of S_0 do not agree with the predictions of the optical model, any more than do the results of measurements on separated isotopes of silver [1], and point to the marked effect of incoming states when a compound nucleus is formed.

Table 1

Sb^{121}				Sb^{123}			
E_0 (эв)	$2g\Gamma_n$ (mV)	$\Delta 2g\Gamma_n$ %	$2g\Gamma_n^0$	E_0 (эв)	$2g\Gamma_n$ (mV)	$\Delta 2g\Gamma_n$ %	$2g\Gamma_n^0$
6,24	2,0	5	0,30	21,0	30	20	6,48
15,4	6,9	6	1,76	80,5	5,3	15	0,75
29,55	7,3	20	1,34	76.7	7,6	10	0.87
37,77	0.013	30	0,0021	104,9	43	15	4,20
53,3	2,1	5	0,29	131,0	1,1	20	0.096
55,01	0,05	20	0,0067	167,0	0,15	50	0.012
64,4	0,65	15	0,081	176,3	0,28	20	0,021
73,78	7,0	15	0,32	186,5	0.32	20	0,023
89,53	6,0	13	0,63	191,6	19,0	20	1,37
90.11	5,0	15	0,53	198.0	0,3	20	0,021
111,4	2,8	15	0.26	219.0	3,8	20	0,26
125,6	23	20	2,04	225,8	0,32	15	0.021
131,9	9,5	15	0,83	236,4	0,30	15	0,020
144,4	10	15	0,85	241,0	14	10	0,90
149,8	30	15	2,44	296,7	1,5	20	0,087
160,7	1,5	20	0,12	300,0	24	7	1,4
167.0	13	15	1,01	324,4	32	10	1.78
177,7	0,07	25	0,0053	332,1	0,9	30	0,049
185,0	0,15	20	0.013	341,5	0,5	30	0,027
192.3	1,3	15	0.094	351,5	6,5	6	0,35
214.2	1.2	15	0.082	374,2	1,7	10	0,088
222,7	4.0	15	2.69	392,9	2,4	20	0.12
230,7	1,0	20	0.066	395,9	29	5	1,46
246,6	0.35	30	0,022	415,4	0,7	20	0,034
249,6	0,4	30	0,025	472,6	4,6	5	0,21
262,3	0,2	50	0.012	483,3	12,5	5	0,57
266,4	0,2	50	0,012	492,9	0,9	25	0,041
270,5	0,3	30	0,013	522.6	1,1	30	0,048
274,8	0,28	15	0,017	533,5	14	5	0,61
287,2	12,6	5	0,75	572,4	28	6	1,17

Table I (cont.)

293,7	0,1	30	0,0058	600,9	9	10	0,37
310,2	3,7	10	0,21	629,4	28	10	1,12
321,2	0,6	30	0,034	645,8	1,6	30	0,063
332,1	2,5	6	0,14	660,7	20	7	0,70
339,5	8,0	5	0,44	693,2	3,2	25	0,12
348,1	0,15	50	0,0080	702,6	1,0	50	0,098
356,3	0,25	25	0,013	719,4	4	30	0,15
368,8	0,4	30	0,021	749,8	150	10	5,49
393,9	22	5	1,11	818,2	25	10	0,87
407,1	1,2	20	0,059	842,6	90	7	3,10
416,1	0,7	30	0,034	874,6	170	8	5,74
422,2	10	10	0,49	887,9	87	8	2,92
432,6	0,2	50	0,0096	896,3	2,8	25	0,094
444,9	25	20	1,18	911,3	24	10	0,79
448,8	25	30	1,18	933,3	22	10	0,72
451,8	16	30	0 75	970,7	39	8	1,25
455,5	160	20	7,48	980,4	5	60	0,16
463,6	1,8	30	0,094	990,2	87	10	2,76
471,3	13,7	6	0,63	1031	14	30	0,48
476,6	0,6	25	0,028	1050	62	7	1,21
483,3	1,5	30	0,058	1086	12	30	0,36
499,2	7,5	15	0,34	1094	6	30	0,18
502,1	1,3	25	0,058	1119	19	25	0,57
510,8	0,7	30	0,031	1120	84	10	2,51
535,9	7,8	10	0,34	1168	90	7	2,63
544,7	95	5	4,08	1228	6	40	0,17
551,2	0,8	50	0,094	1239	5	40	0,14
560,4	19	5	0,80	1259	41	10	1,16
565,4	1,9	20	0,08	1276	48	8	1,94
582,1	1,2	50	0,05	1311	30	12	0,89
601,3	4,2	15	0,17	1333	20	30	0,55
607,5	55	5	2,24	1387	20	10	0,54
615,2	13	8	9,52	1437	5	50	0,13
632,5	40	5	1,59	1458	10	40	0,26
647,9	1,0	40	0,099	1487	170	25	4,40
662,9	32	6	1 24	1497	280	25	7,24
672,8	36	10	1,39	1571	7	25	0,18
678,3	23	15	0,88	1609	25	15	0,63
712,1	18	10	0,67	1624	125	7	3,11
715,8	2,8	30	0,11	1653	44	10	1,08
720,7	34	10	1,27	1675	6	15	0,15
737,6	4,4	15	0,16	1701	162	7	2,93
774,7	76	7	2,73	1740	4	40	0,096
792,0	24	20	0,85	1785	47	30	1,11
797,7	30	20	1,06	1800	266	15	6,27
803,5	100	30	3,53	1864	140	20	3,25
805,0	120	30	4,28	1874	190	20	4,99
841,0	27	10	0,93	1900	6	50	0,14
861,5	14	10	0,48	1938	80	15	1,82
892,1	7,0	20	0,29	1971	16	20	0,36
913,7	8,4	30	0,28	2005	360	8	8,05
919,0	160	25	5,28	2039	10	60	0,22
938,8	4,0	20	0,16	2112	109	15	2,24
949,8	47	10	1,53	2143	170	15	3,68
964,9	38	10	1,22	2156	320	10	6,90
996,2	190	8	4,12	2175	130	15	2,79
1016	32	10	1,00	2207	97	15	2,07
1040	6,4	25	0,20	2241	215	10	4,55
1048	10	20	0,91	2282	49	15	1,03
1069	32	10	0,97	2317	106	15	2,20
1119	120	15	3,60	2360	170	15	3,51
1125	8	30	0,24	2390	60	30	1,23
1147	18	20	0,53	2450	34	25	0,69
1185	278	8	8,08	2489	54	30	1,08
1205	72	10	2,08	2655	30	30	0,97
1222	39	10	1,12	2708	370	20	7,12
1235	66	10	1,86	2782	40	30	0,76
1262	15	40	0,42	2839	130	25	2,44
1311	110	10	3,04	2907	52	30	0,96
1332	33	15	0,90	3020	320	25	5,82
1351	20	30	0,54	3128	145	25	2,59
1367	195	10	3 65	3242	200	40	8,51
1441	93	10	2,45	3265	200	40	9,50

Table I (cont.)

I455	I2	25	0,32	33I4	290	I5	5,04
I487	82	I0	2,I2	3970	150	50	2,58
I524	I6	30	0,4I	340I	200	40	3;43
I533	12	30	0,3I	3530	70	30	1,18
I559	I5	30	0,38	3696	290	30	4,79
I579	I9	30	0,48	3984	400	50	6,34
I599	I20	I5	3,00	4166	I800	80	27,9
I645	35	20	0,86				
I70I	73	I5	1,77				
1729	64	30	I,54				
1743	24	35	0,57				
I770	97	25	2,30				
I804	I73	30	4,07				
I829	I85	25	4,33				
I849	39	25	0,91				
1906	345	30	7;90				
I922	I08	30	2,46				
I982	I37	25	3,08				
2005	220	25	4,9I				
2039	65	25	I,44				
2II2	67	35	I,46				
2I24	68	35	I,48				
2I56	I46	35	3,I5				
2268	I40	40	2,94				
2275	II0	40	2,3I				
23I0	I70	25	3,53				
2367	I50	30	3,08				
2397	290	25	5,92				
2442	II5	30	2,33				
2533	420	40	8,35				

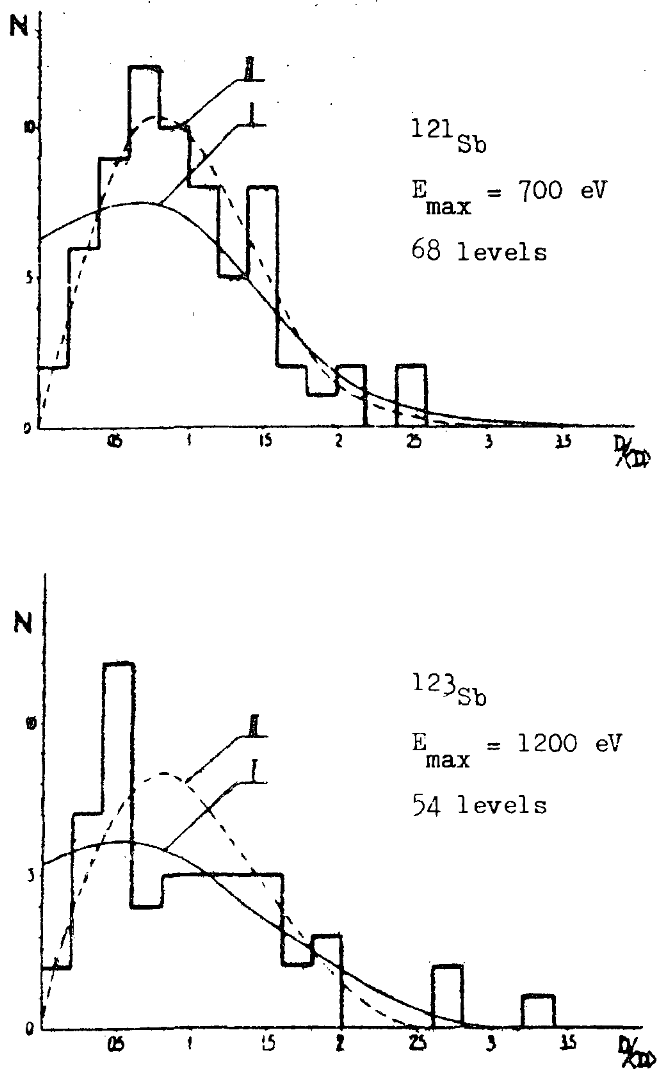

Fig. 1. Level spacing distribution for isotopes ^{121}Sb and ^{123}Sb. Curve II - Wigner distribution for one system of levels; curve I - Wigner distribution for two systems of levels with identical mean spacings.

REFERENCES

[1] G.V. Muradyan, Yu.V. Adamchuk. Nuclear Data for Reactors (Proc. Conf. Paris 1966), I, IAEA, Vienna (1967) 79.

[2] S.W. Ynchank et al. Phys. Rev. 166, B1234 (1968).

[3] H.V. Muradyan and Yu.V. Adamchuk. Nucl. Phys. 68 (1965) 549.

[4] G.V. Muradyan, Yu.G. Shchepkin, Yu.V. Adamchuk, M.G. Arutyunov. Paper presented at the Anglo-Soviet Seminar, Dubna, 1968 (ASS-68/14).

FISSION CROSS-SECTION MEASUREMENTS IN THE RESONANCE ENERGY REGION ON LIQUID-NITROGEN-COOLED URANIUM-235

T.A. Mostovaya, V.I. Mostovoy

(Presented at the Anglo-Soviet Seminar on "Nuclear Constants for Reactor Computations", Dubna, 18-22 June 1968
Paper No. ASS-68/15))

The resolving power of present-day neutron choppers makes it possible to obtain cross-sections in the resonance energy region which are to all intents and purposes distorted only by Doppler broadening. Further information on the actual resonance structure of heavy nuclei, where the level spacing is of the same order as the width of levels, can be obtained by reducing the Doppler effect. The work here described was undertaken with a view to clarifying the ^{235}U fission cross-section data obtained previously by lessening the effect of Doppler broadening [1].

The measurements were carried out on a neutron chopper by the time-of-flight method over a path length of 18.15 m. The Institute's electron linac, giving neutron bursts of duration T_n = 0.2 μsec with a frequency ν = 250 Hz, served as neutron source. A special ionization chamber was used for the measurements.

The background at various neutron energies was measured by means of the customary technique using resonance filters.

Effects from the fission chamber were recorded by a 4096-channel time analyser with a ferrite memory and at a channel width τ = 0.25 μsec. At the same time, the effects from the proportional counter were recorded on a 2048-channel analyser with a magnetic drum memory.

The resolution for measuring fission effects (disregarding the indeterminacy of the flight length due to the neutron source) was 13 nsec/m.

Provisional measurements show that the chamber as constructed is fully suitable for recording fission events when the layer is cooled to the temperature of liquid nitrogen.

Insufficient statistics have as yet been obtained to draw definite conclusions regarding the efficiency of cooling in measuring fission cross-sections on a ^{235}U oxide. Thus, it is purely for illustrative purposes that we give here the fission effects Nf' (including background), as measured directly on the analyser. The results of one source of measurements are given in Figs 1 and 2.

Cooling causes the weak resonances located in the troughs between levels (10.2, 11.7, 12.9, 13.3, 20.1, 20.6, 38.4 eV etc.) and on the descending slopes of strong levels (9.3, 43.3 eV etc.) to show up more clearly. Isolated weak levels with small full widths (20.4, 4.85, 7.1, 11.7 eV etc.) are noticeably elongated in the event of cooling. Fig. 3 illustrates this effect qualitatively taking as an example the level at E = 7.1 eV.

REFERENCES

[1] T.A. Mostovaya; Bulletin of the Nuclear Data Information Centre No. 3 (1966)

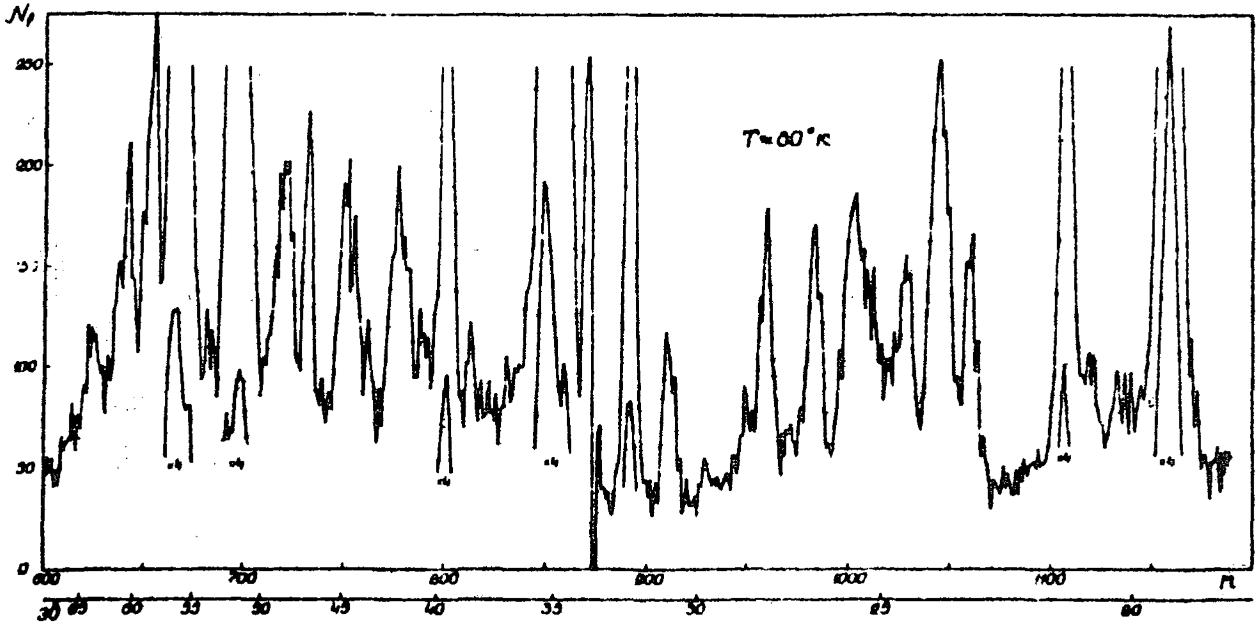

Fig. 1 Effect of fissions (Nf') in the analyser channels (n) with cooling of the fissioning layer.

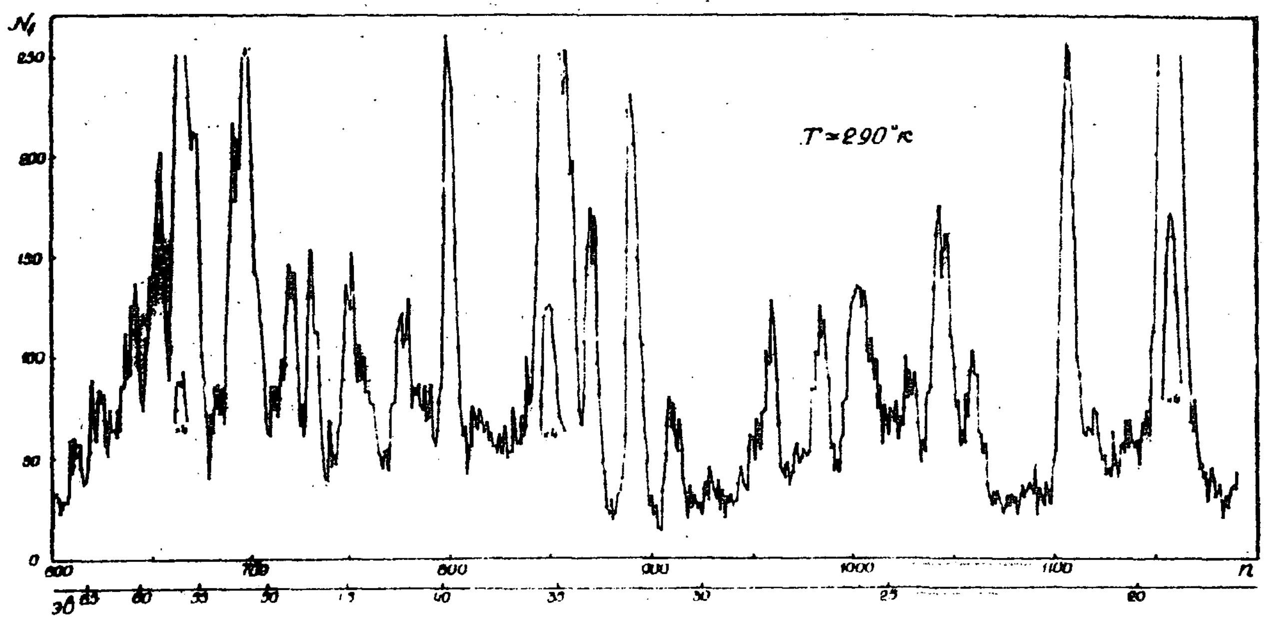

Fig. 2 Effect of fission (Nf') in the analyser channels (n) without cooling of the fissioning layer.

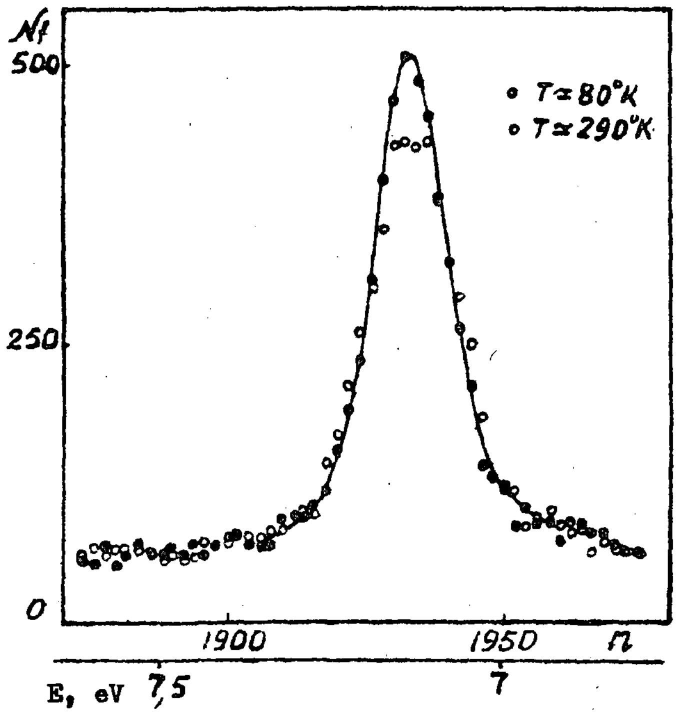

Fig. 3 Effect of cooling on the level at E = 7.1 eV.

ABUNDANCE OF PARTIAL RADIATIVE TRANSITIONS TO THE GROUND AND FIRST EXCITED STATES IN THE RESONANCES OF GADOLINIUM-155

L.S. Danelyan, B.V. Efimov, S.K. Sotnikov

A two-crystal scintillation spectrometer was used to measure the total abundance of partial gamma transitions to the ground and first excited states in 23 resonances of the $^{155}Gd(n,\gamma)^{156}Gd$ reaction. The measurements were performed on the neutron beam of the I.V. Kurchatov Institute of Atomic Energy's electron linac. The gamma spectrometer, which is mounted at a distance of 10.8 m from the target, is designed on the "summation-coincidence" principle and consists of two detectors with sodium iodide crystals measuring 120 x 120 mm. This design made it possible to measure the background due to the summation of pulses from two or more gamma quanta. In order to analyse the pulses in respect of time and pulse height, a multi-dimensional analyser with altogether 2048 channels was used. The sample was enriched to the order of 92% gadolinium-155. The relative abundances of transitions are shown in Table 1.

On the basis of the abundances of two-cascade transitions an attempt was made to show up resonances with spin 1. Owing to the low summation background statistics it was not possible to obtain a clear picture for all resonances studied. Nevertheless, in the case of five resonances it was possible to posit spin 1, while for the remaining 17 resonances the experimental distribution lies between distributions with $\nu = 1$ and $\nu = 2$. If the resonances are broken down by spins in this way, the mean abundance values for transitions from 1 states is approximately ten times greater than for transitions from 2^- states.

Assuming that E_1 transitions predominate, it may then be assumed that transitions from a 2^- spin state to the first excited 2^+ state are forbidden in the ^{156}Gd nucleus.

Table 1

$E_{res.}$ eV	Spin J	Total abundance of transitions 8.44 and 8.52 MeV
62,9		I,9±0,9
59,5		0,4±0,2
53		I,6±0,5
50,3		8,5±0,5
47,I		4,9±0,9
42,7	I x)	I00 ±2,2
37,3		I2,2±I,6
35,I	I x)	20,4±4,9
33,8		9,8±0,7
30,5		I,2±I,2
29,9		0,8±0,4
23,3	I x)	I5,3±I,3
2I,3	I x)	I4,3±I,4
20,2		I,5±0,8
I4,54		2,3±I,0
I2,05		4,4±0,8
II,67	I x)	44,8±4
I0,I2		I,5±0,7
7,8		0,0I±0,07
6,3	2	2,0±0,5
2,57	2	4,5±2,0
2,0I	I	7,9±I,I
0,0268	2	3,6±0,8

x) Assumed spin values from the data on two-cascade transitions.

SPIN MIXING IN INITIATING CHANNELS OF REACTIONS

K.V. Karadzhev, V.I. Manko, F.E. Chukreev

(Submitted to Jadernaja Fizika)

The angular distributions of alpha particles from the reaction $^{31}P\ (p,\alpha_0)\ ^{28}Si$ were used to determine the spin mixing coefficient, which is equal to the ratio Γ_{p0}/Γ_{p1}, where Γ_{p0} and Γ_{p1} are the partial proton widths corresponding to the two possible channels of the $^{31}P\ (p,\alpha_0)\ ^{28}Si$ reaction, with spins 0 and 1 respectively. The distribution of these coefficients does not agree with the calculated distribution based on assumptions that the widths Γ_{p0} and Γ_{p1} are statistically independent and that each of them is subject to Porter–Thomas distribution. The shape of this distribution shows that there is a correlation between the widths Γ_{p0} and Γ_{p1}. This correlation is close to that which must occur in the event that there is jj-bonding and this in turn may mean that even at such high excitation energies (10.0 -12.5 meV) it is possible to speak of the appearance of relatively simple shell configurations.

INTERJACENT STRUCTURE OF THE RELATION OF ^{236}U FISSION PROBABILITY TO EXCITATION ENERGY

P.E. Vorotnikov

(Submitted to Jadernaja Fizika)

The author shows that in the event of neutron-induced fission of ^{235}U the relation (averaged out over the resonances of the compound nucleus) of fission width to neutron energy displays marked peaks with width $\lesssim$ 300 eV and spacing ~ 1 keV.

Institute of Theoretical and Experimental Physics*

NEUTRON POLARIZATION IN (d,n) REACTIONS INVOLVING NUCLEI OF MEAN ATOMIC WEIGHT

I.I. Levintov, V.V. Okorokov, V.M. Serezhin, V.A. Smotryaev, D.L. Tolchenkov, I.S. Trostin, Yu. N. Cheblukov

(Submitted to Jadernaja Fizika)

The authors measured neutron polarization in (d,n) reactions involving the isotopes ^{59}Co, ^{56}Fe, $^{60, 62}$ and ^{64}Ni and $^{64, 66}$ and ^{68}Zr in the range of angles $\Theta_{d,n} = 30^o–50^o$ (Lab. system). The incident deuteron energy E_d was 11.7 MeV (cyclotron belonging to the Institute). Neutron polarization was determined from the azimuthal asymmetry of scattering on carbon, the analysing power of which had been previously found from the scattering of polarized neutrons from the D (d,n) ^{3}He reaction. Neutron polarization for scattering on carbon at an angle of 45^o (Lab. system) P_{n-c} was -0.78 ± 0.18 for 12.6 MeV neutrons and -0.60 ± 0.09 for 10.2 MeV neutrons.

The scattered-neutron spectra were measured by the time-of-flight method. The authors determined the polarization of neutrons corresponding to the ground and adjoining excited states of the residual nucleus (residual nucleus excitation energy range $\Delta E^* \sim$ (0-3.1) MeV + (0-6.7) MeV).

---

* Edited by V.N. Andreev

The following percentage values were obtained for the polarization of neutrons:

Target	Reaction angle $\Theta_{d,n}$ (Lab. system)		
	50^0	40^0	50^0
Co^{59}	-	-5,6±4,0	- 13,4±5,9
Fe^{56}	+3,2±3,8	+0,6±1,9	0,0±5,8
Zn^{64}	-	-10,8±5,2	-8,1±7,5
Zn^{65}	-	-	-6,0±17,5
Zn^{68}	-	-	-8,7±8,0
Ni^{60}	-9,3±5,7	+3,0±8,0	-4,0±5,4
Ni^{62}	-	-	-4,4±2,5
Ni^{64}	-	-	-3,8±5,0

The positive sense of the normal $\vec{n} = \vec{k}_d \times \vec{k}_n$

LONG-RANGE PARTICLES WITH Z ≥ 2 IN TERNARY FISSION OF ^{239}Pu BY THERMAL NEUTRONS

V.I. Andreev, V.G. Nedopekin, V.N. Rogov

This paper deals with a study of the emission of ^{4}He and particles with A > 4 in ^{239}Pu fission by thermal neutrons. The particles were recorded using a detector which at the same time measured the specific ionization, energy and flight path for each particle. Lithium, beryllium, boron and carbon were observed. The ion yields and energy spectra were measured and the isotopic composition of the ions estimated. The ion spectra at the moment of ion formation in the fission process were calculated. The following table gives the experimentally measured ion yields, the minimum detectable-particle energy, and the total ion yield, as determined by extrapolation of the experimental spectra to the low ion-energy range.

Ions	Yield per fission event	E min.	Total yield per fission event
γ-particles	$2,27.10^{-3}$ *)	7	$2,4 . 10^{-3}$ *)
helium	$(4,2 \pm 0,5).10^{-5}$	8,5	$6 . 10^{-5}$
lithium	$(1,76 \pm 0,5).10^{-6}$	15	$3,6 . 10^{-6}$
beryllium	$(4,4 \pm 0,1).10^{-6}$	21	$1,4 . 10^{-5}$
boron	$(1,25 \pm 0,09).10^{-7}$	28	$8 . 10^{-7}$
carbon	$(6,4 \pm 0,2).10^{-7}$	36	$1,2 . 10^{-5}$

*) Reference values.

TOTAL NEUTRON CROSS-SECTION OF ^{230}Th IN THE THERMAL AND RESONANCE ENERGY RANGES

S.M. Kalebin, P.N. Palei, P.I. Ivanova, Z.K. Karalova,
G.M. Kukavadze, E.I. Pyzhova, G.V. Rukolaine

(Presented at the Anglo-Soviet Seminar on Nuclear Data
for Reactor Computations, Dubna, 18-22 June 1968
(Paper No. ASS-68/18))

The heavy-water reactor at the Institute of Theoretical and Experimental Physics was used to study the total neutron cross-sections of ^{230}Th in the thermal and resonance energy ranges. The sample of ^{230}Th was separated from uranium ores (1 gram). The measurements were carried out on a mechanical chopper. The total neutron cross-section of ^{230}Th at the thermal energy (0.025 eV) was (71.8 ± 2) barns, the neutron capture cross-section (56.8 ± 3) barns, and the potential scattering cross-section (15 ± 2) barns.

In the energy range up to 600 eV 29 neutron levels were measured, including one negative level. The level parameters are given. The level parameters were used to calculate the neutron strength function and the total resonance integral, which were equal to $(1.30 \pm 0.3) \times 10^{-4}$ and (1035 ± 85) barns, respectively. The mean neutron level spacing for ^{230}Th is (9.8 ± 1.6) eV.

Neutron level parameters

N	E(eV)	Γ_γ(meV)	Γ_n(meV)	$g\Gamma_n^0$(meV)	Ires (barns)
1	-0,075 ± 0,030	29,0 ± 1,8		13,1 ± 0,2·10^{-3}	
2	1,431 ± 0,014	27,61 ± 1,8	0,39 ± 0,06	0,326 ± 0,050	769,4 ± 622
3	17,50 ± 0,06	29,54 ± 1,8	12,1 ± 1,7	2,91 ± 0,41	112,0 ± 200
4	23,64 ± 0,07	30,9 ± 3,5	9,8 ± 1,0	2,01 ± 0,20	54,0 ± 9,5
5	32,43 ± 0,10	29,9 ± 5,2	3,4 ± 0,5	0,597 ± 0,038	11,83 ± 3,00
6	39,30 ± 0,14	29,1 ± 3,4	7,9 ± 1,8	1,231 ± 0,284	15,9 ± 4,4
7	48,22 ± 0,19	29,0 ± 4,9	11,5 ± 1,1	1,656 ± 0,154	14,50 ± 3,34
8	64,7 ± 0,3	29,0 ± 1,8 assumed	2,35 ± 0,34	0,355 ± 0,043	2,56 ± [illegible]
9	75,8 ± 0,4		4,5 ± 0,5	0,517 ± 0,057	2,85 ± [illegible]
10	85,5 ± 0,4	"	25,6 ± 4,3	[illegible] ± 0,47	8,25 ± 0,67
11	102,8 ± 0,5	"	7,9 ± [illegible]	0,772 ± 0,178	2,32 ± 0,40
12	105,7 ± 0,5	"	1,6 [illegible]	0,154 ± 0,042	0,53 ± 0,14
13	116,4 ± 0,7	"	37,0 ± 13,0	3,45 ± 1,20	4,25 ± 0,84
14	133,8 ± 0,8	"	7,5 ± 2,3	0,648 ± 0,295	1,38 ± 0,42
15	139,0 ± 0,9	"	2,35 ± 1,15	0,199 ± 0,098	0,46 ± [illegible]
16	148,2 ± 1,0	"	5,85 ± 2,70	0,480 ± 0,225	0,89 ± 0,31
17	172,3 ± 1,2	"	8,3 ± 2,8	0,631 ± 0,204	0,87 ± 0,22
18	183,3 ± 1,3	"	39,6 ± 17,8	[illegible] ± 1,31	2,06 ± 0,28
19	193,6 ± 1,5	"	78,5 ± 35,0	5,72 ± 2,52	2,29 ± [illegible]
20	207,4 ± 1,5	"	128,5 ± 33,0	8,92 ± 2,28	2,28 ± 0,17
21	221,0 ± 2,0	"	42,8 ± 15,7	2,87 ± 1,31	1,43 ± 0,24
22	240,0 ± 2,0	"	35,6 ± 15,8	2,36 ± 1,02	1,18 ± 0,18
23	267 ± 3	"	5,3 ± 3,6	0,658 ± 0,215	[illegible] ± 0,13
24	294 ± 3	"	122,5 ± 45,0	7,15 ± 2,53	1,15 ± 0,08
25	346 ± 3	"	170,0 ± 71,0	9,15 ± 3,80	0,65 ± 0,07
26	400 ± 5	"	1250 ± 63,0	6,55 ± [illegible]	0,63 ± 0,05
27	458 ± 5	"	260,5 ± 97,5	12,2 ± 4,5	0,49 ± 0,12
28	485 ± 6	"	123,0 ± 76,0	5,59 ± 3,46	0,41 ± 0,24
29	563 ± 7	"	216,0 ± 73,0	9,1 ± 3,1	0,33 ± 0,03

A.F. Ioffe Physico-Technical Institute, USSR Academy of Sciences*

DEPENDENCE OF GAMMA-RADIATION ANISOTROPY ON THE OVERALL KINETIC ENERGIES OF FRAGMENTS AND ON THEIR MASS RATIO IN THE FISSION OF ^{235}U BY SLOW NEUTRONS

G.V. Valsky, G.A. Petrov, Yu.S. Pleva

(Submitted to Jadernaja Fizika)

The paper describes measurements of:

1. The dependence of gamma-radiation anisotropy on the overall kinetic energies of fragments (Table I, W(30°));

2. The dependence of the number of gamma-quanta emitted in one fission event at an angle of 90° to the line along which the fragments fly apart on the overall kinetic energies of the fragments (B in arbitrary units, Table I);

3. The dependence of gamma-radiation anisotropy on the fragment mass ratio (W(30°) in Table II, given as a function of the mass of a heavy fragment);

4. The dependence of the number of gamma-quanta, emitted in one fission event at an angle of 90° to the line along which the fragments fly apart on the fragment mass ratio (B in Table III, given as a function of the mass of a heavy fragment, in arbitrary units).

5. The dependence of the number of gamma-quanta per unit solid angle emitted by a fragment at an angle of 30° to its direction of movement on the mass of the fragment, (B in Table IV, in arbitrary units).

All the measurements were made for gamma-quanta of energy greater than 100 keV. The anisotropy is determined, without units, as the ratio of the gamma-radiation intensities at angles of 30° and 90° to the line along which the fragments fly apart. No corrections were made for the finite nature of the solid angles.

The mean ratio of the gamma-radiation intensities at angles of 0° and 90°, without units, and with all corrections, is 0.128 ± 0.008.

The mean ratio of the gamma-radiation intensity for the light-fragment group to that for the heavy group is 1.4 ± 0.2.

---

* Edited by G.Z. Borukhovich.

Table 1

Ek	W30°	ΔW30°	B	ΔB
I33,44	-0,0245	0,0393	I2,86	I,97
I37,50	0,0953	0,03I8	I0,26	0,64
I4I,45	0,0645	0,0208	9,45	0,32
I45,36	0,0788	0,0I50	8,67	0,08
I49,I7	0,08I6	0,0I05	8,07	0,06
I53,29	0,0690	0,0082	7,85	0,04
I57,26	0,0798	0,0068	7,53	0,03
I6I,I5	0,0750	0,006I	7,36	0,03
I6I,I6	0,0772	0,0060	7,09	0,03
I68,98	0,0837	0,0062	6,83	0,03
I72,95	0,089I	0,0069	6,55	0,03
I77,00	0,0992	0,0082	6,26	0,03
I80,98	0,I099	0,0I00	6,00	0,04
I84,88	0,II62	0,0I32	5,70	0,05
I88,74	0,II54	0,0I95	5,3I	0,07
I92,64	0,I666	0,0360	4,94	0,I2
I96,52	0,I552	0,0680	4,45	0,46
200,7I	0,I429	0,I574	4,52	0,74

Table II

M	W(30°)	ΔW(30°)
I23,5	0,I56	0,054
I28,I	0,090	0,03I
I3I,2	0,096	0,0I4
I34,2	0,086	0,008
I37,3	0,074	0,007
I40,0	0,082	0,007
I42,9	0,086	0,006
I45,9	0,093	0,008
I48,8	0,085	0,0I2
I5I,9	0,II4	0,02I
I55,2	0,08I	0,040
I58,5	0,07I	0,07I

Table III

M	B	ΔB
I22,33	6,6I7	±0,268
I28,I0	6,49I	±0,I3I
I3I,20	6,202	±0,056
I34,I5	6,283	±0,034
I37,24	6,644	±0,029
I40,04	7,I33	±0,030
I42,86	7,473	±0,03I
I45,85	7,587	±0,038
I48,8I	7,589	±0,070
I49,60	7,466	±0,I00
I5I,I5	7,060	±0,I30
I52,75	7,302	±0,I80
I55,I7	7,396	±0,I92
I58,44	7,402	±0,298

Table IV

M	B	Δ B
77,7	I,90	4,09
80,9	4,83	2,20
84,0	2,94	I.I4
87,2	4,90	0,66
90,I	5,25	0,44
93.I	4,43	0,36
95,9	4,67	0,36
98,8	5,47	0,33
IOI,8	5,44	0,40
I04,8	5,64	0,65
I07,9	7,46	I,53
III,2	2,73	3,23
I22,4	4,96	3,23
I28,I	-0,42	I,53
I3I,2	I,26	0,65
I34,2	I,50	0,40
I37,2	I,77	0.33
I40.I	3,I7	0,36
I42,9	3,85	0,36
I45,9	3,25	0,44
I48,8	3,4I	0,66
I5I,9	5,I3	I,I4
I55,2	3,33	2,20
I58,4	6,06	4,09

YIELD OF LIGHT NUCLEI FORMED DURING FISSION OF ^{235}U BY THERMAL NEUTRONS

A.A. Vorobev, V.T. Grachev, A.P. Komar, A.M. Nikitin, D.N. Seliverstov

(Submitted to Atomnaja Energija)

The yield and energy spectra of hydrogen, helium, lithium and beryllium isotopes formed during ^{235}U fission by thermal neutrons were measured using a magnetic-deflection mass spectrometer. The measured spectra of ^{2}H, ^{3}H, ^{6}He and ^{4}He appear to have an almost Gaussian distribution. The distribution parameters and the yield of ^{2}H, ^{3}H, ^{6}He and ^{4}He are given in Table 1. The yield of lithium and beryllium isotopes and of ^{3}He and ^{8}He in the measured energy ranges is given in Table 2. The data in Table 2 should be regarded as provisional. An anomalously low yield is observed for the isotopes ^{3}He, ^{6}Li and ^{7}Be.

<u>Table 1</u>

Yield and energy distribution of ^{2}H, ^{3}H, ^{4}He, ^{6}He

Isotope	Measured energy range MeV	Energy at distribution max. MeV	HWHM MeV	Yield in measured energy-range for 100 α-particles	Total yield for 100 α-particles*
^{2}H	4,8-I5,0	8,5 ± 0,3	3,4 ± 0,2	0,39 ± 0,03	0,44 ± 0,04
^{3}H	4,2-II,6	8,I ± 0,2	3,I ± 0,I	5,2 ± 0,I5	6,3 ± 0,2
^{4}He	I0,6-34,2	I5,7 ± 0,2	4,8 ± 0,I5	90	I00
^{6}He	9,0-20,I	II,8 ± 0,3	4,5 ± 0,2	I,04 ± 0,07	I,4 ± 0,I

* In calculating the total yield from the measured yield, the energy distribution was assumed to be Gaussian.

Table 2

He, Li and Be isotope yields
(provisional results)

Isotope	Energy range MeV	Yield per 10^4 α-particles*
^{3}He	I0,5 -22,0	≲ 0,5
^{8}He	9,I -I2,2	> I,I
^{6}Li	I6,0 -28,4	≲ 0,04
^{7}Li	I5,7 -26,6	I,9
^{8}Li	I5,7 -24,0	0,80
^{9}Li	I5,3 -22,2	I,I
^{7}Be	24,5 -44,0	≲ 0,00I
^{9}Be	23,4 -37,0	0,5
^{I0}Be	23,7 -35,0	3,2
^{II}Be	24,0 -33,0	0,09
^{I2}Be	24,5 -3I,0	≲ 0,04

* The isotope yield in the measured energy interval is referred to the total yield of alpha particles

V.G. Khlopin Radium Institute, Leningrad*

RADIOCHEMICAL DETERMINATION OF THE YIELD OF RARE-EARTH ELEMENTS IN THE FISSION OF ^{239}Pu AND ^{241}Pu BY SLOW NEUTRONS

N.V. Skovorodkin, A.V. Sorokina, S.P. Bugorkov,
A.S. Krivokhatsky, K.A. Petrzhak

(Submitted to Radiokhimija)

The aim of this work was to determine the cumulative yields of rare-earth elements and yttrium in the fission of ^{239}Pu and ^{241}Pu by slow neutrons.

For extracting rare-earth groups and yttrium from the irradiated compounds and for removing other fission products from them precipitation methods were employed. Plutonium was removed by anion exchange. The rare-earth elements and yttrium were separated chromatographically using ammonium alpha-oxyisobutyrate. The activity was measured in a 4π beta flow counter.

The cumulative yields are all given relative to the cumulative yield of ^{144}Ce. The yields were calculated taking account of accumulation during irradiation and decay when irradiation ceases. The yields obtained are given in the table.

* Edited by A.I. Obukhov.

Table

Cumulative yields of the isotopes of rare-earth elements relative to the cumulative yield of ^{144}Ce, in the fission of ^{241}Pu and ^{239}Pu by slow neutrons

No.	Isotope	Relative yields	
		^{239}Pu	^{241}Pu
I.	La - I4I	I,22 ± 0,04	I,I0 ± 0,02
2.	Ce - I4I	I,32 ± 0,02	I,I6 ± 0,02
3.	Ce - I43	I,04 ± 0,03	0,950 ± 0,02
4.	Pr - I43	I,I0 ± 0,02	I,05 ± 0,0I
5.	Ce - I44	I,000	I,000
6.	Pr - I45	0,9I9 ± 0,020	0,736 ± 0,022
7.	Nd - I47	0,553 ± 0,0II	0,572 ± 0,008
8.	Pm - I47	0,556 ± 0,022	0,570 ± 0,023
9.	Nd - I49	0,297 ± 0,0I0	0,360 ± 0,0I0
I0.	Pm - I49	0,337 ± 0,006	0,369 ± 0,0I4
II.	Pm - I5I	0,I9I ± 0,005	0,207 ± 0,0I0
I2.	Sm - I53	0,0942 ± 0,00I8	0,I27 ± 0,003
I3.	Eu - I55	-	0,0566 ± 0,005I
I4.	Sm - I56	0,0248 ± 0,0006	0,0387 ± 0,00I0
I5.	Eu - I56	0,0322 ± 0,0005	0,4I6 ± 0,0007
I6.	Eu - I57	0,0I98 ± 0,0005	0,03I9 ± 0,0008
I7.	Gd - I59	0,0056I ± 0,00667	0,0II3 ± 0,0002
I8.	Tb - I6I	0,00I34 ± 0,00002	0,00I99 ± 0,00004
I9.	Y - 9I	0,639 ± 0,005	0,407 ± 0,007

THE ENERGY DISTRIBUTION OF ALPHA PARTICLES FROM THE FISSION OF PLUTONIUM-241 AND AMERICIUM-241 BY THERMAL NEUTRONS

Z.I. Soloveva

(Submitted to Jadernaja Fizika)

Type P-9-0 nuclear photographic emulsions were used to study the energy spectra of long-range alpha particles formed during the fission of plutonium-241 and americium-241 by thermal neutrons, using a method previously described [1]. The spectra are closely approximated by a Gaussian distribution, whose parameters are determined, together with the statistical errors, by the least-squares method:

	^{241}Pu	^{241}Am
Most probable energy, E_{max}	15.0 ± 0.6 MeV	15.8 ± 1.2 MeV
Half-height width, Δ E	8.3 ± 0.5 MeV	11.2 ± 0.9 MeV

A comparison is made with the alpha energy spectra in the fission of other isotopes.

REFERENCE

[1] N.A. Perfilov, Z.I. Soloveva, R.A. Filov, G.I. Khlebnikov, Dokl. Akad. Nauk SSSR 136 (1961) 581.

Zh. eksp. teor. Fiz. 44 (1963) 1832.

THE ENERGY SPECTRA OF PROMPT NEUTRONS IN THE FISSION OF ^{244}Cm, ^{242}Pu AND ^{239}Pu

L.M. Belov, M.V. Blinov, N.M. Kazarinov,
A.S. Krivokhatsky, A.N. Protopopov

(Submitted to Jadernaja Fizika)

The time-of-flight method was used to measure the neutron energy spectra for spontaneous fission of ^{244}Cm and ^{242}Pu and the neutron energy spectra for fission of ^{239}Pu by thermal neutrons. "Zero time" was taken as the moment the fission gamma quanta were recorded. The measured neutron spectra can be approximated by a Maxwellian distribution $N(E) \sim \sqrt{E e^{-E/T}}$. The parameters T were found equal to 1.37 ± 0.04 MeV, 1.21 ± 0.07 MeV and 1.35 ± 0.04 MeV for ^{244}Cm, ^{242}Pu and ^{239}Pu respectively. The dependence of the mean neutron energy $\bar{E}_n$ on the average number of neutrons emitted $\bar{\nu}$ agrees with the results of Terrell's calculations for the model of boil-off neutrons from excited fragments.

Table

E-neutron energy in MeV, N(E)-ordinate value in relative units, Δ %-statistical error in %

^{244}Cm				^{242}Pu				^{239}Pu			
E	$N(E)$	$\frac{N(E)}{\sqrt{E}}$	Δ%	E	$N(E)$	$\frac{N(E)}{\sqrt{E}}$	Δ%	E	$N(E)$	$\frac{N(E)}{\sqrt{E}}$	Δ%
6,20	240	97	I0	4,84	I50	70	I4	7	I9I	72	I0
5;I0	464	205	9	4,06	200	I30	I2	5	7II	3I8	8
4,30	835	402	7	3,45	370	200	II	4	I400	700	7
3,80	I033	530	6	2,98	470	273	I0	3	2670	I540	6
3,07	I665	950	6	2,59	620	384	9	2,5	3520	2220	5
2,5	2380	I500	5	2,28	730	485	8	2,0	4780	3380	4
2,07	2920	2020	4,5	2,02	900	633	7	I,75	5300	4020	4
I,90	3040	2200	4,5	I,80	II20	835	7	I,50	5870	4800	4
I,70	3360	2580	4,5	I,6I	I200	I020	7	I,35	6I30	5380	4
I,54	3680	2690	4,5	I,45	I450	I200	7	I,I5	6350	5930	4
I,4I	3920	3300	4,5	I,34	I5I0	I300	7	I,00	6070	6670	4
I,28	4020	3550	4,5	I,20	I570	I435	7	0,90	6760	7I30	5
I,I6	4460	4080	4,5	I,I0	I6I0	I567	7	0,80	6960	7800	5
I,I0	4390	4I90	4,5	I,0I	I630	I635	7	0,70	7030	8400	6
I,03	4200	4200	4,5	0,93	I660	I730	8	0,60	7040	9I00	7
0,95	4770	4900	4,5	0,77	I700	I930	8	0,50	7350	I0400	8
0,88	4500	4800	5	0,65	I550	I930	9	0,40	70I0	IIIOO	9
0,78	4630	5250	5	0,52	I920	2660	I0	0,30	6490	II850	9
0,68	46I0	5600	6	0,37	2030	3300	I0				
0,59	4760	6200	6								
0,49	4340	6200	7								
0,4I	4360	6800	7								
0,39	4I40	7I00	8								
0,29	3220	7I00	9								

X-RAYS FROM FRAGMENTS IN FISSION ACCOMPANIED BY RELEASE OF LONG-RANGE ALPHA PARTICLES

S.M. Solovev, V.P. Eismont

(Submitted to "Jadernaja Fizika")

To determine the nuclear charge of the fragments and the nature of their formation in a fission process involving the release of a long-range alpha particle, the authors measured the yield and energy distribution of the K-series of characteristic rays emitted in this process.

The equipment consisted of three proportional counters, arranged in coincidence, which recorded the X-ray quanta, fragments and alpha particles in the fission of ^{235}U by thermal neutrons (reactor in the Physico-Technical Institute, USSR Academy of Sciences).

The measured K-radiation spectrum is shown in the figure. The main difference from the binary-fission spectrum obtained under the same conditions is the shift in the right-hand (descending) slopes of the peaks for light and heavy fragments by about 2 keV, which corresponds to a change of about two units in the fragment charge.

A value of 0.9 ± 0.2 was obtained for the ratio between the radiation intensity for fission accompanied by release of an alpha particle and that for normal (binary) fission.

The results show the close similarity between normal fission and fission accompanied by the release of a long range alpha particle.

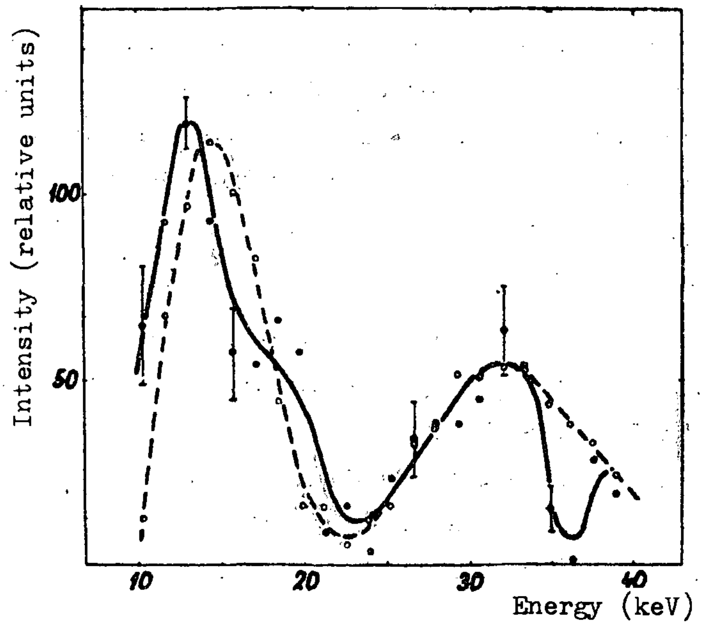

Fig. 1 Measured spectrum of K-radiation from fragments.

• - alpha fission

o - binary fission

Showing statistical errors calculated as errors for difference measurements (the errors for binary fission do not exceed the point size).

ENERGY DISTRIBUTIONS OF RETARDED FRAGMENTS

S.M. Solovev, V.P. Eismont

(Submitted to Atomnaja Energija)

In order to obtain new data on fission-fragment energy losses, a semi-conductor detector was used to measure the kinetic-energy distributions of fragments which had passed through a layer of air of known thickness, in the fission of ^{235}U by thermal neutrons. The authors determined the dependence of the mean energies and energy spread of light and heavy fragments on retardation length.

The experimental "flight path/energy" curve is given in the figure, which also shows Fulmer's data [1], obtained using scintillation detectors, and a curve calculated from the theory of Lindhard et al. [2]. It can be seen that basically the divergence from Fulmer's results does not exceed the limits of experimental error. It can also be seen that theory underestimates fragment-energy losses at the beginning of the flight path.

REFERENCES

[1] C.B. Fulmer, Phys. Rev. 139, B54 (1965)

[2] L. Lindhard, M. Scharff, H.E. Schiøtt, Mat.Fys.Medd.Dan. Vid. Selsk. 33, No. 14 (1963)

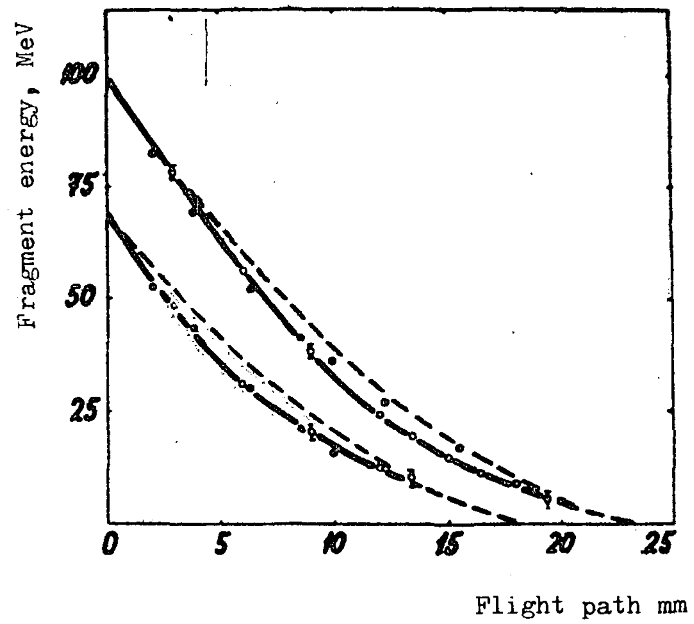

The dependence of the kinetic energy of ^{235}U fission fragments on the flight-path length in normal air for light and heavy fragments (upper and lower curves, respectively).
o - data from the present work, • - Fulmer's data; the dotted curves are calculated from the theory of Lindhard et al. All curves are for initial fragment energies of 69.6 MeV and 100.1 MeV.

COMPARATIVE MEASUREMENTS OF CHARACTERISTIC K-RADIATION IN ^{233}U FISSION

Yu.P. Davydov, S.M. Solovev, V.P. Eismont

(Submitted to Jadernaja Fizika)

To widen the range of nuclei which have been studied and so get a better understanding of the emission of X-rays by fragments and of the properties of nuclear charge distribution in measurements carried out on ^{235}U, data were obtained on the K-radiation of fragments produced through the fission of ^{233}U by thermal neutrons.

The method used was similar to that described in Reference [1]. The value 0.96 ± 0.08 was obtained for the X-ray quantum ratio between ^{233}U and ^{235}U fission.

It was found that for ^{233}U the mean radiation energy for a light fragment was 0.3 ± 0.1 keV less than for ^{235}U, and for a heavy fragment it was 0.2 ± 0.1 keV greater. The difference observed in the energies corresponds to the difference in charge: -0.4 ± 0.1 for light fragments and +0.2 ± 0.1 for heavy fragments, or as an average +0.3 ± 0.1 units of charge.

The result agrees qualitatively with the predicted rule that decay chains should be of equal length and shows that, unlike the mass, the charge of a heavy fragment is not unchanged when the nucleonic state of the fissioning nucleus changes.

REFERENCE

[1] S.M. Solovev, V.P. Eismont, X-rays from fragments in fission accompanied by release of long-range alpha particles, Jadernaja Fizika, 6, (1968) 96.

Institute of Physics, Ukrainian Academy of Sciences, Kiev*

THE ELASTIC SCATTERING OF POLARIZED NEUTRONS OF ENERGY 1.5 MeV BY NUCLEI

I.A. Korzh, V.A. Mishchenko, M.V. Pasechnik, N.M. Pravdivy, I.E. Sanzhur, I.A. Totsky

(Submitted to Ukrainskij Fizičeskij Zhurnal (Ukrainian Journal of Physics))

This study deals with the elastic scattering of polarized neutrons of energy 1.5 MeV on Mg, Al and Si nuclei in the scattering-angle range 20–143°. The measured differential cross-sections of elastic scattering of polarized neutrons (P_1 (33°) = (36 ± 2)%) were used to determine the differential cross-sections of elastic scattering of non-polarized neutrons as a function of scattering angle, and to find the elastic scattering cross-sections and transport cross-sections. The measured differential cross-sections for non-polarized neutrons are given in the form of a Legendre polynomial expansion $\frac{d\sigma_{el}}{d\Omega} = \sum_{i=0}^{5} A_i P_i (\cos \Theta)$. The numerical values of the calculated constants and coefficients A_i are given in Table I. Table II gives the numerical values of the polarizing power of Mg, Al and Si nuclei for the neutron energy studied.

* Edited by I.A. Korzh.

Table I

Nucleus	σ_{el} barn	σ_{tre} barn	$\overline{\text{Cos}\,\Theta}$	A_0 barn/ ster.	A_1 barn/ ster.	A_2 barn/ ster.	A_3 barn/ ster.	A_4 barn/ ster.	A_5 barn/ ster.
Mg	2,542±0,053	I,543±0,075	0,393±0,0I7	0,202	0,I95	0,I3I	0,050	0,007	0,026
Al	2,55I±0,059	I,464±0,080	0,426±0,0I8	0,202	0,223	0,032	0,007	-0,00I	0,006
Si	2,682±0,043	I,859±0,057	0,307±0,0I0	0,2I3	0,I80	0.I48	-0,04I	0,0I2	-0,006

Table II

Θ_{lab}	P_2, %			Θ_{lab}	P_2, %		
	Mg	Al	Si		Mg	Al	Si
20°	I,8±6,6	-0,3±2,6	-5,7±3,8	85°	24,I±4,4	-20,0± 4,8	I6 ±4,2
30°	7,8±3,0	-3,9±2,4	-5,2±3,6	I00°	23,6±5,9	-8,9± 6,9	I7,2±4,6
40°	I4,9±4,8	-I,2±2,0	+2,7±2,9	II5°	6,2±5,0	-8,2± 5,3	II,4±6,2
55°	20,2±5,3	-5,5±4,0	I2,5±3,4	I30°	-5,5±6,3	+2,8±II,6	2,4±6,3
70°	24,7±4,0	-I0,7±2,4	I7,0±4,I	I43°	-6,I±7,I	-7 ±II,4	2,2±6,3

FAST-NEUTRON RADIATIVE-CAPTURE CROSS-SECTION FOR THE ISOTOPES ^{63}Cu, ^{65}Cu, ^{186}W

G.G. Zaikin, I.A. Korzh, N.T. Sklyar and I.A. Totsky

(Submitted to Atomnaja Energija)

The activation method was used to measure the energy dependence of the fast-neutron radiative-capture cross-section for the isotopes ^{63}Cu, ^{65}Cu and ^{186}W in the energy range 200-3100 keV at intervals of 30-60 keV. The activities induced in the samples by fast and thermal neutrons were compared. The reference cross-sections were the fast and thermal-neutron ^{235}U fission cross-sections [1], and the thermal-neutron activation cross-sections for the isotopes ^{63}Cu, ^{65}Cu and ^{186}W, which were taken equal to 4.5 ± 0.2 barns [2], 2.3 barns [3] and 38 ± 2 barns [3] respectively.

Tables I, II and III give the measured radiative-capture cross-sections together with the ^{235}U fission cross-sections. The errors given do not include the errors in the reference cross-sections.

REFERENCES

[1] Neutron Cross-Sections, BNL-325, 2nd edition, Supp. 2, vol. III (1965)

[2] I.V. Gordeev, et al., Jaderno-fiziteskie konstanty (Nuclear Physics Constants), Gosatomizdat, Moscow, 1963

[3] Neutron Cross-Sections BNL-325, 2nd edition, Supp.2, vol IIa (1966)

Table I

	^{63}Cu	
E_n keV	^{235}U σ_f, barn	$\sigma_{n\gamma}$; m barn
230	I,38	23,7± 0,9
350	I,27	I7,8± 0,9
4I0	I,22	I6,0± 0,6
470	I,20	I5,7± 0,6
560	I,I7	I4,2± 0,5
690	I,I8	I2,2± I,I
790	I,I5	I2,8± 0,6
II00	I,27	I2,0± 0,6
I290	I,24	II,I ±0,4
I5I0	I,27	8,74±0,26
I7I0	I,30	6,90±0,20
I9I0	I,3I	6,80±0,20
2II0	I,3I	6,27±0,24
2320	I,3I	6,30±0,30
25I0	I,30	5,50±0,I6
2720	I,30	5,55±0,30
29I0	I,27	5,60±0,38
3II0	I,27	5,I8±0,34

Table II

E_n keV	^{235}U σ_f, barn	$\sigma_{n\gamma}$; m barn
230	I,38	II,9 ± 0,5
350	I,27	I0,6 ± 0,5
4I0	I,22	7,90± 0,60
580	I,I7	8,82± 0,26
690	I,I8	7,80 ± 0,73
790	I,I8	8,I5 ± 0,24
9I0	I,20	6,96 ±0,38
I000	I,23	9,43± 0,I9
II00	I,27	8,62± 0,56
I270	I,24	8,04± 0,41
I330	I,27	7,22± 0,48
I4I0	I,27	7,7I+ 0,46
I5I0	I,27	6,95± 0,25
I630	I,30	6,49± 0,I9
I880	I,3I	6,82± 0,30
I990	I,3I	6,I4± 0,28
2I70	I,3I	5,48± 0,2I
2320	I,3I	5,I9± 0,22
25I0	I,30	5,I9± 0,20
2570	I.27	4,58± 0,I7
3II0	I,27	4,25± 0,40

Table III

^{186}W

E_n keV	^{235}U σ_f, barn	$\sigma_{n,\gamma}$; mbarn
230	1,38	102 ± 9
350	1,27	78 ± 3
410	1,22	62 ± 5
470	1,20	63 ± 4
530	1,17	48,5 ± 1,5
690	1,18	59 ± 6
1100	1,27	43 ± 6
1310	1,24	42,0 ± 3,6
1510	1,27	37,4 ± 1,5
1710	1,30	39,0 ± 1,5
1910	1,31	33,5 ± 1,5
2110	1,31	29,1 ± 0,8
2320	1,31	27,5 ± 1,0
2510	1,30	23,3 ± 1,1
2720	1,30	22,7 ± 0,9
2910	1,27	19,8 ± 1,1
3110	1,27	23,1 ± 1,5

SCATTERING OF 2.9 MeV NEUTRONS ON TITANIUM AND CHROMIUM NUCLEI

M.V. Pasechnik, M.B. Fedorov, T.I. Yakovenko

(Submitted to Ukrainskij Fizičeskij Zhurnal
(Ukrainian Journal of Physics))

The time-of-flight method was used to study the angular distributions of 2.9 MeV neutrons, elastically scattered by titanium and chromium and inelastically scattered with first-level excitation of the main isotopes of these nuclei.

The measured angular distributions of elastically scattered neutrons corrected for multiple scattering and geometric dispersion, are given in Table I:

Table I

$\cos\theta_{lab}$	Differential cross-section in relative units	
	Titanium	Chromium
0,87	21,2 ± 0,6	25,4 ± 0,4
0,70	11,2 ± 0,4	15,2 ± 0,4
0,50	3,8 ± 0,2	4,8 ± 0,3
0,26	0,9 ± 0,2	1,3 ± 0,2
0	1	1
-0,26	1,4 ± 0,3	2,2 ± 0,2
-0,50	2,7 ± 0,3	3,1 ± 0,3
-0,70	3,2 ± 0,3	3,7 ± 0,3

The corresponding results for inelastic scattering are given in Table II:

Table II

$Cos\theta_{lab}$	Differential cross-section in relative units	
	Titanium	Chromium
0,87	0,9 ± 0,I	0,6 ± 0,3
0,70	I,I ± 0,I	I,4 ± 0,I
0,50	0,9 ± 0,I	I,2 ± 0,I
0,26	I,0 ± 0,I	0,9 ± 0,I
0	I	I
-0,26	I,0 ± 0,I	0,9 ± 0,I
-0,50	I,I ± 0,I	I,0 ± 0,I
-0,70	0,9 ± 0,I	I,2 ± 0,I

The absolute values of the differential inelastic-scattering cross-sections for the angle 90° are obtained by a comparison with the known (n,p) scattering cross-section for a polyethylene sample. They are:

For titanium: $d\sigma(90^\circ)/d\Omega = (79 \pm 4)\frac{mb}{ster}$

For chromium: $d\sigma(90^\circ)/d\Omega = (41 \pm 5)\frac{mb}{ster}$

MEASUREMENTS OF TOTAL SCATTERING CROSS-SECTIONS FOR SEPARATED ISOTOPES IN THE THERMAL AND EPITHERMAL RANGES

V.P. Vertebny, N.D. Gnidak, E.A. Pavlenko, M.V. Pasechnik

(Submitted to Ukrainskij Fizičeskij Zhurnal)
(Ukrainian Journal of Physics)

The measurements were carried out using the time-of-flight method and 4π geometry on the VVR-M reactor at the Institute of Physics, Ukrainian Academy of Sciences [1].

With this method it is possible to use small amounts of material (10-100 mg) and thin samples ($n\sigma_t < 0.2$) [2].

The results given in Table I were obtained in relation to lead, whose cross-section was taken equal to 11.5 ± 0.2 barns. Samples of metallic cadmium were used in making the measurements. The results given in Tables II and III are related to vanadium, whose cross-section was taken equal to 5.1 ± 0.1 barns. The dysprosium isotopes were used in the oxide form (Dy_2O_3).

Table IV gives the isotopic composition of the dysprosium samples used. If it is assumed that the error in determining the concentration of impurities in the dysprosium sample is half a unit in the last significant figure, then the error in determining the neutron scattering cross-section for E = 0.025 eV must be increased by 0.13 barns for all isotopes.

REFERENCES

[1] I.V. Koloty, et al., Ukrainskij Fizičeskij Zhurnal, 13, 599, 1968.

[2] V.P. Vertebny, et al., Ukrainskij Fizičeskij Zhurnal, 13, 605, 1968.

Table I

Total scattering cross-sections of cadmium isotopes for E_n = 0.3-9.0 eV

No.	Nucleus	σ_s barn
I.	Cd natural	5,6 ± 0,3
2.	Cd^{III}	5,2 ± 0,3
3.	Cd^{II2}	6,9 ± 0,3
4.	Cd^{II4}	5,2 ± 0,3
5.	Cd^{II6}	6,4 ± 0,3

Table II

Total scattering cross-sections of Pb, C and ^{11}B nuclei in the range E_n = 0.02-15 eV.

No.	Nucleus	$\bar{\sigma}_s$ barn
I	Pb	II,5 ± 0,2
2.	C	4,8 ± 0,I
3.	^{11}B	4,9 ± 0,2

Table III

Total scattering cross-sections of the dysprosium isotopes 161, 162, 163, 164

No.	E, eV	^{161}Dy	^{162}Dy	^{163}Dy	^{164}Dy
1.	0.025	22,0 ± 0,4	2,5 ± 0,8	9,7 ± 0,4	262,0 ± 7,0
2.	0.05	20,0 ± 0,3	4,1 ± 0,7	9,7 ± 0,4	250,0 ± 5,0
3.	0,10	20,0 ± 0,2	2,5 ± 0,6	8,6 ± 0,3	250,0 ± 3,0
4.	0,15	18,8 ± 0,2	1,8 ± 0,6	8,4 ± 0,2	240,0 ± 3,0
5.	0,20	18,0 ± 0,2	1,1 ± 0,6	7,9 ± 0,1	230,0 ± 3,0
6.	0,25	18,0 ± 0,2	0,9 ± 0,5	7,0 ± 0,1	220,0 ± 3,0
7.	0,30	17,9 ± 0,2	0,6 ± 0,5	6,4 ± 0,1	210,0 ± 3,0
8.	0,40	17,2 ± 0,2	0,3 ± 0,4	5,9 ± 0,1	190,0 ± 3,0
9.	0,50	16,8 ± 0,2	0,1 ± 0,3	5,9 ± 0,1	180,0 ± 3,0
10.	0,60	16,5 ± 0,2	0 ± 0,3	5,7 ± 0,1	160,0 ± 3,0
11.	0,7	16,0 ± 0,2	0 ± 0,3	5,2 ± 0,1	150,0 ± 3,0
12.	0,8	15,5 ± 0,2	0 ± 0,3	4,6 ± 0,1	145,0 ± 3,0
13.	0,9	15,0 ± 0,2	0 ± 0,3	4,3 ± 0,2	140,0 ± 3,0
14.	1,0	14,3 ± 0,2	0 ± 0,3	4,0 ± 0,2	130,0 ± 3,0
15.	1,2	14,1 ± 0,2	0 ± 0,3	4,0 ± 0,2	120,0 ± 3,0
16.	1,5		0,2 ± 0,3		92,0 ± 3,0
17.	2,0		0,7 ± 0,3		76,0 ± 3,0
18.	3,0		8,0 ± 0,3		58,0 ± 2,0
19.	4,0				48,4 ± 2,0
20.	5,0				42,0 ± 1,5
21.	6,0				38,0 ± 1,5
22,0	7,0				33,5 ± 1,5
23.	8,0				32,0 ± 1,5
24.	9,0				28,5 ± 1,5
25.	10,0				27,0 ± 1,5

Table IV

Isotopic composition of dysprosium samples

	Chemical compound	Isotopic composition in %						
Dysprosium 161	Dy_2O_3	-	-	0,6	94,2	3,5	1,1	0,6
" 162	-"-	-	-	0,2	1,6	94,0	3,3	0,9
" 163	-"-	-	-	0,2	0,4	2,1	92,3	4,5
" 164	-"-	-	-	0,1	0,3	0,8	1,8	97,0

NEUTRON RESONANCES IN THE ISOTOPES ^{130}Ba AND ^{132}Ba

V.P. Vertebny, A.I. Kalchenko, M.V. Pasechnik and Zh.I. Pisanko

(Submitted to Ukrainskij Fizičeskij Zhurnal (Ukrainian Journal of Physics))

The time-of-flight method was used on the VVR-M reactor to measure the transmission of samples of natural barium and the barium isotopes 130 and 132 in the energy interval 3-1000 eV (with a resolution of 0.05 msec/m and 0.03 μsec/m). In making the measurements use was made of steel containers with slit dimensions 28 x 2 x 8 mm. The parameters of the samples are given in the table. ^{130}Ba levels were observed with energy 46.4 ± 0.4 eV and 58.24 ± 0.7 eV, and neutron widths of Γ_n = 27 ± 7 meV and Γ_n = 144 ± 27 meV respectively. It is probable that levels 137 ± 3 eV and 186 ± 4 eV are also associated with ^{130}Ba. For the isotope ^{134}Ba no levels were observed in the range of interest.

Composition and concentration of nuclei in samples

Isotope sample	Natural Ba		^{130}Ba		^{132}Ba	
	C	n	C	n	C	n
I30	0,I0I	0,0738	I4,4	6,5723	0,I	0,0535
I32	0,097	0,0709	I	0,4564	8,2	4,386I
I34	2,42	I,7680	4,3	I,9626	I0,8	5,7768
I35	6,59	4,8I45	7,7	3,5I43	II,0	5,8839
I36	7,8I	5,7058	8,0	3,65I3	8,6	4,600I
I37	II,32	8,2702	I0,3	4,70I0	9,6	5,I349
I38	7I,66	52,353	54,5	24,783I	5I,7	27,6538

n = number of nuclei per cm^2 in units of 10^{20} cm^{-2}

C = concentration of nuclei in %

NEUTRON RESONANCES OF RARE ISOTOPES OF GADOLINIUM

V.P. Vertebny, A.I. Kalchenko, M.V. Pasechnik, Zh.I. Pisanko, V.K. Rudyshin

(Submitted to Ukrainskij Fizičeskij Zhurnal (Ukrainian Journal of Physics))

The time-of-flight method was used on the VVR-M reactor to measure the transmission of the rare isotopes gadolinium 152 and 154, and of natural gadolinium, for neutrons in the energy range 0.7-3 eV (resolution 0.2 μsec/m) and 3-1000 eV (resolution 0.05 μsec/m). The sample data are given in Table I. The levels were identified and the neutron widths calculated for the isotopes 152 and 154 (Table II). The mean spacing obtained between levels is given together with data for other gadolinium isotopes taken from the literature (Table III).

REFERENCE

[1] Gilbert, A., Cameron, A., Can. Journ. Phys. 43, 1446 (1965)

Table I

Isotope	Sample					
	152		154		natural	
	n	C	n	C	n	C
I52	I0,86	30,9	-	-	0,09	0,2
I54	3,23	9,3	I9,63	57,0	I,05	2,I5
I55	7,4I	2I,5	II,I9	32,7	7,I6	I4,73
I56	5,2I	I5,2	I,80	5,3	9,88	20,47
I57	2,93	8,6	0,7I	2,I	7,52	I5,68
I58	2,94	8,7	0,64	I,9	II,85	24,87
I60	I,94	5,8	0,33	I,0	I0,3I	2I,9

n = number of nuclei per cm^2 in units of 10^{20} cm^{-2}

C = concentration of nuclei in %

Table II

Gadolinium 152 E_0(eV)	Gadolinium 152 Γ_n^o(meV)	Gadolinium 154 E_0(eV)	Gadolinium 154 Γ_n^o(meV)
3,3I ± 0,04	0,0I	9,4I ± 0,04	0,0I
9,55 ± 0,04	0,03	II,6 ± 0,06	0,I2
I2,5 ± 0,07	I,3	22,7 ± 0,2	2,3
2I,2 ± 0,2	0,I5	30,I ± 0,3	I,4
37,I ± 0,4	I3,0	36,0 ± 0,3	-
39,7 ± 0,4	7,0	47,4 ± 0,5	2,7
43,I ± 0,4	I,I	50,I ± 0,6	-
75,3 + I	6,7	53,5 + 0,8	I,7
88,0 + I	(5,7)?	66,0 + 0,8	2,9
93,5 ± I,5	(9,8)?	70,4 ± 0,9	I,3
		79,6 ± I	-
		I0I ± 2	(I5,5)?
		I40 ± 3	(29,4)?
		I48 ± 3	(24,6)?

Table III

Istotope	I52	I54	I56	I58	I60	I55	I57	
E (MeV)	6,48	6,46	6,35	6,03	5,64	8,53	7,92	
U (MeV)	5,5I	5,50	5,38	5,06	4,67	6,64	6,23	
$D_{obs.}$(eV)	II,5	I0,2	33(I)	-	-	I,8(I)	5,6(I)	

E = binding (excitation) energy

U = effective excitation energy U = E - P(N) - P(Z)

P(N),P(Z)=pair-interaction energy

$D_{obs.}$ = observed spacing between levels

NEUTRON CROSS-SECTIONS OF CADMIUM ISOTOPES

V.P. Vertebny, M.F. Vlasov, N.D. Gnidak, E.I. Grishanin, R.A. Zatserkovsky
A.L. Kirilyuk, V.I. Lependin, M.V. Pasechnik, N.A. Trofimova,
A.F. Fedorova

(Presented at the Anglo-Soviet Seminar on Nuclear Constants
for Reactor Computations, Dubna, 18-22 June 1968
(Paper ASS-68/20))

A neutron spectrometer, intended for working with small amounts of material [1] was used on the VVR-M reactor at the Institute of Physics, Ukrainian Academy of Sciences, to measure total neutron cross-sections of the isotopes ^{111}Cd, ^{112}Cd, ^{114}Cd and ^{116}Cd. The measurements were made using the time-of-flight method with a resolution of 6.7 μsec/m (thermal-neutron energy range). The samples used were in the form of the oxide CdO.

To reduce the amount of the strongly absorbing isotope ^{113}Cd in the samples, the latter were irradiated in the active zone of the VVR-M reactor using an integral neutron flux $\theta = 4.3 \times 10^{20}$. The isotopic composition of the enriched cadmium samples is given in Table I. After irradiation, the concentration of the impurity ^{113}Cd in the samples of ^{111}Cd, ^{112}Cd, ^{114}Cd and ^{116}Cd was $4.5 \times 10^{-4}\%$, $8.6 \times 10^{-4}\%$, $2.6 \times 10^{-4}\%$ and $5.7 \times 10^{-4}\%$, respectively. The integral neutron flux was determined by measuring the neutron transparency of the samples of natural cadmium and boron before and after irradiation.

In addition, the total neutron scattering cross-sections were measured in 4π geometry on non-irradiated samples of metallic cadmium. The experimental equipment is described in reference [2]. The measurements were carried out using the time-of-flight method with a resolution of 3 μsec/m in the energy range 0.3-9 eV. In view of the absence of low-lying levels in the cadmium isotopes 111, 112, 114 and 116, the nuclear scattering cross-section was supposed independent of the neutron energy. Table II gives the total neutron cross-sections, the total scattering cross-sections, the CdO lattice scattering cross-sections (NaCl type lattice), and the capture cross-sections in the form $(\sigma_t - \sigma_s)$ for the isotopes 111, 112, 114 and 116, for $E_n = 0.0253$ Ev.

Table I

Isotopic composition of enriched cadmium samples (in %)

Isotope	Production certificate No.	106	108	110	111	112	113	114	116
III	232	0,2	0,3	II,5	66,7	I4,4	2,5	3,9	0,5
II2	237	0,2	0,4	2,I	I3,I	69,6	4,8	8,7	I,I
II4	279	-	-	0,6	0,7	I,24	I,43	94,86	I,27
II6	233	0,2	0,2	2,6	3,I	6,5	3,2	II,8	72,4

Table II

Neutron cross-sections of cadmium isotopes for E_n = 0.0253 eV (in barns)

Cadmium isotope	Total cross-section	Total scattering cross-section	Lattice scattering cross-section	Capture cross-section $(\sigma_t - \sigma_s)$
III	II ± I,5	5,2 ± 0,3	5 ± I	6 ± I,5
II2	9,4 ± 2,0	6,9 ± 0,3	7,5 ± 0,5	0,75 x/
II4	II,6 ± I,0	5,2 ± 0,3	6,0 ± 0,5	5,6 ± I,2
II6	9,0 ± I,0	6,4 ± 0,3	7,5 ± 0,7	I,5 ± I,0
Natural mixture	-	5,6 ± 0,3	-	-

x/ This is a reactor cross-section determined for balanced concentrations of the isotopes ^{112}Cd and ^{113}Cd.

[1] Vlasov, M.F., Kirilyuk, A.L. Ukrainskij Fizičeskij Zhurnal (Ukrainian Physics Journal) 8, 947, 1963.

[2] Gnidak, N.L., Vertebny, V.P., Pavelenko, E.A. Contribution to the 18th Annual Meeting on Nuclear Spectroscopy and Nuclear Structure, Riga, 1968. Izvestija AN SSSR (in press).

Kiev State University, Department of Nuclear Physics

ANGULAR CORRELATIONS BETWEEN NEUTRONS FROM THE (n,2n) REACTION ON LEAD AND BISMUTH NUCLEI

V.A. Voitenko, G.A. Prokopets, V.I. Strizhak

The authors measured the angular distributions of neutrons from the (n,2n) reaction on lead and bismuth nuclei in the horizontal plane for the range $\alpha = 13^\circ$-180° relative to the direction of release of one of the neutrons - the direction making an angle $\Theta_{II} = 65^\circ$ to the incident flux. The energy of the incident neutrons was $E_n = 14$ MeV. The angular indeterminacy $\Delta\alpha = \pm 15^\circ$. The results for lead and bismuth nuclei are given in the Table.

A certain anisotropy of the angular distributions was noted for both lead and bismuth. There was an increased probability for the release of one of the neutrons in the direction of the incident beam. Both distributions pass through a smooth minimum in the region $\alpha = 135^\circ$ ($\Theta_I = 70^\circ$), after which they increase again to $\alpha = 165^\circ$ ($\Theta_I = 200^\circ$)*. In the range of small relative angles between the two neutron release paths, there is symmetry of the differential cross-section relative to the beam. However, this symmetry is destroyed for very small relative angles $\alpha \approx 10^\circ$. There is an increased probability for the release of two neutrons in one spatial direction ($\alpha \simeq 0^\circ$): the ratio between the cross-section for $\alpha = 13^\circ$ ($\Theta_I = -52^\circ$) and the cross-section for a symmetrical angle (relative to the beam) $\alpha = 117^\circ$ ($\Theta_I = 52^\circ$) is approximately three for both lead and bismuth. This leads to the following conclusions. The identical behaviour of the angular distributions of neutrons from the (n,2n) reaction for bismuth and lead for $\Theta_{II} = 65^\circ$ indicates that only the structure of the neutron states in the nucleus has a significant effect on the process; this structure is the same for ^{209}Bi and for the basic lead isotope ^{208}Pb. Moreover, it cannot be considered that the (n,2n) reaction for $E_n = 14$ MeV has a purely statistical character.

Different types of direct interaction probably also play a part in the mechanism of the (n,2n) reaction in heavy nuclei for $E_n = 14$ MeV. In this event the observed preferential release of two neutrons in one spatial direction shows that it is obviously important to take into account the interaction of neutrons in the end state and does not exclude the possibility of simultaneous release of a correlated neutron pair from the nucleus.

---

* The positive values of Θ_I correspond to the case of the two detectors situated in different half-planes and the negative values correspond to the case of one half-plane.

$$\frac{d^2\sigma}{d\Omega_1\, d\Omega_2}$$

(In arbitrary units)

α^o	Lead	Bismuth
I3,5	I9 ± 9	20 ± 3
25	I0,4± 3,4	9 ± 3
35	2I ± 7	I8 ± 6
85	I6,6± 2,8	I9 ± I
I00	9,2± 0,6	9,7 ± I,4
II0	8,9± 0,6	9 ± I,4
I25	-	8,3 ± 2,4
I35	6,4± 3,4	-
I40	-	4,5 ± I,4
I60	I2,8± I,5	I4,8 ± I,7
I80	9,2± 2,I	II ± 3,4

The errors indicated are averaged over 10-15 cycles of measurements for each point.

Joint Institute of Nuclear Research, Dubna*

NEUTRON CROSS-SECTION AND STRENGTH FUNCTIONS FOR GERMANIUM ISOTOPES

Kh. Maletski, L.B. Pikelner, I.M. Salamatin, E.I. Sharapov

(JINR Preprint R3-3456)

The pulsed reactor at the Joint Institute was used under operating conditions with an electron cyclotron to measure the transmission and radiative capture of neutrons, with a resolution of 3 nsec/m and 12 nsec/m respectively, on separated germanium isotopes. Table I gives the parameters of the levels under study. On the basis of these data the authors calculated the strength functions S_o, the mean radiation widths $\bar{\Gamma}_\gamma$, the mean spacing $\bar{D}_\gamma$ between levels, and the level density parameters a for each germanium isotope. These mean parameters are given in Table II.

---

* Edited by Yu.P. Popov.

Table I

Neutron resonance parameters for germanium isotopes

Target nucleus	E_o eV	ΔE_o eV	Γ_n eV	$\Delta\Gamma_n$ eV	Γ_γ eV	$\Delta\Gamma_\gamma$ eV
^{70}Ge	III5	4	4,6	I,0	0,I60	0,025
	I469	5	0,70	0,I2	0,I50	0,025
	I935	8	0,030	0,006		
	3I40	I5	0,046	0,0I0		
	4230	25	0,055	0,025		
	4378	25	5,9	I,2	0,I85	0,040
	5570	35	33	7		
	6750	35	I5	5		
	8635	45	5I	I2		
	9890	60	52	II		
	I03I0	90	77	I6		
	II040	I00	8,3	4,7		
	II780	I00	22	I0		
	I3200	I00	95	I2		
	I8440	I50	63	24		
	23820	300	75	26		
	25860	300	94	33		
	27600	350	I4I	60		
	28600	400	75	34		
^{72}Ge	252,0	0,5	0,00034	0,000I0		
	736	2	0,0025	0,0008		
	2I80	7	0,046	0,009		
	26I4	8	0,79	0,39	0,I35	0,030
	2743	8	0,40	0,I8	0,230	0,040
	3650	I2	0,83	0,43	0,I20	0,030
	4560	I7	I5	3		
	4949	I9	27	5		
	8980	50	4I	6		
	9640	55	8	5		

	I1170	60	22	4		
	I2070	70	26	7		
	I9080	I30	I46	30		
	29400	300	3I	I7		
^{73}Ge	I02,6	0,2	I,30	0,I2	0,I92	0,030
	204,0	0,4	0,23	0,02	0,2I0	0,030
	224,7	0,4	0,45	0,04	0,I98	0,030
	320,6	0,7	0,23	0,04	0,I90	0,030
	332,0	0,7	I,36	0,I2		
	367,I	0,6	0,72	0,06	0,200	0,030
	408,2	0,6	0,25	0,03	0,200	0,030
	490,3	0,9	2,00	0,I5	0,I85	0,030
	5I6	I	0,038	0,005		
	557	I	0,39	0,04	0,I90	0,030
	668	I	0,026	0,008		
	735	2	0,0I7	0,005		
	752	2	0,020	0,006		
	807	2	0,02I	0,006		
	849	2	0,I4	0,02		
	9I9	2	0,I5	0,02		
	I028	2	0,09	0,02		
	I056	2	0,23	0,06		
	II45	2	2,I	0,6		
	I2I8	3	I,3	0,2	0,2I0	0,030
	I3I3	3	I,3	0,2	0,2I0	0,030
	I353	3	0,29	0,05		
	I526	3	I,2	0,2		
	I650	4	2,5	0,2		
	I802	4	I,6	0,2	0,I90	0,030
	I925	5	0,33	0,20		
	I934	5	0,5	0,2		
	I950	5	0,8	0,3		
	20II	6	4,0	0,4	0,I85	0,030
	2256	6	I,7	0,2		
	2286	6	3,2	0,3		
	2434	8	0,6	0,2		
	2558	9	2,I	0,3		

	2676	I0	I,3	0,2		
	2940	II	2,6	0,3		
	4040	I5	8,4	I,0		
	4238	I7	6,0	0,9		
	4440	I9	5,5	I,0		
	4623	22	I,4	0,6		
	5200	25	3,0	0,9		
	5357	25	II	2		
	5746	30	5,5	I,I		
	6200	40	2,7	I,3		
	6320	40	2,3	I,0		
	6585	45	II,0	2,0		
	7770	50	I6,5	2,5		
	8530	60	36	3		
^{74}Ge	2846	8	8,0	2,0	0,I60	0,040
	3035	I2	I,0	0,6	0,230	0,040
	4I70	25	0,064	0,020		
	4990	30	94	I3		
	I2030	70	24	I3		
	I9450	I50	I20	25		
	2I9I0	200	50	I8		
	25I00	250	44	2I		
	42800	500	500	II0		
	6I040	900	8I0	260		
^{76}Ge	550	I	0,35	0,08	0,II5	0,025
	4760	20	4,2	I,8	0,I20	0,025
	I3940	90	I2	8		
	I5050	I00	84	II		
	2I040	200	4I	I7		
	22460	200	I95	22		
	29600	300	760	I90		
	48700	600	230	I20		

Table II

Average parameters for germanium isotopes

Isotope	Ge-70	Ge-72	Ge-73	Ge-74	Ge-76
$S_0 \cdot 10^4$	$2,3^{+1,0}_{-0,9}$	$1,0^{+0,6}_{-0,4}$	$2,0^{+0,7}_{-0,6}$	$1,3^{+1,1}_{-0,6}$	$2,3^{+2,1}_{-1,0}$
$\bar{\Gamma}_\gamma$ eV эВ	0,162±0,025	0,160±0,025	0,197±0,029	0,195±0,040	0,120±0,025
D_J eV эВ	1330±210	1550±270	124±14	3900±770	4[illegible]±825
a MeV МэВ$^{-1}$	10,79±0,25	12,08±0,34	12,60±0,32	11,95±0,38	12,74±0,41

NEUTRON RESONANCES OF NEODYMIUM ISOTOPES

E.N. Karzhavina, Nguen Nguen Fong, A.B. Popov, A.I. Taskaev

(JINR Preprint P3-3564)

The neutron spectrometer in the Neutron Physics Laboratory at the Joint Institute (resolution 80 nsec/m to 6 nsec/m) was used to measure transmission and neutron-capture gamma-ray emission for samples of natural neodymium and of neodymium enriched by the isotopes ^{142}Nd, ^{143}Nd, ^{144}Nd, ^{145}Nd, ^{146}Nd, ^{148}Nd, ^{150}Nd. The isotopes ^{143}Nd and ^{145}Nd were studied in the energy range up to 1000 eV, and the remaining were studied in the range up to 10 keV. For the neodymium isotopes ^{142}Nd, ^{143}Nd, ^{144}Nd, ^{145}Nd, ^{146}Nd, ^{148}Nd and ^{150}Nd, respectively, the following level spacings D were obtained: 1000 ± 250, 38 ± 6, 520 ± 70, 20 ± 3, 310 ± 43, 200 ± 21, 230 ± 28, and the following strength functions S_o: $(0.6 \pm 0.3) \times 10^{-4}$, $(4.3 \pm 1.4) \times 10^{-4}$, $(4.8 \pm 2.0) \times 10^{-4}$, $(3.0 \pm 0.7) \times 10^{-4}$, $(4.5 \pm 1.9) \times 10^{-4}$, $(3.6 \pm 1.1) \times 10^{-4}$, $(2.0 \pm 0.8) \times 10^{-4}$.

Table 1

^{142}Nd Resonance parameters

No.	E_0, eV	Γ_n, meV	Γ_n^o, meV
I.	I685 ± I0	I8I ± 73	4,4 ± I.8
2.	2539 ± I4	I200[illegible] ± [illegible]	238 ± 40
3.	3992 ± 28	780±400	I2 ± 6
4.	4547 ± 34	8300±830	I23 ± I[illegible]
5.	5533 ± 45	4550±600	6I ± 8
6.	63I5 ± 56	I000±I000	I3 ± I3
7.	9987 ± II0	I2000±3500	I20 ± 35

Table 2

^{143}Na Resonance parameters

No.	E_0, eV	Γ, meV	$g\Gamma_n$, meV	$2g\Gamma_n^o$	Γ_γ, meV
I.	55,4±0,2		20±2	5,4±0,5	80±20
2.	I27,4±0,4	450±I50	I80±30	32±5	94±I4
3.	I35,4±0,4		3I±5	5,3±0,9	70±23
4.	I59,0±0,5	I300±500	600±60	95±9	83±I3
5.	I79,7±0,5		320±50	48±7	6I±9
6.	I87,0±0,6	I600±500	850±50	I24±8	89±I3
7.	306 ±I		355±70	4I±8	67±I0
8.	324 ±I		2I5±60	24±8	
9.	338 ±I		260±40	28±5	
I0.	358 ± I,5		300±70	32±8	
II.	40I ±I,5		520±I00	52±I0	
I2.	408 ±I,5		230±40	23±4	
I3.	446 ±2		900±80	85±8	73±II
I4.	507 ±2		I0±2	0,9±0,2	
I5.	524 ±2,5		84±I6	7,3±I,4	75±I5
I6.	555 ±3		35±7	3,0±0,6	
I7.	576 ±3		7I±I4	6,I±I,2	
I8.	658 ±4		290±50	22±4	70±I0
I9.	705 ±4		I87±40	I4±3	
20.	775 ±5		580±80	42±6	76±II
2I.	806 ±5		4±I	0,28±0,07	
22.	822 ±5		3,4±0,7	0,25±0,05	
23.	840 ±6		480±70	33±5	
24.	853 ±6				
25.	976 ±6				
26.	988 ±7				
27.	I0I0 ±7				
28.	I028 ±7				
29.	I085 ±8				
30.	II27 ±8				
3I.	II67 ±8				
32.	I2I4 ±9				
33.	I265 ±9				
34.	I3I0 ±I0				

Table 3

^{144}Nd Resonance parameters

No.	E_0, eV	Γ_n, eV	Γ_n^o, meV	Γ_γ^o, meV
I.	374 ± 2	I5 ± I	790 ± 52	
2.	736 ± 4	0,58±0,05	2I,4 ± I,8	78 ± I2
3.	I280 ± 6	27,5 ±I,5	770 ± 42	
4.	I635 ± 8	4,3 ±0,3	I06 ± 8	I50 ± 80
5.	I980 ± I0	I4 ±I,6	3I5 ± 36	
6.	2784 ± 20	4 ±I	76 ± I9	
7.	3567 ± 24	I7 ±2	285 ± 34	
8.	3760 ± 27		< I0	
9.	4985 ± 40	26 ± 4	370 ± 57	
I0.	5200 + 45		< I0	
II.	5697 ± 50	2 ± I	26 ± I3	
I2.	6207 ± 60	8 ± 2	I0I ± 25	
I3.	69I0 ± 70	43 ± 5	5I7 ± 60	
I4.	7594 ± 75	3,I±I,5	36 ± I8	
I5.	8300 ± 85	9,0±2,4	99 ± 26	
I6.	96II ± I00	22 ± 4	225 ± 40	
I7.	9930 ± II5	24 ± 4	240 ± 40	
I8.	I0930 ± I30	34 ± 5	325 ± 48	
I9.	II730 ± I50	(8,0)	(74)	
20.	I3540 ± 200	45 ± 8	390 ± 70	

Table 4

^{145}Nd Resonance parameters

No.	E_0, eV	Γ, meV	$g\Gamma_n$, meV	$2g\Gamma_n^o$	Γ_γ, meV
1	2	3	4	5	6
I.	42,6 ± 0,I	394 ± 43	I55 ± I6	47 ± 5	
2.	85,7 ± 0,2		7,9±0,9	I,7 ± 0,2	
3.	96,0 ± 0,2		2,I±0,3	0,43±0,06	
4.	I02,2 ± 0,2		56 ± 4	II ± 0,8	
5.	I03,5 ± 0,2		I8,5±2,0	3,6 ±0,4	
6.	I47,3 ± 0,4		I0 ± I	I,65±0,I6	
7.	I5I,7 ± 0,4		7,8±0,9	I,26±0,I4	
8.	I69,8 ± 0,5		I,2±0,3	0,I8±0,5	
9.	I89,5 ± 0,6		2I ± 2	3,0 ±0,3	
I0.	233,4 ± 0,8		3,3±0,5	0,43±0,6	
II.	242,5 ± 0,9		34 ± 3	4,4 ±0,4	60 ± I0
I2.	249,4 ± 0,9		3,2±0,6	0,4I±0,08	
I3.	259,3 ± 0,9		56 ± 5	7,0 ±0,6	59 ± I0
I4.	275 ± I		67 ± 6	8,I ±0,7	6I ± I0
I5.	307 ± I		29 ± 6	3,3 ±0,7	
I6.	3I2 ± I,2		I5I ± I5	I7 ±I,7	5I ± 8
I7.	3I9 ± I,3		2,8±0,4	0,32±0,4	
I8.	343 ± I,4		5,5±0,8	0,60±0,08	
I9.	376 ± I,6		26 ± 4	2,7 ±0,4	
20.	39I ± I,7		23 ± 4	2,3 ±0,4	
2I.	399 ± I,7		8 ± I	0,8 ±0,I	
22.	405 ± 2		336 ± 58	33 ± 6	
23.	447 ± 2		II8 ± I3	II,I ±I,2	53 ± I3
24.	466 ± 2	847 ± 255	309 ± 5I	29 ± 5	46 ± 7
25.	488 ± 2		I98 ± I5	I7,9 ±I,4	58 ± 9
26.	499 ± 2		I87 ± 57	I6,7 ±4,5	
27.	507 ± 2	784 ± I82	350 ± 35	3I ± 3	67 ± I0
28.	5I6 ± 2		7 ± I	0,62±0,08	
29.	543 ± 2	628 ± 248	265 ± 30	23 ± 3	55 ± I2
30.	570 ± 3		570 ± 55	48 ± 5	67 ± I0
3I.	590 ± 3		4,I±0,6	0,34±0,05	
32.	607 ± 3		2,9±0,5	0,24±0,05	

I	2	3	4	5	6
33.	64I ± 3		206 ± 4I	I6 ± 3	62 ± 9
34.	650 ± 3		24 ± 4	I,9 ± 0,3	
35.	66I ± 3		4,I ± 0,6	0,32±0,05	
36.	69I ± 3		(I7)	(I,3)	
37.	699 ± 3		(I9)	(I,4)	
38.	7I0 ± 4		(I3)	(0,98)	
39.	7I9 ± 4		(I3)	(0,97)	
40.	758 ± 4		600 ± 60	43 ± 5	
4I.	790 ± 4		I,8 ± 0,3	0,I3±0,02	
42.	83I ± 4		I8I ± 3I	I3±2	
43.	850 ± 4		I450 ± 200	99±I4	
44.	888 ± 4			< I0	
45.	906 ± 5		(I50)	(I0)	
46.	9I9 ± 5		(200)	(I3)	
47.	948 ± 5		233 ± 28	I5±2	
48.	978 ± 5		403 ± 5I	27±4	
49.	I0I0 ± 5		620 ± 60	39±4	

Table 5

^{146}Nd Resonance parameters

No.	E_0, eV	Γ meV	Γ_n, meV	Γ_n^o	Γ_γ, meV
I.	36I ± I		43 ± 7	23 ± 0,4	55 ± 8
2.	625 ± 3			< 2	
3.	8I3 ± 3	I200 ± 450	II60±I00	4I ± 3,5	55 ± 8
4.	II75± 4		I3500±I000	394± 29	
5.	I5II± 7		3400±300	87,5± 7,7	
6.	I83I± 9		I540±60	36± 3,6	
7.	2049± II		4200±400	93±9	
8.	26I5± 20		25000±2000	490± 39	
9.	2880± 20			< I0	
I0.	2998± 25		3680±360	67± 6,7	
II.	3255± 25		2000±400	35 ± 7	
I2.	3677± 25		22000±2000	345± 34	
I3.	4026±30		I4000±I500	220± 24	
I4.	5I04± 40			< 30	
I5.	5227± 45			< 30	
I6.	5465± 50		4900±II00	66± I5	
I7.	6456± 60		(7500)	(93)	
I8.	6723±65		(8000)	(97)	

Table 6

^{148}Nd Resonance parameters

No.	E_0, eV	Γ_n, meV	Γ_n^0	Γ_γ, meV
1.	155 ± 0,5	1610 ± 240	129 ± 19	100 ± 15
2.	288 ± 1	2600 ± 200	153 ± 12	96 ± 14
3.	399 ± 1,5	410 ± 30	20,5 ± 1,5	65 ± 10
4.	717 ± 2	2000 ± 100	75 ± 4	74 ± 11
5.	876 ± 3	199 ± 36	6,7 ± 1,2	
6.	1060 ± 5	2350 ± 150	72 ± 5	
7.	1183 ± 6	2700 ± 200	79 ± 6	148 ± 24
8.	1355 ± 6	1680 ± 110	46 ± 3	
9.	1544 ± 7	3590 ± 150	91 ± 4	
10.	1818 ±		< 10	
11.	2195 ± 12	8400 ± 700	179 ± 15	
12.	2403 ± 13	3900 ± 300	80 ± 6	
13.	2546 ± 14	2400 ± 300	48 ± 6	
14.	2594 ± 20	7900 ± 800	155 ± 16	
15.	2795 ± 20	1400 ± 500	26 ± 9	
16.	3010 ± 25	2000 ± 500	36 ± 9	
17.	3525 ± 25		< 15	
18.	3688 ± 25		< 10	
19.	3950 ± 30		< 10	
20.	4121 ± 30	13000 ± 1000	203 ± 16	
21.	4318 ± 31	6500 ± 650	99 ± 10	
22.	4463 ± 33	2400 ± 600	36 ± 9	
23.	4704 ± 36	6700 ± 1000	98 ± 15	
24.	5377 ± 44	(4400)	(60)	
25.	6342 ± 56		< 30	
26.	7172 ± 70	13000 ± 2000	153 ± 24	
27.	7485 ± 75	(7400)	(85)	
28.	7819 ± 80	17000 ± 2000	192 ± 23	
29.	8781 ± 90	28000 ± 3000	300 ± 32	

Table 7

^{150}Nd Resonance parameters

No.	E_0, eV	Γ, meV	Γ_n, meV	Γ_n^o	Γ_γ, meV
I.	78,9 ± 0,I	I27 ± 20	I5,I ± I,6	I,7 ± 0,2	II5 ± 20
2.	3I6 ± I		420 ± 20	23,7 ± I,4	66 ± I0
3.	487 ± 2		II30 ± I00	5I ± 5	74 ± II
4.	774 ± 3		560 ± 40	20 ± I,4	84 ± I3
5.	I035 ± 5		I600 ± I40	50 ± 4,4	82 ± I2
6.	I340 ± 6		588 ± 80	I6 ± 2	
7.	I476 ± 7		I830 ± I30	47,6 ± 3,4	
8.	I724 ± 8		2000 ± 200	48 ± 5	
9.	I784 ± 9		I360 ± I60	32 ± 4	
I0.	I87I ± 9		I62 ± 7I	3,7 ± I,6	
II.	2550 ± I4		I770 ± I90	35 ± 4	
I2.	2750 ± I6		I0000 ± I000	I90 ± I9	
I3.	2870 ± I7		2900 ± 300	54 ± 6	
I4.	3I95 ± 20		440 ± 330	8 ± 6	
I5.	352I ± 25		5500 ± 550	93 ± 9	
I6.	3843 ± 30		6500 ± 600	I05 ± I0	

Table 8

Mean parameters of Nd isotopes

Isotope	E max. eV	n-number of resonances for determination	D, eV	D*, eV	S_0 max. true $X.10^{-4}$	$S_0 = \frac{\Sigma \Gamma_n^0}{\Delta E}$ $X.10^{-4}$	$\bar{\Gamma}_\gamma$, meV
Nd^{I42}	6300	6	I000±250	670	$I,0^{+I,2}_{-0,5}$	0,6±0,3	-
Nd^{I43}	840	23	38±6	-		4,3±I,4	76±II
Nd^{I44}	7000	I4	520±70	540	$4,5^{+3,I}_{-I,8}$	4,8±2,0	78±I2
Nd^{I45}	I000	50	I9±3	-	-	3,0±0,7	58±8
Nd^{I46}	4000	I3	3I0±43	290	$4,6^{+3,2}_{-I,6}$	4,5±I,9	55±8
Nd^{I48}	4500	23	200±2I	I98	$3,5^{+I,7}_{-I,I}$	3,6±I,I	96±I4
Nd^{I50}	4000	I6	230+28	255	$I,8^{+I,I}_{-0,6}$	2,0±0,8	84±I2

Table 9

No.	Target nucleus	Spin I	E_0 MeV	σ_p MeV	σ_n MeV	U MeV	$2\rho_{no\,\omega} = \sum_{J,\pi} \rho(J,\pi)$ X.10^{-3}, MeV^{-1}	a MeV^{-1}	σ
I.	$_{60}Nd^{I42}$	0	6,I0	I,30		4,77	2,98±0,62	I7,3±0,5	4,69
2.	Nd^{I43}	7/2	7,8I	I,38	0,99	5,44	57 ± 8	I7,7±0,4	4,89
3.	Nd^{I44}	0	5,97	I,27		4,67	3,84±0,52	I8,2±0,4	4,75
4.	Nd^{I45}	7/2	7,53	I,27	0,9I	5,40	I05 ± I7	I9,I±0,4	5,0
5.	Nd^{I46}	0	5,I4	I,27		3,84	6,46±0,90	23,0±0,5	4,82
6.	Nd^{I48}	0	4,94	I,27		3,64	I0 ± I	25,4±0,5	4,90
7.	Nd^{I50}	0	4,8I	I,27		3,5I	8,7 ± 0,7	25,9±0,5	4,90

NEUTRON RESONANCES OF GADOLINIUM ISOTOPES

E.N. Karzhavina, Nguen Nguen Fong, A.B. Popov

(JINR Preprint P3-3882)

The LNF neutronspectrometer at the Joint Institute was used for transmission and radiative-capture measurements on the isotopes ^{152}Gd, ^{154}Gd, ^{155}Gd, ^{156}Gd, ^{157}Gd, ^{158}Gd, ^{160}Gd. The neutron-resonance parameters of these isotopes were obtained by area analysis. Resonance parameter data are given in Tables I, II and III. Table IV gives the mean level spacing D, the strength functions S_o, the mean radiation width Γ_γ and the level density parameter a for the Gd isotopes. This same table also gives the mean level spacing for the isotopes ^{152}Sm and ^{154}Sm. The radiative neutron capture was also measured for these isotopes, so that the position of the neutron resonances could be determined (data given in Table V).

Table I

Resonance parameters of even Gd isotopes

E_o eV	Γ, meV	Γn, meV	Γγ meV	Γn^o
		Gd^{152}		
8,00±0,02		5,0		I,8
I2,35±0,04		2,2 ± 0,2		0,62±0,06
36,86±0,05	I40 ± I0	84 ± 6	56 ± I2	I3,8 ±I,0
39,3 ±0,I	97 ± I7	39 ± 3	58 ± I7	6,2 ±0,5
42,7 ±0,I		3,I ± 0,6		0,47±0,09
74,3 ±0,2	I02 ± I5	55 ± I3	47 ± 20	6,4 ±I,5
85,I ±0,2		3,6 ± 0,6		0,39±0,06
92,4 ±0,2	2I2 ± 38	I60 ± 37		I6,6 ±3,8
I00,0±0,4		(9,0)		(0,9)
I24,0±0,4		(8,0)		(0,7)
I40,4±0,4	I70 ± I7	I24 ± I6	46 ± 24	I0,5 ±I,3
I85,2±0,6	I67 ± 27	I05 ± 30	62 ± 40	7,7 ±2,2
202 ± I		200 ± 40		I4 ± 3
223 ± I		300 ± I00		20 ± 6
23I ± I		I00 ± 40		6,6 ± 2,6
238 ± I				
252 ± I,5				
293 ± I,5				
	—	Gd^{154}		
II,49±0,04		0,34±0,08		0,I0±0,03
22,4 ±0,I		I3±2		2,7 ±0,4
47,0 ±0,I		4,5 ±0,9		0,66±0,I3
49,5 ±0,I		2,4 ±0,4		0,34±0,06
65,0 ±0,I	93 ± I4	36,5 ±4,2	57 ± I5	4,5 ±0,5
I00,5 ±0,2	I44 ± 50	43 ± 7	I00 ± 50	4,3 ±0,7
I05,6 ±0,2		7,7 ±I,8		0,75±0,20
I23,8 ±0,3		I30 ±23		I2±2

I	2	3	4	5
I39,3±0,3		I25±32		II ± 3
I48,0±0,4		50±I2		4,2±I,0
I64,9±0,5	I89±I3	I20±8	69±I5	9,3±0,6
2II ±0,7		43±6		3,0±0,5
244 ±0,8		27±7		I,8±0,5
		Gd^{156}		
33,I2±0,04	86±I3	I4±2	72±I4	2,4±0,3
80,2 ±0,2		79±8		8,8±0,9
I50,1± 0,4		42±5		3,4±0,4
I98,I ±0,5		275±33		I9,5±2,3
20I,6 ±0,5		I7±5		I,2±0,4
244,0 ±0,7		3,I±0,5		0,20±0,03
340 ±1		(20)		(I,I)
377 ±I		226±23		II,6±I,2
452 ±I		II6±35		5,5±I,6
477 ±I,2		I20±40		5,5±I,7
5I5 ±I,5		I45±43		6,4±I,9
707 ±2		(420)		(I5,8)
7I4 ±2		(420)		(I5,7)
732 ±2,2		300±I00	70 ± I4	I2 ±4
796 ±2,5		94±32		3,3±I,I
823 ±3		I000±300	94 ± I5	35 ±I0
845 ±3		350±I20	97 ± 20	I2 ±4
856 ±3		2I±3		0,72±0,I0
900 ±3		390±I40	79 ± I6	I3 ±5
982 ±3,5		I85±58		5,9±I,8
I035 ±		30±6		0,94±0,I9
I054 ±4		50±I0		I,5±0,3
I094 ±4		I5±3		0,45±0,09
II43 ±4,5		900±200		27±6
II54 ±4,5				
II85 ±5		230±70		6,7±2,0
I239 ±5				
I254 ±5				

I	2	3	4	5
I318±6		(59)		(I,6)
I339±6		(60)		(I,6)
I392±6		I70±40		4,6 ± I,I
I427±6		205±55		5,4 ± I,4
I49I±7				
I5II±7				
I550±7				
		Gd^{158}		
22,3±0,I	98±I3	6,I±0,6	92±I3	I,29±0,I3
I0I,0±0,4		0,8±0,2		0,08±0,02
243,0±0,5		68±6		4,4 ±0,4
278,0±0,5		24±4		I,4 ±0,2
345 ±0,7		I94±50		I0,4 ±2,6
409 ±I		343±57	88±I7	I7 ± 3
505 ±I,2		334±43	80±I6	I5 ± 2
589 ±I,6		84±26		3,5 ± I,I
694 ±2		740±I00	90±I4	28 ± 4
848 ±3		I8I0±I50	I09±I5	62 ± 5
92I ±3		508±I50	75±I5	I7 ± 5
I074 ±4		300±I50		9 ± 4
I225 ±5		II60±I90		33 ± 5
I299 ±5		660±I80		I8 ± 5
I356 ±6		слабый		
I346 ±6		620±I50		26 ± 4
I460 ±7		980±2I0		I6 ± 6
I554 ±7		390±I20		I0 ± 3
I655 ±8		слабый		(4,8)

I	2	3	4	5
		(200)		(4,8)
		(200)		(4,8)
I880±I0		I60±50		3,8±I,2
I952±I0		850±250		I9±6
20I2±I0		940±250		2I±6
2II8±II		слабый		
2250±I2		(I50)		(3)
2338±I2		440±300		9±6

Gd^{I60}

222,0±0,5		60±I0		4,0±0,7
447±I		4,6±0,7		0,22±0,04
480±I,2		370±40		I7±I,7
570±I,5		6±I		0,25±0,04
750±2		5±I		0,I8±0,04
903±3		4440±340	I05±I5	I48±I2
984±4		4,6±0,7		0,I4±0,03
I243±5		3000±500	9I±I4	85±I4
I425±5		II20±360	98±I5	30±9
I694±8		(I5)		(0,36)
I8I2±9		8000±700		I88±I6
I964±I0		330±240		(7,5)
2283±I2		I3I0±280		27±6
2405±I3		3600±400		73±8
2525±I5		3600±480		7I±I0
2656±I5		2870±480		56±I9

Table II

^{155}Gd Resonance parameters

E_o eV	Γ meV	$g\Gamma_n$ meV	Γ_γ meV	$2g\Gamma_n^o$
I	2	3	4	5
6,28±0,02	I22±I3	I,I4±0,09	I20±I3	0,9I±0,07
7,7I±0,02	85±I6	0,68±0,II	05±I6	0,49±0,08
9,96±0,03		0,097±0,008		0,060±0,00
II,49±0,04		0,I9±0,02		0,II±0,0I
II,99±0,04		0,5I±0,03		0,29±0,02
I4,48±0,05		I,3±0,I		0,68±0,05
I7,70±0,06		0,24±0,02		0,II±0,0I
I9,87±0,06	II6±I6	3,0±0,3	II0±I6	I,34±0,I3
20,96±0,06	97±I8	I0,9±I,3	75±I9	4,8±0,6
23,60±0,04		I,5±0,2		0,62±0,08
27,48±0,04		0,4I±0,03		0,I6±0,0I
29,50±0,05	I3I±6I	3,5±0,4	I24±6I	I,28±0,I6
30,03±0,05	I04±38	8,9±I,6	87±39	3,25±0,58
3I,64±0,05		0,78±0,I5		0,28±0,04
33,I4±0,06		(0,6)		(0,II)
34,68±0,06		2,3±0,2		0,78±0,07
35,36±0,06		I,2±0,2		0,40±0,07
36,83±0,07	94±I4	4,0±0,4	86±I5	I,32±0,I3
33,89±0,08		0,72±0,08		0,23±0,03
43,82±0,09		8,4±I,0		2,53±0,30
45,94±0,09	—	I,6±0,2		0,47±0,06
46,74±0,09	I07±39	3,7±0,4	I00±39	I,08±0,I2
47,56±0,I		0,24±0,03		0,70±0,09
5I,23±0,I		I0±I		2,79±0,28
5I,9±0,I	I20±56	9,5±I,3	I00±56	2,64±0,36
52,8±0,I		(0,9)		(0,25)
53,6±0,I		6,0±0,5		I,64±0,I4
56,0±0,I		I,3±0,2		0,35±0,05
59,2±0,I	I68±55	4,3±0,5		I,II±0,I3
62,7±0,2	I7I±50	5,4±0,6		I,36±0,I5
65,0±0,2		0,60±0,I0		0,I5±0,03
69,4±0,I		3,9±0,4		0,94±0,I0
76,8±0,I		I,0±0,5		0,23±0,II

I	2	3	4	5
80,0±0,I		2,2±0,2		0,49±0,05
80,6±0,I		I,4±0,2		0,3I±0,05
83,9±0,I		4,I±I,0		0,89±0,22
84,8±0,I		I,2±0,2		0,26±0,04
90,4±0,I		0,67±0,07		0,I4±0,02
92,3±0,I		I,7±0,2		0,36±0,04
92,7±0,I		2,7±0,4		0,55±0,07
95,6±0,I		2,6±0,3		0,53±0,05
96,3±0,I		2,6±0,3		0,53±0,06
98,2±0,2		7,2±0,I		I,45±0,20
I00,I±0,2		0,83±0,08		0,I7±0,02
I0I,3		2,8±0,7		0,56±0,I4
I02,0		(0,85)		(0,I7)
I04,3		3,6±0,4		0,7I±0,08
I05,8		2,4±0,2		0,46±0,05
I07,0		4,I±0,4		0,79±0,08
I09,6		I,8±0,2		0,35±0,04
III,3		6,I±0,7		I,I5±0,I4
II3,7		8,9±I,2		I,67±0,23
II6,4		6,0±0,8		I,II±0,I6
II8,5		0,83±0,09		I,52±0,I7
I23,3		23±4		4,I5±72
I24,3		4,5±0,5		0,8I±0,09
I25,9		7,8±I,0		I,4±0,2
I29,8		(I,7)		(0,30)
I30,7		I9±3		3,3±0,5
I32,9		I,3±0,2		0,22±0,03
I33,7		I,0±0,I5		0,I7±0,03
I34,7		0,07		0,0I
I37,7±0,2		I,5±0,2		0,25±0,04
I45,5±0,3		3,9±0,4		0,65±0,07
I46±0,3		I,7±0,3		0,28±0,04
I48,2±0,3		I,7±0,3		0,29±0,04
I49,6		(I3,4)		(2,2)
I50,0		(I4)		(2,3)
I52,2		2,9±0,4		0,47±0,07

I	2	3	4	5
I56,24		4,7±0,7		0,75±0,II
I60,0		7,7±0,8		I,I2±0,I2
I6I,6		9,5±I,2		I,5 ±0,2
I68,I		I2±I,5		I,8±0,2
I70,3		5,4±0,8		0,83±0,I2
I71,3		5,4±0,8		0,83±0,I2
I73,4		2I±3		3,3±0,5
I77,9±0,3		3,3±0,5		0,50±0,08
I80,2±0,4		5,I±0,8		0,76±0,I2
I83,2		3,5±0,5		0,52±0,07

Table III

^{157}Gd Resonance parameters

E_o, eV	Γ, meV	gΓn meV	Γγ meV	$2g\Gamma n^o$
I	2	3	4	5
I6,I7±0,06		(0,2I)		(0,I0)
I6,77±0,06	97±I0	8,0±0,7	8I±I0	3,9±0,3
20,49±0,03	97±20	7±I	85±20	3,I±0,4
23,23±0,04		0,30±0,05		0,I2±0,02
25,33±0,04	77±I3	I,03±0,09	75±I3	0,4I±0,04
40,06±0,08		0,45±0,03		0,I4±0,0I
44,07±0,09	I00±I9	5,5±0,9	89±I9	I,7±0,3
48,7±0,I	II7±II	I7,8±I,2	82,I2	5,I±0,3
58,I3±0,I3	I25±II	23,I±I,5	79±I2	6,0±0,4
66,44±0,I6		4,7±0,5		I,I±0,I
8I,2±0,I		6,4±0,8		I,4±0,2
82,0		3,7±0,5		0,82±0,II
87,0	I9I±55	4,4±0,6	I73±65	0,94±0,I3
96,5±0,I	97±26	8,0±I,0	8I±26	I,6±0,2
I00,0±0,2	I27±I8	I9±3	89±I9	3,8±0,5
I04,8		I8±3		3,5±0,6
I07,3		5,8±0,4		I,I2±0,08

I	2	3	4	5
I08,9		(0,3)		(0,06)
II0,0	I4I±I9	29±4	83±2I	5,5±0,8
II5,2	I50±75	I0±2	I30±75	I,9±0,4
I20,7	268±2I	92±7	84±24	I6,7±I,2
I37,9		29±6		5,0±I,0
I38,8±0,2		(3,8±0,4)		0,64±0,07
I43,7±0,3		40±4		6,7±0,7
I43,3		9±2		I,5±0,3
I56,4		II±2		I,8±0,3
I64,8		I2±3		2,8±0,5
I68,2		(0,86)		(0,I3)
I69,5		(I,0)		(0,I5)
I71,3±0,3		I9±3		2,9±0,5
I78,6±0,4		I0±2		I,5±0,3
I82,9		I0±2		I,5±0,3
I90,6		9±2		I,3±0,3
I94,4		28±5		4,0±0,7
202,8		3,6±0,5		0,50±0,07
205,2		(0,6I±0,09)		(0,08±0,0I)
207,7±0,4	2I9±I8	75±I0	69±23	I0,4±I,4
2I7,2±0,5		3,0±0,3		0,4I±0,04
22I,I		I,5±0,3		0,20±0,04
228,3±0,5		4,I±0,6		0,54±0,08
239,2±0,6	243±I8	95±I0	53±30	I2,3±I,3
246,4		5,8±0,6		0,74±0,08
250,2		2,I±0,3		0,27±0,04
255,0		I,4±0,2		0,I7±0,03
260,I		8,2±I,0		I,0±0,I
265,8±0,6		4,0,4		0,49±0,05
268,2±0,7		6,5±0,9		0,80±0,II
28I,8		24±4		2,8±0,5
287,6		8,9±I,0		I,0±0,I
290,8±0,7		25±3		2,9±0,4
293±0,8		25±3		2,7±0,4
300,9		20±5		2,3±0,6
306,4±0,8		I,8±0,3		0,20±0,03

Table IV. Mean parameters of Gd and Sm isotopes

Target nucleus	Max. neutron energy	No. of resonances	$D_{obs.}$ eV	$S_0 = \frac{\Sigma g \Gamma_n^0}{\Delta E}$ $\times 10^4$	S_0 max. true $\times 10^4$	Γγ MeV	Bn MeV	$\Delta = \Delta_p + \Delta_n$ MeV	U MeV	a MeV^{-I}
I52	230	I4	I5±2	4,6±I,8	$4,0^{+2,6}_{-I,5}$	57±I5*) (2)	6,4I	0,97	5,44	25,3
I54	230	I3	I5,5±2,3	2,4±I,0	$2,I^{+I,5}_{-0,7}$	63±I5	6,4I	0,97	5,44	25,2
I55	I80	80	I,8±0,3	2,I0±0,35		I00±I0	8,5I	I,89	6,62	22,6
I56	I200	24	47±4	I,8±0,6	$I,6^{+0,8}_{-0,5}$	82±I2 (8)	6,36	0,97	5,39	22,8
I57	300	54	5,6±0,7	2,I6±0,45		86±I0 (I0)	7,92	I,70	6,22	2I,6
I58	2000	22	85±9	I,5±0,5	$I,4^{+0,7}_{-0,4}$	89±I3 (6)	6,I5	0,97	5,I8	22,2
I60	2500	I6	I70±2I	2,6±I,0	$2,7^{+I,7}_{-0,9}$	98±I5 (3)	5,79	0,97	4,82	22,I
I52	700	I5	45±5				5,75	I,22	4,53	26,6
I54	I300	20	90±I0				5,27	I,22	4,05	27,6

* In the column Γγ, the figure in brackets is the number of resonances for which the mean value of the radiation width was determined.

Table V. Neutron resonance energies for Sm isotopes

^{152}Sm	8,03; 62,I; 87,7; I53,7; I85,2; 237; 260; 3I5; 326; 384;4I5; 484; 508; 586; 60I; 642; 772; 792; 853; 929; 956; 99I; I050; I086; III5; I229; I3I2
^{154}Sm	93,0; 26I; 34I; 457; 578; 6I6; 703; 7I8; 828; I077; II58; II8I; I244; I280; I470; I552; I6I0; I650; I734; I768; I835.

ALPHA-PARTICLE SPECTRA IN THE DECAY OF EXCITED STATES OF ^{148}Sm WITH 3^- AND 4^- SPINS

Yu.P. Popov, M. Stempinsky

(JINR Preprint P6-3605)

The paper gives the first results of a study of the alpha-particle spectra obtained with the decay of the different states of samarium-148 excited by resonance neutron capture on the ^{147}Sa nucleus. An analysis of the alpha-particle spectra makes it possible to identify the resonances in terms of the spins. For the resonances E_0 = 3.4 eV and 18.3 eV spins 3 and 4 can be confirmed respectively, and for the resonance E_0 = 27.1 eV the value 3 was obtained.

The paper discusses the influence of pâir-correlation effects of the last nucleons on the reduced alpha widths in the ^{147}Sm (n,α) reaction (see Table).

Table

Characteristics of daughter-nucleus levels and reduced probability of alpha-transitions to these levels in the reaction $^{147}Sm(n,\alpha)^{144}Nd$

E_{exc} MeV	I^{π}	E_0 = 3.4 eV; $j^{\pi} = 3^-$ N_α	$\Gamma_{\alpha i}$ $\mu eV^{x)}$	δ_i^2 $eV^{xx)}$	E_0 = 18.3 eV; $j^{\pi} = 4^-$ N_α	$\Gamma_{\alpha i}$ $\mu eV^{x)}$	δ_i^2 $eV^{xx)}$
0	0^+	627	0,70±0,03	I,6±0,I	-	-	-
0,696	2^+	7I6	0,80±0,03	5,2±0,2	78	0,05±0,02	I,0±0,4
I,3I	4^+	98	$0,II^{+0,05}_{-0,08}$	$7,2^{+3,3}_{-5,2}$	I70	0,II±0,02	7,2±I,2
I,50	(3)	I97	0,22±0,05	I2±3	62	0,04±0,02	3,2±I,6
I,56	2^+						
2,29	4^+						
2,37	2^+	~35	0,04±0,03	I00±80	~I0	0,027±0,026	26±22

x) For unresolved-energy transitions to levels 1.50–1.56 MeV and 2.29–2.37 MeV the overall widths are given.

xx) For unresolved transitions the mean reduced widths are given. The errors indicated in the table do not include the standard errors.

THE EFFECT OF NUCLEAR DEFORMATION ON NEUTRON-RESONANCE DENSITY IN THE RARE-EARTH RANGE

V.I. Furman, A.B. Popov

(JINR Preprint P4-3925)

The extensive data available on neutron-resonance density have been repeatedly analysed on the basis of the statistical model of the nucleus [1]. The results of such analyses indicate that the dependence of the statistical-model parameter a on the atomic weight A corresponds to the concept of a nucleus as a gas of weakly interacting fermions (a on average proportional to A), while the dips in the dependence of a on A, corresponding to the magic numbers, clearly show the existence of shell effects. In reference [2] the maximum in the dependence of a on A at A ≈ 150 is of interest; this maximum appears more clearly in the dependence of a on the number of neutrons N, at N ≈ 90 (see Fig. 1). Although the presence of minima in the plot a (A) can be qualitatively explained by the filling of shells of spherical nuclei [3], the existence of the maximum at A ≈ 150 is not explained in this way.

The authors discuss the significance of this maximum and try to explain it by the filling of a system of single-particle states of deformed nuclei [4].

Using this system it is possible to estimate the density of the single-particle states close to the Fermi surface g_{shell}. For this, the authors assumed that the effective experimental deformation of the nucleus corresponds to the deformation of the neutron system and that the proton deformation changes only slightly for each isotope family.

Fig. 2 gives a comparison between the values of g_{shell} obtained with an averaging interval of the order of the nuclear temperature and the experimental values $g_{exp.} = \frac{6}{\pi^2} a$. From Fig. 2 it can be seen that in the functions g_{shell} (N) and $g_{exp.}$ (N) there is a correlation, although systematically $g_{shell} \leq g_{exp}$. Thus, the presence of the maximum in $g_{exp.}$ (N) at N ≈ 90 can be easily understood from the function g_{shell} (N). It can be stated that the rise in g_{shell} (N) in the transition region (A ≈ 150) is caused by an increase in the shell density due to the mixing of the sub-shells for small deformations ($\beta \approx A^{-2/3}$). The drop in g_{shell} after A≈155 and the ensuing slope are due to the change to large deformations ($\beta \approx A^{-1/3}$), which lead to discharges in the level system for the centre of the neutron shell.

REFERENCES

[1] A.V. Malyshev, Vsesojuznaja letnjaja shkola po jadernoj spektroskopii (All-Union Summer School on Nuclear Spectroscopy) 3-19 July 1966, Obninsk.

A. Gilbert, A. Cameron, Canad. J. Phys. 43 (1965) 1446
U. Facchini, Saetta-Menichella, Ener. Nucleare 15 (1968) 54.

[2] E.N. Karzhavina, et al., JINR Preprint P3-3564, 1967
E.N. Karzhavina, et al., JINR Preprint P3-3882, 1968.

[3] T. Newton, Canad. J. Phys. 34 (1956) 804.

[4] F. Gareev, S. Ivanova, et al., JINR Preprint P4-3607, 1967.

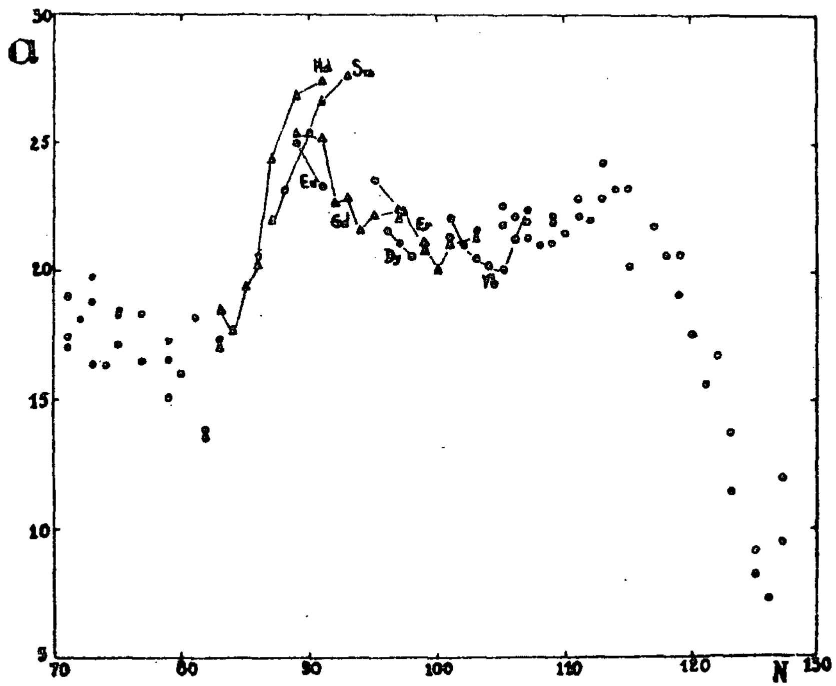

Fig. 1 Dependence of the parameter a on the number of neutrons.
Dots - data from the work by Facchini [1].
Triangles - data from work [2].

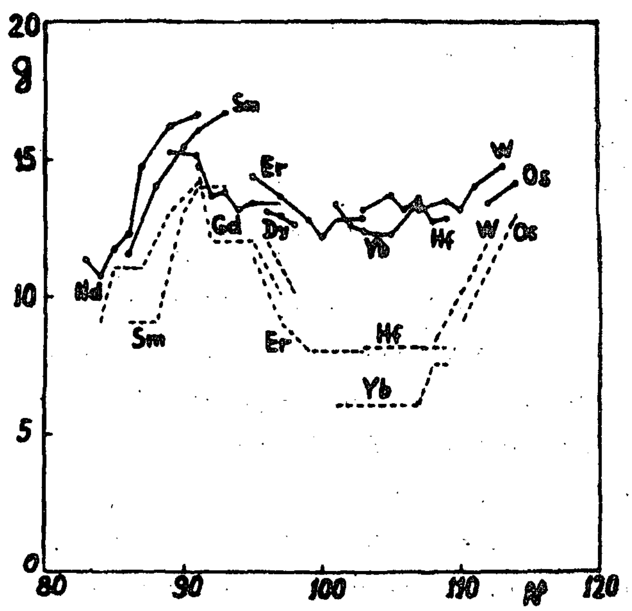

Fig. 2 Comparison between $g_{exp.}(N)$ (full lines) and $g_{shell}(N)$ (dotted lines).

NEW EXPERIMENTAL INSTALLATIONS

In July of this year an electron accelerator (microtron) was put into operation at the Institute of Physics and Power Engineering. The main characteristics of the accelerator are as follows:

Maximum electron energy 30 MeV,
Pulse current 80 mA,
Pulse length 2–5 μsec,
Pulse frequency up to 100 pulses/sec.

The beam of accelerated electrons is directed at a target in the centre of the core of the adjacent BFS reactor. The short neutron bursts produced in the target by photo-nuclear reactions can be used in various reactor-physics studies, especially for measuring the energy spectra of neutrons emitted from the core using the time-of-flight method. For this purpose the installation is designed for a flight path of about 800 m with intermediate stations for installing detectors, at distances of 50 and 200 m from the reactor. In addition, the installation will be used for research on reactor kinetics, neutron cross-section measurements and the study of photo-nuclear reactions.

CONTENTS

---

* The page number of the beginning of each article in the English translation corresponds to that of the Russian original.